ISSN 1881-7831 Online ISSN 1881-784X

DD&T

Drug Discoveries & Therapeutics

Volume 7, Number 6
December, 2013

IRCA BSSA

IACMHR

www.ddtjournal.com

DD&T
Drug Discoveries & Therapeutics

ISSN: 1881-7831
Online ISSN: 1881-784X
CODEN: DDTRBX
Issues/Year: 6
Language: English
Publisher: IACMHR Co., Ltd.

Drug Discoveries & Therapeutics is one of a series of peer-reviewed journals of the International Research and Cooperation Association for Bio & Socio-Sciences Advancement (IRCA-BSSA) Group and is published bimonthly by the International Advancement Center for Medicine & Health Research Co., Ltd. (IACMHR Co., Ltd.) and supported by the IRCA-BSSA and Shandong University China-Japan Cooperation Center for Drug Discovery & Screening (SDU-DDSC).

Drug Discoveries & Therapeutics publishes contributions in all fields of pharmaceutical and therapeutic research such as medicinal chemistry, pharmacology, pharmaceutical analysis, pharmaceutics, pharmaceutical administration, and experimental and clinical studies of effects, mechanisms, or uses of various treatments. Studies in drug-related fields such as biology, biochemistry, physiology, microbiology, and immunology are also within the scope of this journal.

Drug Discoveries & Therapeutics publishes Original Articles, Brief Reports, Reviews, Policy Forum articles, Case Reports, News, and Letters on all aspects of the field of pharmaceutical research. All contributions should seek to promote international collaboration in pharmaceutical science.

Editorial Board

Editorial and Head Office:

Pearl City Koishikawa 603,
2-4-5 Kasuga, Bunkyo-ku,
Tokyo 112-0003, Japan
Tel.: +81-3-5840-9697
Fax: +81-3-5840-9698
E-mail: office@ddtjournal.com

Drug Discoveries & Therapeutics

Editorial and Head Office

Pearl City Koishikawa 603, 2-4-5 Kasuga, Bunkyo-ku,
Tokyo 112-0003, Japan

Tel: +81-3-5840-9697, Fax: +81-3-5840-9698
E-mail: office@ddtjournal.com
URL: www.ddtjournal.com

Editorial Board Members

CONTENTS

Volume 7, Number 6, 2013

Reviews

Brief Report

Original Articles

CONTENTS (*Continued*)

Index

Guide for Authors

Copyright

Review

DOI: 10.5582/ddt.2013.v7.6.212

Traditional Chinese medicine and related active compounds: A review of their role on hepatitis B virus infection

Fanghua Qi[1,*], Zhixue Wang[1,*], Pingping Cai[1], Lin Zhao[1], Jianjun Gao[2], Norihiro Kokudo[2], Anyuan Li[1], Junqing Han[3,], Wei Tang[2,**]**

[1] *Department of Traditional Chinese Medicine, Shandong Provincial Hospital affiliated to Shandong University, Ji'nan, China;*
[2] *Hepato-Biliary-Pancreatic Surgery Division, Department of Surgery, Graduate School of Medicine, The University of Tokyo, Tokyo, Japan;*
[3] *Department of Tumor Research and Therapy Center, Shandong Provincial Hospital affiliated to Shandong University, Ji'nan, China.*

ABSTRACT: Since the significant public health hazard of Hepatitis B virus (HBV) infection and obvious drug resistance and dose-dependent side effects for common antiviral agents (*e.g.*, interferon-alpha, lamivudine, and adefovir), continuous development of agents to treat HBV infection is urgently needed. Traditional Chinese medicine (TCM) is an established segment of the health care system in China. Currently, it is widely used for chronic hepatitis B (CHB) in China and many parts of the world. Over a long period of time in clinical practice and in basic research progress, the effectiveness and beneficial contribution of TCM on CHB have been gradually known and confirmed. Based upon our review of related papers and because of our prior knowledge and experience, we have selected some Chinese medicines, including Chinese herbal formulas (*e.g.*, Xiao-Chai-Hu-Tang, Xiao-Yao-San, and Long-Dan-Xie-Gan-Tang), single herbs (*e.g.*, *Phyllanthus niruri*, *Radix astragali*, *Polygonum cuspidatum*, *Rheum palmatum*, and *Salvia miltiorrhiza*) and related active compounds (*e.g.*, wogonin, artesunate, saikosaponin, astragaloside IV, and chrysophanol 8-*O*-beta-D-glucoside) and Chinese medicine preparations (*e.g.*, silymarin, silibinin, kushenin, and cinobufacini), which seem effective and worthy of additional and in-depth study in treating CHB, and we have given them a brief review. We conclude that these Chinese herbal medicines exhibit significant anti-HBV activities with improved liver function, and enhanced HBeAg and HBsAg sero-conversion rates as well as HBV DNA clearance rates in HepG2 2.2.15 cells, DHBV models, or patients with CHB. We hope this review will contribute to an understanding of TCM and related active compounds as an effective treatment for CHB and provide useful information for the development of more effective antiviral drugs.

Keywords: Hepatitis B virus (HBV), chronic hepatitis B (CHB), traditional Chinese medicine (TCM), active compounds

1. Introduction

Hepatitis B virus (HBV) infection is a serious global public health problem, which can lead to liver failure, acute and chronic hepatitis, liver cirrhosis, and liver cancer. Approximately 2 billion people worldwide are reportedly infected with HBV, and more than 350 million of them are chronic carriers (*1*). It is estimated that worldwide more than 600,000 individuals die from HBV-related liver disease each year (*2*). Vaccination is considered to be the most effective way to control the spread of HBV and implementation of the HBV vaccine has led to a significant reduction in viral transmission; however, it remains highly endemic in many areas of the world, particularly in eastern Asia, India, and Pakistan (*3*). Currently, there are six agents approved for the treatment of chronic hepatitis B (CHB) by the US Food and Drug Administration (FDA), including interferon (interferon-alpha (IFN-α) and pegylated interferon-alpha (peg IFN-α)), nucleoside (lamivudine, entecavir, and telbivudine) and nucleotide analogues (adefovir) (*4*). However, their therapeutic effect is not satisfactory with obvious drug resistance and dose-dependent side effects

* Drs. Fanghua Qi and Zhixue Wang contributed equally to this article.
***Address correspondence to:*
Dr. Wei Tang, Hepato-Biliary-Pancreatic Surgery Division, Department of Surgery, Graduate School of Medicine, The University of Tokyo, 7-3-1 Hongo, Bunkyo-ku, Tokyo 113-8655, Japan.
E-mail: TANG-SUR@h.u-tokyo.ac.jp
Dr. Junqing Han, Department of Tumor Research and Therapy Center, Shandong Provincial Hospital affiliated to Shandong University, No. 324, Jingwuweiqi Road, Ji'nan 250021, Shandong, China.
E-mail: hanjunqing1960@126.com

(*5*). Therefore, development of novel antiviral drugs and more effective therapies for the treatment of CHB are urgently needed.

Traditional Chinese medicine (TCM) has been widely used in Asia for more than two thousand years. At present, TCM serves as an established segment of the public health system in China and in recent years it has been gaining interest and acceptance as alternative or complementary medicine in Western countries. An estimated 1.5 billion people now use Chinese herbal medicine, an important category of TCM, for the treatment of various diseases including chronic HBV infection worldwide (*6*). In China, it is used as a treatment adjunct or alternative to anti-HBV drugs and accounts for 30% to 50% of total medicine consumption for CHB treatment (*7*). Because of its low cost and low toxicity, about 80% of the patients with CHB in China rely on Chinese herbal medicine (*8*). A number of clinical trials have been performed to assess the therapeutic efficacy and safety of Chinese herbal medicines in CHB treatment. According to the results from meta-analysis of clinical trials, they indicated that: (*i*) Chinese herbal medicines alone may have an equivalent or better effect when compared with interferon or lamivudine in CHB treatment as evidenced by HBeAg and HBsAg sero-conversion as well as HBV DNA clearance; (*ii*) Chinese herbal medicines combined with interferon or lamivudine significantly enhanced the anti-viral activities of these agents; (*iii*) Chinese herbal medicines have a beneficial effect on improving liver function (*7,8*).

Although Chinese herbal medicines are widely used in the clinic in China, their active ingredients are complex and their mechanisms in CHB treatment are not clear, so that at present it is difficult for them to be popular in the world. In recent decades, as the HBV-transfected cell lines and duck HBV (DHBV) model are widely used for the study of anti-HBV drugs *in vitro* and *in vivo*, the anti-viral effects of many Chinese herbal medicines and their active ingredients have been gradually known and confirmed, which will provide evidence for developing novel antiviral drugs. Therefore, in this article, the authors review some Chinese herbal medicines, including Chinese herbal formulas, single herbs and their active ingredients, and Chinese medicine preparations, which are widely reported to have antiviral effects in basic or clinical studies. We hope this review will contribute to an understanding of Chinese herbal medicines as an effective treatment for CHB and provide useful information for the development of more effective antiviral drugs.

2. Traditional Chinese herbal formulas commonly used with anti-HBV activities

Traditional Chinese herbal formulas (or Kampo in Japanese) are a combination of compatible herbs in fixed dosages, most of which come from classical or well-known Chinese textbooks of medicine (*e.g.*, "Shang Han Lun" and "Jin Gui Yao Lue", two classics of traditional medicine edited by Zhang Zhongjing, a well-known Chinese physician during the Han Dynasty) (*9*). Currently, several traditional Chinese herbal formulas, such as Xiao-Chai-Hu-Tang (also called Sho-saiko-to in Japan), have been found to have a potentially beneficial effect for treating CHB (*10*). A brief outline of the antiviral pharmacology of the most commonly used traditional Chinese herbal formulas is presented below (Table 1).

2.1. *Xiao-Chai-Hu-Tang*

Xiao-Chai-Hu-Tang, a famous traditional Chinese herbal formula originally recorded in "Shang Han Lun", has been used to treat liver diseases especially chronic hepatitis for thousands of years in China and Japan. It consists of seven medicinal herbs (*Bupleurum falcatum*, *Scutellaria baicalensis*, *Panax ginseng*, *Zizyphus jujube*, *Pinellia ternate*, *Zingiber officinale*, and *Glycyrrhiza glabra*) (*11*). Much pharmacological research has shown that Xiao-Chai-Hu-Tang has potent anti-inflammation, anti-oxidation, immunomodulation, hepatoprotective, anti-hepatic fibrosis, and antitumor properties (*12-16*). Recently, a lot of basic or clinical studies have been conducted to assess the beneficial effects and safety of Xiao-Chai-Hu-Tang for CHB treatment. Chang *et al.* found that Xiao-Chai-Hu-Tang could inhibit the replication of HBV DNA and decrease the expression of HBeAg in HepG2 2.2.15 cells (*17*). Tajiri *et al.* found that Xiao-Chai-Hu-Tang could promote the clearance of HBeAg in children with chronic HBV infection (*18*). Qin *et al.* gave a systematic review of randomized trials on treatment of CHB using Xiao-Chai-Hu-Tang (*19*). Sixteen randomized trials (involving 1,601 CHB patients) were included in this review. The pooled results showed that Xiao-Chai-Hu-Tang combined with antiviral drugs (*e.g.*, lamivudine and IFN-α) was more effective in serum loss of hepatitis B viral markers and in improving liver function compared to antiviral drugs alone. Moreover, there were no adverse effects reported in the trials regarding Xiao-Chai-Hu-Tang.

2.2. *Xiao-Yao-San*

Xiao-Yao-San is a famous Chinese herbal formula originally recorded in "Tai Ping Hui Min He Ji Ju Fang" (a classical Chinese medicine book of the Song Dynasty). It is a mixture of eight crude herbs (*Bupleurum falcatum*, *Angelica sinensis*, *Paeonia lactiflora*, *Atractylodes lancea*, *Wolfiporia cocos*, *Zingiber officinale*, *Mentha arvensis*, and *Glycyrrhiza uralensis* (*20*). This herbal prescription is reported to possess hepatoprotective, anti-inflammation, anti-oxidation, anti-cancer, and immunomodulation activities, and is commonly used in the clinic to treat functional dyspepsia, postmenopausal women with

Table 1. Traditional Chinese herbal formulas commonly used with anti-HBV activities

Common name	Source	Composition	Biological activity	Evidence of anti-HBV activity	*Ref.*
Xiao-Chai-Hu-Tang	"Shang Han Lun" (the Eastern Han Dynasty (25-220 AD))	Includes 7 herbs: *Bupleurum falcatum*, *Scutellaria baicalensis*, *Panax ginseng*, *Zizyphus jujube*, *Pinellia ternate*, *Zingiber officinale*, *Glycyrrhiza glabra*	Hepatoprotective, anti-hepaticfibrosis, anti-inflammation, anti-oxidation, immunomodulation, anti-tumor	In HepG2 2.2.15 cells: inhibits HBV DNA replication and HBeAg secretion; In patients: (*i*) promotes the clearance of HBeAg; (*ii*) combined with antiviral drugs (*e.g.* lamivudine and IFN-α) exhibits more effectiveness in serum loss of HBV markers and in improving liver function	*11-19*
Xiao-Yao-San	"Tai Ping Hui Min He Ji Ju Fang" (the Song Dynasty (960-1279 AD))	Includes 8 herbs: *Bupleurum falcatum*, *Angelica sinensis*, *Paeonia lactiflora*, *Atractylodes lancea*, *Wolfiporia cocos*, *Zingiber officinale*, *Mentha arvensis*, *Glycyrrhiza uralensis*	Hepatoprotective, anti-inflammation, anti-oxidation, immunomodulation, anticancer	In patients: improves the negative conversion rates of HBV markers (HBeAg and HBV-DNA) and liver function	*20-23*
Long-Dan-Xie-Gan-Tang	"Tai Ping Hui Min He Ji Ju Fang" (the Song Dynasty (960-1279 AD))	Includes 10 herbs: *Gentiana scabra*, *Scutellaria baicalensis*, *Gardenia jasminoides*, *Alisma plantago*, *Plantago asiatica*, *Akebia trifoliate*, *Rhemannia glutinosa*, *Angelica sinensis*, *Bupleurum chinense*, *Glycyrrhiza uralensis*	Anti-inflammation, anti-oxidation, hepatoprotective, immunomodulation, anti-herpetic virus, anti-HBV	In CCl_4-induced hepatic injury rats: improves liver function; In patients: combined with IFN-α improves the negative conversion rates of HBeAg	*24-27*

climacteric symptoms, premenstrual dysphoric disorder, mood stabilizer swings, insomnia, depressive disorders, breast cancer, and so on (*21*). Recently, some studies have shown that Xiao-Yao-San has a potent effect on treating CHB. Xiao-Yao-San could improve the clinical symptoms (*e.g.*, weak, inappetence, and hepatalgia) of patients with CHB. Furthermore, the patients' liver function (ALT and AST) and liver fibrosis indexes, including hyaluronic acid (HA), laminin (LN), pro-collagen III peptide (P-III-P), and collagen type IV (IV-C), were improved significantly after treatment with Xiao-Yao-San (*22*). Furthermore, Xiao-Yao-San combined with adefovir dipivoxil could significantly improve the negative conversion rates of HBeAg and HBV-DNA in the treatment of CHB (*23*). Although Xiao-Yao-San has its unique advantages in treating CHB, a far larger body of literature only exists in Chinese language journals. It is reasonable to publish some well-designed, efficacy-based basic or clinical trials to evaluate the efficacy of Xiao-Yao-San in treating CHB in the future in Englishlanguage journals.

2.3. *Long-Dan-Xie-Gan-Tang*

Long-Dan-Xie-Gan-Tang is a famous Chinese herbal formula which also originally came from "Tai Ping Hui Min He Ji Ju Fang". It was recorded to have inhibitive effects on inflammatory diseases of the liver or gall bladder. There are ten medicinal herbs in Long-Dan-Xie-Gan-Tang including *Gentiana scabra*, *Scutellaria baicalensis*, *Gardenia jasminoides*, *Alisma plantago*, *Plantago asiatica*, *Akebia trifoliate*, *Rhemannia glutinosa*, *Angelica sinensis*, *Bupleurum chinense* and *Glycyrrhiza uralensis*. Recently, much pharmacological research has shown that Long-Dan-Xie-Gan-Tang has potent anti-inflammation, anti-oxidation, immune modulation, anti-herpetic virus, and anti-HBV properties (*24,25*). It is reported that Long-Dan-Xie-Gan-Tang is the most commonly prescribed Chinese herbal formula for subjects with CHB in Taiwan (*25*). It has a hepatoprotective effect on CCl4-induced hepatic injury in rats with the level of serum ALT and AST decreased significantly after treatment with Long-Dan-Xie-Gan-Tang (*26*). In addition, Long-Dan-Xie-Gan-Tang combined with IFN-α could significantly improve the negative conversion rates of HBeAg in the treatment of CHB (*27*).

3. Single Chinese herbs commonly used with anti-HBV activities

In 1982, Thyagarajan *et al.* confirmed *Phyllanthus niruri* with anti-HBV activity for the first time. Since then, the anti-HBV activity of single Chinese medicines has gradually got the attention of researchers. Many single Chinese medicines have been found to have potentially beneficial effects treating CHB. However, because the majority of herbs were administered in combination with other herbs in Chinese herbal formulas, it is not possible to determine exactly which

individual herbs in the formulas have the greatest therapeutic potential in the treatment of CHB. Thus, based upon our review of the related papers and upon our prior knowledge and experience, we have selected some herbs (Table 2) that seem effective and worthy of additional and in-depth study, and we will give them a brief commentary below. Especially these 5 herbs (*Phyllanthus niruri*, *Radix astragali*, *Polygonum cuspidatum*, *Rheum palmatum*, and *Salvia miltiorrhiza*) will be introduced in detail concerning their anti-HBV activities.

3.1. *Phyllanthus niruri*

Phyllanthus niruri (Ye Xia Zhu or Zhen Zhu Cao) is widely distributed in most tropical and subtropical countries of the globe (*e.g.*, China, South Asia, and America) and have long been used as traditional medicines to treat chronic liver disease, as well as a wide number of traditional ailments such as kidney disease, urinary bladder and intestinal infections, jaundice, gonorrhea, frequent menstruation, diabetes, skin ulcers, sores, swelling, and itchiness (*28-30*). It is reported to have many pharmacological effects including antiviral, antibacterial, antihepatotoxic, antihypertensive, and anticancer properties (*31,32*). Many active compounds, such as gallic acid, geraniin, quercetin glucoside, and quercetin rhamnoside, have been identified from *Phyllanthus niruri* (*32*). Since *Phyllanthus niruri* has been used to treat chronic liver disease for thousands of years, a lot of basic or clinical studies have been conducted recently to assess the beneficial effects and safety of *Phyllanthus niruri* for CHB treatment. Lam *et al.* showed that the ethanolic extract of *Phyllanthus niruri* exhibited potent antiviral activity against HBV (*33*). It produced a suppressive effect on HBsAg secretion, HBsAg mRNA expression, and HBV replication in vitro. Liu *et al.* conducted a systematic review of randomized trials on the treatment of CHB using *Phyllanthus niruri* (*34*). Twenty-two randomized trials (n = 1,947) were included in this review. The combined results showed that: (*i*) *Phyllanthus niruri* had a positive effect on clearance of serum HBsAg compared with placebo or no intervention; (*ii*) There was no significant difference on clearance of serum HBsAg, HBeAg and HBV DNA between *Phyllanthus niruri* and IFN; (*iii*) There was a better effect of *Phyllanthus niruri* plus IFN combination

Table 2. Single Chinese herbs commonly used with anti-HBV activities

Common name	Name in Chinese	Major active compounds	Biological activity	Evidence of anti-HBV activity	*Ref.*
Phyllanthus niruri	Ye Xia Zhu, Zhen Zhu Cao	Gallic acid, ellagic acid geraniin, quercetin glucoside, quercetin rhamnoside	Antiviral, antibacterial, antihepatotoxic, antihypertensive, anticancer	In HepG2 2.2.15 cells: inhibits HBsAg secretion, HBsAg mRNA expression, and HBV replication; In patients: combined with IFN exhibits more effectiveness on the clearance of serum HBsAg, HBeAg and HBV DNA	*33,34*
Radix astragali	Huang Qi	Astragaloside, calycosin-7-*O*-beta-D-glucoside, calycosin, formononetin	Immunomodulation, anticancer, anti-fatigue, antiviral	In patients: improves the negative conversion rates of HBeAg and HBV DNA	*35-37*
Polygonum cuspidatum	Hu Zhang	Resveratrol, polydatin	Antiviral, antimicrobial, hepatoprotective, neuroprotective, cardioprotective	In HepG2 2.2.15 cells: inhibits HBeAg secretion and HBV DNA replication	*8,38-40*
Rheum palmatum	Da Huang	Emodin, rhein, sennoside A, chrysophanol	Antiviral, antibacterial	In HepG2 2.2.15 cells: inhibits HBV DNA production and HBsAg secretion; In DHBV models: inhibits HBV DNA production	*38, 41-44*
Salvia miltiorrhiza	Dan Shen	Tanshinone, salvianic acid, protocatechuic aldehyde, cryptotanshinone	Antiviral, antibacterial, hepatoprotective cardioprotective, anti-thrombosis	In patients: improves the negative conversion rates of HBeAg and liver function	*46-48*
Curcuma longa	Jiang Huang	Curcumin, demethoxycurcumin, bisdemethoxycurcumin	Antiviral, anti-inflammation, anti-oxidation, anticancer	In HepG2.2.15 cells: suppresses the secretion of HBsAg, the production of HBV particles and the level of intracellular HBV RNAs	*35,49*
Glossogyne tenuifolia	Lu Jiao Cao	Luteolin-7-*O*-β-D-glucopyranoside, luteolin	Anti-inflammation, antiviral, antipyretic, hepatoprotective	In PLC/PRF/5 cells: inhibits HBsAg secretion	*50*
Arenaria kansuensis	Xue Ling Zhi	Arenarine, tricin, β-sitosterol-3β-D-glucopyranoside, isoscoparin	Antiviral, immunomodulation, hepatoprotective	In HepG2.2.15 cells: inhibits HBsAg and HBeAg secretion	*51*

on clearance of serum HBeAg and HBV DNA than IFN alone; (*iiii*) No serious adverse event was reported.

3.2. *Radix astragali*

Radix astragali (Huang Qi) has been used in China for thousands of years and is one of the most widely prescribed Chinese herbs in many formulas. The major active constituents of *Radix astragali* are saponins and flavonoids, such as astragaloside, calycosin-7-*O*-beta-D-glucoside, calycosin, and formononetin. It is traditionally considered to be a tonic that can improve the functioning of the lungs, adrenal glands, and the gastrointestinal tract, increase metabolism, promote healing, and reduce fatigue (*35*). Currently, some reports have indicated that *Radix astragali* possess many pharmacologic activities including immunomodulatory, anticancer, anti-fatigue, and antiviral activities (*35,36*). Moreover, it can balance serum hormone levels and improve liver function in patients with chronic viral hepatitis (*37*). A clinical evaluation of *Radix astragali* was performed in 208 patients with CHB (*37*). The treatment group (n = 116) was treated with the *Radix astragali* compound (containing *Radix astragali* and adjuvant components), and the control group (n = 92) was treated with regular drugs used for viral hepatitis. The results indicated that negative conversion rates of HBeAg and HBV DNA were significantly higher in the treatment group than in the control group.

3.3. *Polygonum cuspidatum*

Polygonum cuspidatum (Hu Zhang), as an herbaceous perennial plant, is widely distributed in the world and has been used as folk medicine in countries such as China, Japan and Korea for thousands of years. It is frequently prescribed by TCM practitioners for the treatment of hepatitis, cough, jaundice, amenorrhea, leucorrhoea, arthralgia, hyperlipidemia, scalding and bruises, snake bites, and carbuncles, *etc.* (*38*). The major active compounds isolated from this herb include resveratrol, polydatin, and anthraquinones (*e.g.*, emodin and its glycoside) (*39*). Recent pharmacological and clinical studies have indicated that *Polygonum cuspidatum* has antiviral (*e.g.*, HBV and HIV), antimicrobial, hepatoprotective, neuroprotective, and cardioprotective functions (*39,40*). It is also reported that *Polygonum cuspidatum* is widely used for treating CHB. Zhang *et al.* published a review to summarize and critically meta-analyze the results of randomized, controlled, clinical trials of TCM formulations reported from China in 1998-2008 for treatment of CHB. They found that *Polygonum cuspidatum* is ranked in the top five of individual herbs used most frequently in TCM formulations for CHB (*8*). Chang *et al.* found that the water extract of *Polygonum cuspidatum* at higher concentrations (30 μg/mL) could inhibit the expression of HBeAg. Furthermore, the ethanol extract of *Polygonum cuspidatum* could inhibit the production of HBV DNA dose-dependently with an effective minimal dosage (10 μg/mL) (*40*).

3.4. *Rheum palmatum*

Rheum palmatum (Da Huang) is an important Chinese medicinal herb with a long history of over 2,000 years and has been commonly used as an antibacterial or laxative agent in treating gastroenteritic and viral diseases (*38*). About 200 chemical compounds have been isolated or identified in *Rheum palmatum*, among which anthraquinone and its derivatives (*e.g.*, emodin, rhein, sennoside A, and chrysophanol) are considered as the main active ingredients (*41*). Recent pharmacological and clinical studies have indicated that *Rheum palmatum* and its active ingredients have showed activities against some viruses including vesicular stomatitis virus, herpes simplex virus types 1 and 2, parainfluenza, vaccinia virus, human cytomegalovirus and poliovirus (*42*). It is also reported that *Rheum palmatum* could inhibit HBV. Both the aqueous extract and ethanol extract of *Rheum palmatum* demonstrated inhibitory effects on HBV DNA production and HBsAg expression in HepG2.2.15 cells (*42,43*). Furthermore, in DHBV models, the aqueous extract of *Rheum palmatum* showed suppression of plasma HBV DNA levels and HBV DNA polymerase activity (*44*).

3.5. *Salvia miltiorrhiza*

Salvia miltiorrhiza (Dan Shen) was originally recorded in "Shen Nong Ben Cao Jing" (a classical Chinese herbal medicine book of the Dong-Han Dynasty). As a promoting blood circulation and removing blood stasis herb of the nontoxic superior class, it has been widely used for more than 2000 years to prevent and treat various human diseases, such as hepatitis, coronary artery disease, apoplexy, tumor growth and immunological disorders (*45*). Currently, there are numerous pharmaceutical dosage forms (*e.g.*, tablets, capsules, granules, injections, and oral liquids) of Chinese medicine preparations containing *Salvia miltiorrhiza*, such as Fufang Dan Shen tablet, Dan Shen injection, and Fufang Dan Shen dripping pills, which are commercially widely available for use in clinics in China (*38*). According to the pharmacological investigations, the major active constituents of *Salvia miltiorrhiza* can be divided into two groups: the water soluble phenolic acids such as, salvianic acid, protocatechuic aldehyde, rosemarinic acid and salvianolic acid B, and the lipophilic tanshinones such as, tanshinone I, dihydrotanshinone I, cryptotanshinone, tanshinone IIA, tanshinone IIB and hydroxtanshinone (*46*). According to pharmacological and clinical studies,

Salvia miltiorrhiza and its active constituents are not only used in coronary artery disease but also widely used for treating CHB. In a clinical evaluation, 30 patients with CHB were treated with *Salvia miltiorrhiza* (*47*). After 3 months of treatment, the negative conversion rate of HBeAg was 16.7%. A follow up of 3 and 9 months after the end of treatment showed the negative conversion rates of HBeAg were 22.7% and 25.0%, respectively. Ye *et al.* found that different dosages of *Salvia miltiorrhiza* injection (Dan Shen injection, 8 mL, 16 mL, and 24 mL) could improve the clinical symptoms and significantly reduce the level of ALT, total bilirubin (TBIL), and liver fibrosis indexes (pro-collagen type III (PC III), collagen type IV (IV-C) and hyaluronic acid (HA)) in hepatitis B cirrhosis patients. Furthermore, the large dosage (24 mL) of *Salvia miltiorrhiza* injection had the best effect treating the HBV-induced cirrhosis patients, particularly in patients with compensated cirrhosis (*48*).

3.6. *Others*

Except for the above 5 herbs, we will give a brief commentary on some other Chinese herbs commonly used for treating CHB. *Curcuma longa* (Jiang Huang), a rhizomatous herbaceous perennial plant of the ginger family, has been used for treating various liver diseases caused by HBV in Asia for many years with antiviral, anti-inflammation, and anti-oxidation activities (*35,49*). Kim *et al.* found that the aqueous extract of *Curcuma longa* could suppress the secretion of HBsAg, the production of HBV particles and the level of intracellular HBV RNAs in HepG2.2.15 cells (*49*). They also found that the anti-HBV activity of *Curcuma longa* was mediated through enhancing the cellular accumulation of p53 protein by trans-activating the transcription of the p53 gene as well as increasing the stability of p53 protein. *Glossogyne tenuifolia* (Lu Jiao Cao) is a special medicinal plant of the compositae family in the Pescadores Islands. It has been shown to exhibit good anti-inflammatory and antiviral activity, as a traditional antipyretic and hepatoprotective herb used in Chinese medicine. Wu *et al.* found that *Glossogyne tenuifolia* had potent anti-HBV effects on the human hepatocellular carcinoma cell line PLC/PRF/5 (*50*). *Glossogyne tenuifolia* exhibited a dose-dependent inhibition of the release of HBsAg by repressing the expression of HBsAg with an IC_{50} of 0.093 mg/mL. *Arenaria kansuensis* (Xue Ling Zhi) is from the highest elevation for flowering green plants in the world. It belongs to the family Caryophyllaceae and is mainly located in the Qinghai-Tibet Plateau near the permanent snowline around 4,700 to 5,500 meters above sea level. *Arenaria kansuensis* has been shown to exhibit good antiviral and immunomodulation activity. Tang *et al.* found that both the ethanol extract and aqueous extract of *Arenaria kansuensis* could inhibit the release of HBsAg and HBeAg in HepG2.2.15 cells (*51*). Moreover, the aqueous extract of *Arenaria kansuensis* exhibited more obvious anti-HBV activity with lower toxicity than that of the ethanol extract. The maximum inhibition rates of the aqueous extract of *Arenaria kansuensis* on the levels of HBsAg and HBeAg at 96 h were 52.5% and 72.8%, respectively.

4. The active compounds of Chinese medicines commonly used with anti-HBV activities

Although Chinese medicines play an important role in drug discovery and human health, the actual value of them has not been fully recognized worldwide due to their complex components and uncontrollable quality. In recent years, with the developing modernization of TCM and continuing emergence of new theories, methods and techniques, very rapid and significant development has been achieved in the pharmacology of TCM. Many active compounds of Chinese medicines have been found and their activities have been studied. Some active compounds isolated from Chinese herbal medicines have been reported to possess anti-HBV activities. Zuo *et al.* gave a summary of the active compounds of Chinese herbal medicines with anti-HBV activities (*52*). They reported that these anti-HBV active compounds mainly included alkaloids, flavonoids, terpenoids, glycosides, lignans, plant polyphenols, saccharides, and so on. Based upon our review of the related papers, we have selected some active compounds of Chinese herbal medicines with anti-HBV activities (Table 3) that seem effective and worthy of additional and in-depth study in treating CHB, and we will give them a brief commentary below.

4.1. *Alkaloids*

Alkaloids are a group of naturally occurring chemical compounds that contain mostly basic nitrogen atoms, which can be isolated from many Chinese herbal medicines. Matrine, oxymatrine, sophoridine and sophocarpine are the major bioactive alkaloids extracted from Chinese herbal medicine *Sophora flavescens* (Ku Shen) (*28*). Ye *et al.* found that the aqueous extract of *Sophora flavescens* possessed anti-DHBV activity (*53*). Furthermore, they found the above four alkaloids (matrine, oxymatrine, sophoridine and sophocarpine) were identified in the duck serum, of which oxymatrine, sophoranol and matrine were the effective substances for anti-HBV activity in aqueous extracts of *Sophora flavescens*. Ma *et al.* investigated the anti-HBV activity of the combination of 3TC and either oxymatrine or matrine on HepG2 2.2.15 cells (*54*). They found that the combination of 3TC (30 μg/mL) with oxymatrine (100 μg/mL) or matrine (100 μg/mL) showed significant inhibitory effects on the secretion of HBsAg, HBeAg, and HBV-DNA into culture media, that were higher

Table 3. Typical active compounds of Chinese medicines commonly used with anti-HBV activities

Category	Typical compounds	Source	Biological activity	Evidence of anti-HBV activity	*Ref.*
Alkaloids	Oxymatrine	*Sophora flavescens* (Ku Shen)	Antiviral, antifibrotic, hepatoprotective, immunomodulation	In HepG2.2.15 cells: inhibits the secretion of HBsAg, HBeAg, and HBV-DNA; In patients: combined with lamivudine exhibits higher HBeAg/anti-HBe seroconversion rate	*28,53-58*
Flavonoids	Wogonin	*Scutellaria baicalensis* (Huang Qin)	Antiviral, hepatoprotective	In MS-G2 cells: suppresses HBsAg secretion and HBV DNA production; In HepG2.2.15 cells: inhibits the secretion of HBsAg, HBeAg, and HBV-DNA; In DHBV models: inhibits DHBV DNA polymerase; In human HBV-transgenic mice: inhibits plasma HBsAg levels	*28,60,61*
	Ellagic acid	*Phyllanthus niruri* (Ye Xia Zhu, Zhen Zhu Cao)	Antiviral, immunomodulation	In HepG2 2.2.15 cells: inhibits HBeAg secretion; In HBeAg-producing transgenic mice: blocks immune tolerance caused by HBeAg	*62,63*
Terpenoids	Artesunate	*Artemisia annua* (Qing Hao)	Antiviral, antimalarial, antipyretic, anti-inflammation	In HepG2 2.2.15 cells: (*i*) inhibits HBsAg secretion and HBV DNA production; (*ii*) exhibits a synergic anti-HBV effect combined with lamivudine	*66,67*
Glycoside	Saikosaponin c	*Bupleuri radix* (Chai Hu)	Anti-hepatitis, anti-nephritis, antihepatoma, anti-inflammation, immunomodulation, antibacterial	In HepG2 2.2.15 cells: inhibits HBsAg secretion and HBV DNA production	*68*
	Astragaloside IV	*Radix astragali* (Huang Qi)	Antiviral, anti-oxidation, anti-inflammation, anti-cancer, immunomodulation, regulation of the calcium balance	In HepG2 2.2.15 cells: suppresses the secretion of HBsAg and HBeAg; In DHBV models: reduces serum DHBV DNA levels	*36,41, 69*

than or equivalent to the use of 3TC alone at 100 μg/mL. Chen *et al.* conducted a study to investigate the effect of lamivudine, IFN-α and the combination of lamivudine and oxymatrine on surviving hepatic failure patients with HBV infection (*55*). They found that the HBeAg/anti-HBe seroconversion rate in patients treated with the combination of lamivudine and oxymatrine was lower than that in patients treated with IFN-α, but was higher than that in patients treated with lamivudine alone. Moreover, lamivudine or lamivudine in combination with oxymatrine significantly inhibited the intrahepatic inflammatory activities of subacute or acute-on-chronic hepatic failure survivals. Li *et al.* prepared liposome-encapsulated matrine and studied its anti-HBV effect on HepG2 2.2.15 cells and DHBV models (*56*). They found that liposome-encapsulated matrine could evidently inhibit the replication of hepatitis B virus *in vitro* and *in vivo*, and its anti-HBV effect was better than that of matrine. Nie *et al.* conducted a series of studies to investigate the anti-HBV activities of sophoridine and sophocarpine in HepG2 2.2.15 cells (*57,58*). The results showed that sophoridine could significantly inhibit the secretion of HBsAg, HBeAg, and pre-antigen S1. When the HepG2 2.2.15 cells were treated with 0.001 μmmol/L sophoridine for 9 days, the inhibition rate of the secretion of pre-antigen S1 was 62.20%. Furthermore, they made a comparison between sophocarpine and lamivudine on inhibiting the secretion of HBeAg. The results showed that the inhibition rate of the secretion of HBeAg in the sophocarpine group was higher than that in the lamivudine group. In summary, these alkaloids are much cheaper than INF-α for the treatment of CHB, which makes them attractive therapeutic options and warrants further clinical and basic trials. Moreover, if some other alkaloids possess anti-HBV activity they need further study.

4.2. *Flavonoids*

Flavonoids are a group of plant secondary metabolites with variable phenolic structures and can be found in many Chinese herbal medicines. They are usually divided into seven classes including flavonols, flavones, flavanones, flavononol, flavanols, isoflavones, and anthocyanidins. Some of these flavonoids have been reported to have activities in treatment of various diseases such as heart disease, cancer, and virus infection (*e.g.*, HBV and HCV) as well as potential protective activity against artificially induced-liver damage (*59*).

Wogonin is a flavone derived from the Chinese herbal medicine *Scutellaria baicalensis* (Huang Qin), which has been widely used for treatment of inflammatory and liver diseases for thousands of years in Asia (*28*). In recent years, wogonin has been found to have anti-HBV activity. Huang *et al.* found that

wogonin could suppress HBsAg secretion and HBV DNA production in a HBV transfected liver cell line (MS-G2) without cytotoxicity (*60*). Guo *et al.* found that wogonin effectively suppressed the secretion of HBsAg and HBeAg with an IC_{50} (drug concentration inducing 50% inhibition in HBsAg or HBeAg or HBV DNA release) of 4 μg/mL and reduced HBV DNA levels in a dose-dependent manner in HepG2.2.15 cells (*61*). They also found that in DHBV-infected ducks wogonin dramatically inhibited DHBV DNA polymerase with an IC50 of 0.57 μg/mL, and significantly improved duck liver function in histopathological evaluations. In addition, wogonin significantly reduced plasma HBsAg levels in human HBV-transgenic mice.

Ellagic acid, a flavonoid isolated from Phyllanthus niruri, exhibited a unique anti-HBV function in a HBV infected cell line and in HBeAg transgenic mice. It has been found to effectively block HBeAg secretion in HepG2 2.2.15 cells with an IC50 of 0.07 μg/mL, but does not have any effects on HBV polymerase activity, HBV replication or blockage of HBsAg secretion (*62*). Furthermore, since HBeAg is involved in immune tolerance during HBV infection, ellagic acid might be a new candidate therapeutic against immune tolerance in HBV-infected individuals. It could effectively block the immune tolerance caused by HBeAg in HBeAg-producing transgenic mice (*63*).

Oenanthe javanica or water dropwort (Xi Qin), mainly cultivated in east Asian countries such as China, Korea and Japan, is not only consumed as a spicy vegetable with good amounts of vitamins and great taste, but also as a Chinese herbal medicine widely used in treatment of various diseases including, jaundice, hypertension, polydipsia, and CHB (*64*). Wang *et al.* conducted a study to investigate the antiviral effect of *Oenanthe javanica* flavones on the human hepatoma HepG2.2.15 culture system and DHBV infection (*65*). They reported that *Oenanthe javanica* flavones comprised approximately 2.2% of the whole plant content and were one of the main active ingredients against HBV. *Oenanthe javanica* flavones significantly inhibited HBsAg and HBeAg secretion in HepG2.2.15 cells after 9 days of treatment. Moreover, DHBV-DNA levels decreased significantly after treatment with 0.50 and 1.00 g/kg of Oenanthe javanica flavones in the DHBV model. However, it is worthy of further study to find which *Oenanthe javanica* flavones possess the highest anti-HBV activity.

4.3. *Terpenoids*

Terpenoids are the largest and most widespread class of secondary metabolites. They can be found in all classes of living things especially in Chinese herbal medicines. Terpenoids are a rich reservoir of candidate compounds for drug discovery and they are under investigation for antibacterial, anti-neoplastic, antiviral and other pharmaceutical functions. Recently, some of these terpenoids have been reported to have anti-HBV activities.

Artemisia annua (Qing Hao) has been used as a Chinese herbal medicine to treat fever and malaria in China for thousands of years. Artemisinin is a family of sesquiterpene trioxane lactones derived from *Artemisia annua* and it has been identified as the best medicine with the highest efficiency, the most effective and the lowest toxicity in treating ague, which represents one of the great events in medicine in the latter third of the 20th Century (*66*). In recent years, artemisinin and its derivative artesunate has been reported to have an antiviral effect against HBV. Both artemisinin and artesunate inhibit HBsAg secretion and HBV DNA production in HepG2 2.2.15 cells at concentrations at which host cell viability was not affected, and artesunate had better anti-HBV effects than artemisinin. Artesunate inhibited HBsAg secretion with an IC_{50} of 2.3 μmol/L and reduced the HBV DNA level with an IC_{50} of 0.5 μmol/L. In addition, although the anti-HBV effect of artesunate was not as good as lamivudine which inhibited HBsAg secretion with an IC_{50} of 0.2 μmol/L and reduced the HBV DNA level with an IC_{50} of 0.3 μmol/L, and by combining both agents, a synergic anti-HBV effect could be observed (*67*). This warrants further evaluation of artemisinin and artesunate as antiviral agents against HBV infection.

4.4. *Glycoside*

Glycosides are the major active ingredients isolated from Chinese herbal medicines. They are rich with candidate compounds for drug discovery and possess many pharmaceutical functions including antibacterial, anti-neoplastic, antiviral, and so on. Recently, some of the glycosides have been reported to have anti-HBV activities.

Bupleuri Radix (Chai Hu) is one of the most important traditional Chinese crude drugs for treating hepatitis, malaria and intermittent fever. Saikosaponins, the main active constituents of *Bupleuri Radix*, have been shown to possess various biological activities, specifically anti-hepatitis, anti-nephritis, antihepatoma, anti-inflammation, immunomodulation, and antibacterial effects. Chiang *et al.* conducted a study to evaluate the cytotoxicity and anti-HBV activities of saikosaponins a, c and d. The results showed that, compared with saikosaponins a and d, saikosaponin c showed a significant effect on inhibiting HBsAg secretion and HBV DNA production without cytotoxicity in HepG2 2.2.15 cells (*68*).

Astragaloside IV, a cycloartane-type triterpene glycoside, is one of the major active constituents of *Radix astragali*. It is used as a marker compound for quality control of *Radix astragali* in the Chinese Pharmacopoeia (2005 version), and has various

pharmacological activities including antiviral, anti-oxidation, anti-inflammation, anti-cancer, immunomodulation, regulation of the calcium balance, and so on (*69*). Wang *et al.* conducted a study to investigate the anti-HBV activities of astragaloside IV in HepG2 2.2.15 cells and DHBV-infected ducklings (36). The results showed that astragaloside IV effectively suppressed the secretion of HBV antigens with inhibition rates of 23.6% for HBsAg and 22.9% for HBeAg at100 μg/mL after 9 days of treatment in HepG2 2.2.15 cells. The inhibitory activity of astragaloside IV on the secretion of HBV antigens is more potent than that of 3TC without significant cytotoxicity. Furthermore, in DHBV-infected ducklings, astragaloside IV caused 64.0% inhibition at 120 mg/kg on serum DHBVs after 10 days of treatment and also reduced serum DHBV DNA levels. In summary, these results demonstrated that astragaloside IV possessed potent anti-HBV activity.

In addition, the compound chrysophanol 8-*O*-beta-D-glucoside isolated from *Rheum palmatum* was found to display strong anti-HBV activity. Li *et al.* isolated six anthraquinones from the ethanol extract of *Rheum palmatum* by using reverse phase-high performance liquid chromatography (RP-HPLC) and evaluated their anti-HBV activities (*41*). The results showed that five free anthraquinones showed weak or slightly inhibitory activities against HBV, and the only combined anthraquinone chrysophanol 8-*O*-beta-D-glucoside exhibited significant activity against HBV DNA production with an IC_{50} of 36.98 μg/mL and antigens expression with an IC_{50} value of 237.4 μg/mL for HBsAg and 183.41 μg/mL for HBeAg. Furthermore, they observed that chrysophanol 8-*O*-beta-D-glucoside is a potential inhibitor of HBV-DNA polymerase. Therefore, they concluded that the combined anthraquinone chrysophanol 8-*O*-beta-D-glucoside was the major active compound in the ethanol extract of *Rheum palmatum* and could be a promising candidate for the development of new anti-HBV drugs in the treatment of HBV infection.

5. The Chinese medicine preparations commonly used with anti-HBV activities

Chinese medicine preparations are a form of Chinese medicines that are isolated from single herbs or traditional herbal formulas and that are prepared using modern advanced pharmaceutical technology. There are various dosage forms including injections, tablets, pills, capsules, and liquids. Compared to traditional decoctions, Chinese medicine preparations are safer, more effective, and easier to use. Thus, Chinese medicine preparations are becoming increasingly popular in China and are attracting worldwide attention. Based upon our review of the related papers, we have selected some Chinese medicine preparations with anti-HBV activities (Table 4) which have been approved by the State Food and Drug Administration (FDA) of China and seem effective and worthy of additional and in-depth study, and we will give them a brief commentary below.

5.1. *Silymarin and Silibinin*

Silybum marianum or milk thistle (Shui Fei Ji), a member of the Asteraceae family, is one of the most ancient and extensively used medicinal plants for its beneficial effects on liver and other organs (*38*). Silymarin is a standardized extract from the fruits and seeds of *Silybum marianum* and it is composed of a mixture of several flavonolignans, with the most important being silibinin, isosilibinin, dehydroisosilibinin, silidianin and silichristin. Some studies demonstrate that silymarin possesses powerful antioxidant and hepatoprotective activities. It has beneficial effects on various hepatic disorders, including cirrhosis, fatty liver hepatitis, viral hepatitis, and so on (*70*). Recently, some Chinese medicine preparations containing silymarin (*e.g.*, Silymarin tablet and Silibinin capsule) have been approved for the treatment of hepatic diseases such as CHB in China. Xie *et al.* conducted a study to evaluate

Table 4. Chinese medicine preparations commonly used with anti-HBV activities

Common name	Source	Dosage form	Biological activity	Evidence of anti-HBV activity	*Ref.*
Silymarin	*Silybum marianum* (Shui Fei Ji)	Tablet, capsule	Antioxidant, hepatoprotective, antiviral	In patients: improves liver function	*70,71*
Silibinin	*Silybum marianum* or milk thistle (Shui Fei Ji)	Tablet, capsule	Antioxidant, hepatoprotective, antiviral	In patients: prevents liver necrosis and repairs liver cells	*70,72*
Kushenin	*Sophora flavescens* (Ku Shen)	Injection, tablet, capsule	Antiviral, anti-fibrosis, anti-arrhythmia, anti-inflammation, antibacterial, immunomodulation, enhancing leukocytes	In patients: improves the level of ALT, the negative rate of HBV DNA and HBeAg, and the positive rate of HBeAb	*73,74*
Cinobufacini	*Bufo bufo gargarizans* Cantor	Injection, tablet, oral solution, capsule	Antiviral, anticancer	In HepG2 2.2.15 cells: inhibits the secretion of HBsAg, HBeAg, and HBcrAg; In patients: improves the level of ALT and the negative conversion rates of HBV DNA and HBeAg combined with IFN-α 2b	*75,78,79*

the efficacy of Silymarin tablets on patients with CHB (*71*). After treatment for 12-weeks, ALT and AST levels decreased significantly in the Silymarin tablet group compared to the control group, which indicated that Silymarin tablets might be an effective agent for CHB treatment. Guo *et al.* conducted a study to observe the effect of Silibinin capsules on patients with CHB (*72*). The results showed that the total effective rate and symptom normalization of the Silibinin capsule group improved significantly compared to the control group with ALT, AST and TBIL levels decreased significantly after treatment for three months. These indicated that Silibinin capsules could effectively prevent necrosis of liver cells and repair liver cells in CHB treatment.

5.2. *Kushenin*

Kushenin is a mixed alkaloid of oxymatrine with a little oxysophocarpine, extracted from the root of Chinese herbal medicine *Sophora flavescens*. It has various pharmacological activities including antiviral, anti-fibrosis, anti-arrhythmia anti-inflammation, antibacterial, immunomodulation, enhanced leukocytes, and so on (*73*). Nowadays, many dosage forms containing kushenin, such as injection, tablets, and capsules, have been prepared and approved for treatment of CHB. Yu *et al*. conducted a study to investigate the effect of kushenin on patients with CHB (*74*). In this study, 196 patients were randomly divided into four groups (kushenin group, kushenin + arabinofuranosyl adenine monophosphate (Ara-AMP) group, IFN-α 1b group, and glucose group), and the levels of ALT, AST and viral markers were observed. After treatment for 30 days, the improvement on the level of ALT, the negative rate of HBV DNA and HBeAg, and the positive rate of HBeAb were similar in the kushenin group, kushenin + Ara-AMP group, and IFN-α 1b group, which were better than that of glucose group ($P < 0.05$). After 12 months follow up, the total effective rates were 40.8%, 60.8% and 43.1% in the kushenin group, kushenin + Ara-AMP group, and IFN-α 1b group, respectively. These indicated kushenin might havea better long term efficacy for treating CHB.

5.3. *Cinobufacini*

Cinobufacini (Huachansu), an aqueous extract from the skin and parotid venom glands of the toad (*Bufo bufo gargarizans* Cantor) that contains Chansu which has been widely used in China as an anodyne, cardiotonic, antimicrobial, local anesthetic, and antineoplastic agent for thousands of years (*35,75*). Pharmacological studies demonstrate that the major active constituents of cinobufacini are bufodienolides (which primarily include bufalin, cinobufagin, resibufogenin, bufotalin, and Lumichrome), biogenic amines, alkaloids, peptides, and proteins (*75*). Recently, many dosage forms containing cinobufacini, such as injection, tablets, oral solution, and capsules, have been prepared and approved by the Chinese State Food and Drug Administration (SFDA) (ISO9002) and widely used in clinical cancer and CHB therapy in China (*76*). Our research team has committed to the anti-cancer and anti-HBV activities of cinobufacini for several years. We found that cinobufacini and its active compounds (bufalin and cinobufagin) could induce human hepatocellular carcinoma (HCC) cells apoptosis *via* Fas- and mitochondria-mediated pathways (*75,77*). We also found that after treatment for 6 days in HepG2 2.2.15 cells, cinobufacini at 1 μg/mL effectively inhibited the secretion of HBsAg, HBeAg, and HBcrAg by 29.58, 32.87, and 42.52%, respectively, which was more potent than lamivudine (100 g/mL) (*78*). Furthermore, some clinical studies have indicated that cinobufacini used alone or in combination with other anti-HBV agents (*e.g.*, IFN-α and lamivudine) possesses a significant effect on patients with CHB. Yu *et al.* conducted a study to observe the efficacy of the combination of cinobufacini and IFN-α 2b on patients with CHB (*79*). In this study, 142 patients were randomly divided into two groups (cinobufacini + IFN-α 2b group and IFN-α 2b group). After treatment for 48 weeks, the level of ALT and the negative conversion rates of HBV DNA and HBeAg were improved significantly in the cinobufacini + IFN-α 2b group compared to the IFN-α 2b group ($P < 0.05$). These findings indicated that IFN-α combined with cinobufacini could effectively improve liver function and inhibit HBV DNA replication.

6. Conclusion

Given the significant public health hazard of CHB and the high rates of non-response to interferon and nucleoside antiviral agents, continuous development of agents to treat HBV infections is urgently needed. Over a long period in clinical practice and with progress in basic research, especially advanced and interdisciplinary technology and methodology, the effectiveness and beneficial contribution of Chinese herbal medicines on CHB have been gradually discovered and confirmed, which will provide evidence for development of novel antiviral drugs. Based upon our review of the related papers and upon our prior knowledge and experience, we have selected some Chinese herbal medicines (including Chinese herbal formulas, single herbs and related active compounds, and Chinese medicine preparations) that seem effective and worthy of additional and in-depth study in treating CHB, and we have given them a brief review. According to basic and clinical studies, we conclude that these Chinese herbal medicines exhibit significant anti-HBV activities which improve liver function, and enhance HBeAg and HBsAg sero-conversion rates as well as HBV

DNA clearance rates in HepG2 2.2.15 cells, DHBV models, and patients with CHB. We hope this review will contribute to an understanding of Chinese herbal medicines as an effective treatment for CHB and provide useful information for the development of more effective antiviral drugs. However, more information is needed regarding anti-HBV Chinese herbal medicines, including preparation, standardization, identification of active ingredients, and toxicological evaluation. Moreover, further investigation in well-designed trials with a better understanding of mechanisms, therapeutic effects, and the safety profile, will be helpful for developing effective anti-HBV Chinese medicines.

Acknowledgements

This project was supported by Grants-in-Aid from the Ministry of Education, Science, Sports, and Culture of Japan.

References

1. Song PP, Feng XB, Zhang KM, Song TQ, Ma KS, Kokudo N, Dong JH, Yao LN, Tang W. Screening for and surveillance of high-risk patients with HBV-related chronic liver disease: Promoting the early detection of hepatocellular carcinoma in China. Biosci Trends. 2013; 7:1-6.
2. Zhang CY, Zhong YS, Guo LP. Strategies to prevent hepatitis B virus infection in China: Immunization, screening, and standard medical practices. Biosci Trends. 2013; 7:7-12.
3. Chu D, Yang JD, Lok AS, Tran T, Martins EB, Fagan E, Rousseau F, Kim WR. Hepatitis B screening and vaccination practices in asian american primary care. Gut Liver. 2013; 7:450-457.
4. Papatheodoridis GV, Manolakopoulos S, Dusheiko G, Archimandritis AJ. Therapeutic strategies in the management of patients with chronic hepatitis B virus infection. Lancet Infect Dis. 2008; 8:167-178.
5. Lau DT, Bleibel W. Current status of antiviral therapy for hepatitis B. Therap Adv Gastroenterol. 2008; 1:61-75.
6. Dobos GJ, Tan L, Cohen MH, McIntyre M, Bauer R, Li X, Bensoussan A. Are national quality standards for traditional Chinese herbal medicine sufficient? Current governmental regulations for traditional Chinese herbal medicine in certain Western countries and China as the Eastern origin country. Complement Ther Med. 2005; 13:183-190.
7. McCulloch M, Broffman M, Gao J, Colford JM Jr. Chinese herbal medicine and interferon in the treatment of chronic hepatitis B: A meta-analysis of randomized, controlled trials. Am J Public Health. 2002; 92:1619-1628.
8. Zhang L, Wang G, Hou W, Li P, Dulin A, Bonkovsky HL. Contemporary clinical research of traditional Chinese medicines for chronic hepatitis B in China: An analytical review. Hepatology. 2010; 51:690-698.
9. Yu F, Takahashi T, Moriya J, Kawaura K, Yamakawa J, Kusaka K, Itoh T, Morimoto S, Yamaguchi N, Kanda T. Traditional Chinese medicine and Kampo: A review from the distant past for the future. J Int Med Res. 2006; 34:231-239.
10. Chen FP, Kung YY, Chen YC, Jong MS, Chen TJ, Chen FJ, Hwang SJ. Frequency and pattern of Chinese herbal medicine prescriptions for chronic hepatitis in Taiwan. J Ethnopharmacol. 2008; 117:84-91.
11. Zheng N, Dai J, Cao H, Sun S, Fang J, Li Q, Su S, Zhang Y, Qiu M, Huang S. Current understanding on antihepatocarcinoma effects of xiao chai hu tang and its constituents. Evid Based Complement Alternat Med. 2013; 2013:529458.
12. Kusunose M, Qiu B, Cui T, Hamada A, Yoshioka S, Ono M, Miyamura M, Kyotani S, Nishioka Y. Effect of Sho-saiko-to extract on hepatic inflammation and fibrosis in dimethylnitrosamine induced liver injury rats. Biol Pharm Bull. 2002; 25:1417-1421.
13. Shiota G, Maeta Y, Mukoyama T, Yanagidani A, Udagawa A, Oyama K, Yashima K, Kishimoto Y, Nakai Y, Miura T, Ito H, Murawaki Y, Kawasaki H. Effects of Sho-Saiko-to on hepatocarcinogenesis and 8-hydroxy-2'-deoxyguanosine formation. Hepatology. 2002; 35:1125-1133.
14. Huang XX, Yamashiki M, Nakatani K, Nobori T, Mase A. Semi-quantitative analysis of cytokine mRNA expression induced by the herbal medicine Sho-saiko-to (TJ-9) using a Gel Doc system. J Clin Lab Anal. 2001; 15:199-209.
15. Taira Z, Yabe K, Hamaguchi Y, Hirayama K, Kishimoto M, Ishida S, Ueda Y. Effects of Sho-saiko-to extract and its components, baicalin, baicalein, glycyrrhizin and glycyrrhetic acid, on pharmacokinetic behavior of salicylamide in carbon tetrachloride intoxicated rats. Food Chem Toxicol. 2004; 42:803-807.
16. Chen MH, Chen JC, Tsai CC, Wang WC, Chang DC, Lin CC, Hsieh HY. Sho-saiko-to prevents liver fibrosis induced by bile duct ligation in rats. Am J Chin Med. 2004; 32:195-207.
17. Chang JS, Wang KC, Liu HW, Chen MC, Chiang LC, Lin CC. Sho-saiko-to (Xiao-Chai-Hu-Tang) and crude saikosaponins inhibit hepatitis B virus in a stable HBV-producing cell line. Am J Chin Med. 2007; 35:341-351.
18. Tajiri H, Kozaiwa K, Ozaki Y, Miki K, Shimuzu K, Okada S. Effect of sho-saiko-to(xiao-chai-hu-tang) on HBeAg clearance in children with chronic hepatitis B virus infection and with sustained liver disease. Am J Chin Med. 1991; 19:121-129.
19. Qin XK, Li P, Han M, Liu JP. Xiaochaihu Tang for treatment of chronic hepatitis B: A systematic review of randomized trials. Zhong Xi Yi Jie He Xue Bao. 2010; 8:312-320. (in Chinese)
20. Zhang Y, Han M, Liu Z, Wang J, He Q, Liu J. Chinese herbal formula xiao yao san for treatment of depression: A systematic review of randomized controlled trials. Evid Based Complement Alternat Med. 2012; 2012:931636.
21. Yin SH, Wang CC, Cheng TJ, Chang CY, Lin KC, Kan WC, Wang HY, Kao WM, Kuo YL, Chen JC, Li SL, Cheng CH, Chuu JJ. Room-temperature super-extraction system (RTSES) optimizes the anxiolytic- and antidepressant-like behavioural effects of traditional Xiao-Yao-San in mice. Chin Med. 2012; 7:24.
22. Zhan BL, Chen L, Xu SM. The analysis of clinical therapeutic effect on chronic hepatitis B treated with modified Xiao-Yao-San. Journal of practical traditional Chinese medicine. 2013; 29:333-334. (in Chinese)
23. Zhang J. Clinical effect of Xiaoyao Pill auxiliary adefovir dipivoxil on patients with chronic hepatitis B. Practical pharmacy and clinical remedies. 2013; 16:215-217. (in Chinese)

24. Jin Y. A combined use of acupuncture, moxibustion and long dan xie gan tang for treatment of 36 cases of chronic pelvic inflammation. J Tradit Chin Med. 2004; 24:256-258.
25. Chen FP, Kung YY, Chen YC, Jong MS, Chen TJ, Chen FJ, Hwang SJ. Frequency and pattern of Chinese herbal medicine prescriptions for chronic hepatitis in Taiwan. J Ethnopharmacol. 2008; 117:84-91.
26. Shi H, Zhou Y, Zhang FH, Zhang JP, Li JY, Wu MF, Xu HZ, Li Q. Influence of Long-Dan-Xie-Gan-Tang on the liver transfer function in rats treated by CCl_4. Liao Ning Zhong Yi Za Zhi. 2006; 33:1041-1042. (in Chinese)
27. Zhang YX, Li HG, Su YH. The clinical observation about Long-Dan-Xie-Gan-Tang combined with IFN-α for the treatment of chronic hepatitis B. Zhong Yuan Yi Kan. 1997; 24:30-31. (in Chinese)
28. Cui X, Wang Y, Kokudo N, Fang D, Tang W. Traditional Chinese medicine and related active compounds against hepatitis B virus infection. Biosci Trends. 2010; 4:39-47.
29. Amin ZA, Alshawsh MA, Kassim M, Ali HM, Abdulla MA. Gene expression profiling reveals underlying molecular mechanism of hepatoprotective effect of *Phyllanthus niruri* on thioacetamide-induced hepatotoxicity in Sprague Dawley rats. BMC Complement Altern Med. 2013; 13:160.
30. Naik AD, Juvekar AR. Effects of alkaloidal extract of *Phyllanthus niruri* on HIV replication. Indian J Med Sci. 2003; 57:387-393.
31. Lee SH, Jaganath IB, Manikam R, Sekaran SD. Inhibition of Raf-MEK-ERK and hypoxia pathways by Phyllanthus prevents metastasis in human lung (A549) cancer cell line. BMC Complement Altern Med. 2013; 13:271.
32. Bagalkotkar G, Sagineedu SR, Saad MS, Stanslas J. Phytochemicals from *Phyllanthus niruri* Linn. and their pharmacological properties: A review. J Pharm Pharmacol. 2006; 58:1559-1570.
33. Lam WY, Leung KT, Law PT, Lee SM, Chan HL, Fung KP, Ooi VE, Waye MM. Antiviral effect of *Phyllanthus nanus* ethanolic extract against hepatitis B virus (HBV) by expression microarray analysis. J Cell Biochem. 2006; 97:795-812.
34. Liu J, Lin H, McIntosh H. Genus *Phyllanthus* for chronic hepatitis B virus infection: A systematic review. J Viral Hepat. 2001; 8:358-366.
35. Qi F, Li A, Inagaki Y, Gao J, Li J, Kokudo N, Li XK, Tang W. Chinese herbal medicines as adjuvant treatment during chemo- or radio-therapy for cancer. Biosci Trends. 2010; 4:297-307.
36. Wang S, Li J, Huang H, Gao W, Zhuang C, Li B, Zhou P, Kong D. Anti-hepatitis B virus activities of astragaloside IV isolated from *Radix astragali*. Biol Pharm Bull. 2009; 32:132-135.
37. Tang LL, Sheng JF, Xu CH, Liu KZ. Clinical and experimental effectiveness of Astragali compound in the treatment of chronic viral hepatitis B. J Int Med Res. 2009; 37:662-667.
38. The State Pharmacopoeia Commission of the People's Republic of China. Pharmacopoeia of the People's Republic of China 2010. China Medical Science and Technology Press, Beijing, China, 2010.
39. Zhang H, Li C, Kwok ST, Zhang QW, Chan SW. A Review of the pharmacological effects of the dried root of *Polygonum cuspidatum* (Hu Zhang) and its constituents. Evid Based Complement Alternat Med. 2013; 2013:208349.
40. Chang JS, Liu HW, Wang KC, Chen MC, Chiang LC, Hua YC, Lin CC. Ethanol extract of *Polygonum cuspidatum* inhibits hepatitis B virus in a stable HBV-producing cell line. Antiviral Res. 2005; 66:29-34.
41. Li Z, Li LJ, Sun Y, Li J. Identification of natural compounds with anti-hepatitis B virus activity from *Rheum palmatum* L. ethanol extract. Chemotherapy. 2007; 53:320-326.
42. Sun Y, Li LJ, Li J, Li Z. Inhibition of hepatitis B virus replication by *Rheum palmatum* L. ethanol extract in a stable HBV-producing cell line. Virol Sin. 2007; 22:14-20.
43. Kim TG, Kang SY, Jung KK, Kang JH, Lee E, Han HM, Kim SH. Antiviral activities of extracts isolated from *Terminalis chebula* Retz., *Sanguisorba officinalis* L., *Rubus coreanus* Miq. and *Rheum palmatum* L. against hepatitis B virus. Phytother Res. 2001; 15:718-720.
44. Chung TH, Kim JC, Lee CY, Moon MK, Chae SC,Lee IS, Kim SH, Hahn KS, Lee IP. Potential antiviral effects of *Sanguisorba officinalis*, *Terminalis chebula*, *Rubusanus migua*, and *Rheum palmatum* against duck hepatitis B virus (DHBV). Phytother Res. 1997; 11:179-182.
45. Song YH, Liu Q, Lv ZP, Chen YY, Zhou YC, Sun XG. Protection of a polysaccharide from *Salvia miltiorrhiza*, a Chinese medicinal herb, against immunological liver injury in mice. Int J Biol Macromol. 2008; 43:170-175.
46. Cheng HT, Li XL, Li XR, Li YH, Wang LJ, Xue M. Simultaneous quantification of selected compounds from Salvia herbs by HPLC method and their application. Food Chem. 2012; 130:1031-1035.
47. Xiong LL. Therapeutic effect of combined therapy of Salvia Miltiorrhiza and Polyporus Umbellatus Polysaccharide in treating chronic Hepatitis B. Zhong Guo Zhong Xi Yi Jie He Za Zhi. 1993; 13:533-535, 516-517. (in Chinese)
48. Ye F, Liu Y, Qiu G, Zhao Y, Liu M. Clinical study on treatment of cirrhosis by different dosages of salvia injection. Zhong Yao Cai. 2005; 28:850-854. (in Chinese)
49. Kim HJ, Yoo HS, Kim JC, Park CS, Choi MS, Kim M, Choi H, Min JS, Kim YS, Yoon SW, Ahn JK. Antiviral effect of *Curcuma longa* Linn extract against hepatitis B virus replication. J Ethnopharmacol. 2009; 124:189-196.
50. Wu MJ, Weng CY, Ding HY, Wu PJ. Anti-inflammatory and antiviral effects of *Glossogyne tenuifolia*. Life Sci. 2005; 76:1135-1146.
51. Tang QN, Feng M, Gong SJ, Dai ZK, Zhou YZ, Xu Q. The effects of extracts from *Arenaria kansuensis* on the levels of HBsAg and HBeAg in HepG2.2.15 cells. Zhong Yao Cai. 2008; 31:1212-1216. (in Chinese)
52. Zuo GY, Liu SL, Xu GL. The research progress on the in vitro anti-HBV activities of ingredients isolated from medicinal plants over the past 20 years. World Chin J Dig. 2006; 14:1241-1246. (in Chinese)
53. Ye G, Zhu HY, Li ZX, Ma CH, Fan MS, Sun ZL, Huang CG. LC-MS characterization of efficacy substances in serum of experimental animals treated with *Sophora flavescens* extracts. Biomed Chromatogr. 2007; 21:655-660.
54. Ma ZJ, Li Q, Wang JB, Zhao YL, Zhong YW, Bai YF, Wang RL, Li JY, Yang HY, Zeng LN, Pu SB, Liu FF, Xiao DK, Xia XH, Xiao XH. Combining oxymatrine or matrine with lamivudine increased its anti-replication effect against the hepatitis B virus *in vitro*. Evid Based Complement Alternat Med. 2013; 2013:186573.
55. Chen CX, Liu B, Ma Y, Zhou YJ, Pan XN, Zhen RD, Wang QC, Wang MR, He CL, Fu QC, Chen CW. Lamivudine,

interferon-α and oxymatrine treatment for the surviving hepatic failure patients with hepatitis B. Zhonghua Gan Zang Bing Za Zhi. 2009; 17:505-508. (in Chinese)
56. Li CQ, Zhu YT, Zhang FX, Fu LC, Li XH, Cheng Y, Li XY. Anti-HBV effect of liposome-encapsulated matrine *in vitro* and *in vivo*. World J Gastroenterol. 2005; 11:426-428.
57. Nie HM, Chen JJ, Gao YQ, Jin SG, Wang LT. The research on the anti-HBV effect of sophoridine *in vitro*. Beijing Journal of TCM. 2007; 26:678-680. (in Chinese)
58. Nie HM, Wang LT, Chen JJ, Wang R, Jin SG, Gao YQ. Inhibitory effects of sophocarpine on HBsAg and HBeAg *in vitro*. Liao Ning Zhong Yi Za Zhi. 2006; 33:1478-1479. (in Chinese)
59. Xia JF, Gao JJ, Inagaki Y, Kokudo N, Nakata M, Tang W. Flavonoids as potential anti-hepatocellular carcinoma agents: Recent approaches using HepG2 cell line. Drug Discov Ther. 2013; 7:1-8.
60. Huang RL, Chen CC, Huang HL, Chang CG, Chen CF,Chang C, Hsieh MT. Anti-hepatitis B virus effects of wogonin isolated from *Scutellaria baicalensis*. Planta Med. 2000; 66:694-698.
61. Guo QL, Zhao L, You QD, Yang Y, Gu HY, Song GL, Lu N, Xin J. Anti-hepatitis B virus activity of wogonin *in vitro* and *in vivo*. Antiviral Res. 2007; 74:16-24.
62. Shin MS, Kang EH, Lee YI. A flavonoid from medicinal plants blocks hepatitis B virus-e antigen secretion in HBV-infected hepatocytes. Antiviral Res. 2005; 67:163-168.
63. Kang EH, Kown TY, Oh GT, Park WF, Park SI, Park SK, Lee YI. The flavonoid ellagic acid from a medicinal herb inhibits host immune tolerance induced by the hepatitis B virus-e antigen. Antiviral Res. 2006; 72:100-106.
64. Huang ZM, Yang XB, Cao WB, Liu HZ, Xu HD. Modern study and clinic application of *Oenanthe javanica*. Pharm J Chin PLA. 2001; 17: 266-269. (in Chinese)
65. Wang WN, Yang XB, Liu HZ, Huang ZM, Wu GX. Effect of *Oenanthe javanica* flavone on human and duck hepatitis B virus infection. Acta Pharmacol Sin. 2005; 26:587-592.
66. Klayman DL. Qinghaosu (artemisinin): An antimalarial drug from China. Science. 1985; 228:1049-1055.
67. Romero MR, Efferth T, Serrano MA, Castaño B, Macias RI, Briz O, Marin JJ. Effect of artemisinin/artesunate as inhibitors of hepatitis B virus production in an "*in vitro*" replicative system. Antiviral Res. 2005; 68:75-83.
68. Chiang LC, Ng LT, Liu LT, Shieh DE, Lin CC. Cytotoxicity and anti-hepatitis B virus activities of saikosaponins from *Bupleurum* species. Planta Med. 2003; 69:705-709.
69. Ren S, Zhang H, Mu Y, Sun M, Liu P. Pharmacological effects of astragaloside IV: A literature review. J Tradit Chin Med. 2013; 33:413-416.
70. Basiglio CL, Sánchez Pozzi EJ, Mottino AD, Roma MG. Differential effects of silymarin and its active component silibinin on plasma membrane stability and hepatocellular lysis. Chem Biol Interact. 2009; 179:297-303.
71. Xie YM. Evaluation of silymarin in the treatment of chronic hepatitis B. Chinese Journal of New Drugs. 2006; 15:725-727. (in Chinese)
72. Guo JS. Observation on efficacy of Silibinin capsule for chronic hepatitis B. Zhong Guo Gan Zang Bing Za Zhi. 2010; 2:22-24. (in Chinese)
73. Li ZR. The pharmacological and clinical research progress of kushenin. West China Journal of Pharmaceutical Sciences. 2003; 18:435-437. (in Chinese)
74. Yu YY, Wang QH, Zhu LM, Zhang QB, Xu DZ, Guo YB, Wang ZQ, Guo SH, Zhou XQ, Zhang LX. A clinical research on kushenin for the treatment of chronic hepatitis B. Zhonghua Gan Zang Bing Za Zhi. 2002; 10:280-282. (in Chinese)
75. Qi F, Li A, Zhao L, Xu H, Inagaki Y, Wang D, Cui X, Gao B, Kokudo N, Nakata M, Tang W. Cinobufacini, an aqueous extract from *Bufo bufo gargarizans* Cantor, induces apoptosis through a mitochondria-mediated pathway in human hepatocellular carcinoma cells. J Ethnopharmacol. 2010; 128:654-661.
76. Qi F, Li A, Inagaki Y, Kokudo N, Tamura S, Nakata M, Tang W. Antitumor activity of extracts and compounds from the skin of the toad *Bufo bufo gargarizans* Cantor. Int Immunopharmacol. 2011; 11:342-349.
77. Qi F, Inagaki Y, Gao B, Cui X, Xu H, Kokudo N, Li A, Tang W. Bufalin and cinobufagin induce apoptosis of human hepatocellular carcinoma cells *via* Fas- and mitochondria-mediated pathways. Cancer Sci. 2011; 102:951-958.
78. Cui X, Inagaki Y, Xu H, Wang D, Qi F, Kokudo N, Fang D, Tang W. Anti-hepatitis B virus activities of cinobufacini and its active components bufalin and cinobufagin in HepG2.2.15 cells. Biol Pharm Bull. 2010; 33:1728-1732.
79. Yu Q, Xi QH. Observation on the effect of cinobufacini and IFN-α 2b treating chronic hepatitis B. Capital Medicine. 2011; 16:48-49. (in Chinese)

(Received November 10, 2013; Revised December 21, 2013; Accepted December 25, 2013)

Review

DOI: 10.5582/ddt.2013.v7.6.225

The connotation of the Quantum Traditional Chinese Medicine and the exploration of its experimental technology system for diagnosis

Xiaolei Zhao[1,2], Jinxiang Han[1,*]

[1] *Shandong Academy of Medical Sciences, Medical Biotechnology Center, Ji'nan, Shandong, China;*
[2] *University of Ji'nan-Shandong Academy of Medical Sciences, School of Medicine and Life Sciences, Ji'nan, Shandong, China.*

ABSTRACT: Traditional Chinese Medicine (TCM) developed based on ancient Chinese philosophy. Its characteristics include abstract theories, fuzzy concepts, subjective diagnostic methods and it lacks clarity, and rigor as well as vindication from modern sciences, which makes development of TCM remain stagnant. Thus, how to free the theory of TCM from heavy philosophy to achieve separation of medicine and philosophy, and to use the contemporary cutting-edge science and technology to transform the theory of TCM and then to achieve its scientific paradigm shift, is a way for TCM to get out of the woods. This article, focusing on the problems existing in the development of the modernization of TCM, introduces the concept, the connotation as well as the important role of Quantum TCM in the modernization of TCM. Additionally, based on the view that the body's electromagnetic radiation can characterize the human "Qi" in TCM, we discuss several experimental technology systems for the diagnosis of Quantum TCM in detail. By analyzing and comparing these technology systems, we come to the conclusion that the biophoton analytical technology (BPAT) is more worthy of further study in building the experimental technology system for the diagnosis of Quantum TCM.

Keywords: TCM, Quantum TCM, experimental technology system, biophoton detection system, superconducting quantum interferometer device (SQUID), infrared thermal imager

1. Introduction

Traditional Chinese Medicine (TCM) developed on the basis of ancient Chinese philosophy, and the characteristics of it include abstract theories, fuzzy concepts, subjective examination methods and it lacks the clarity, and rigor and vindication of modern sciences, which makes development of TCM remain stagnant. Although in the early 80's of the last century, medical providers have carried out lots of research and practice in the modernization of TCM, and have achieved some results, however, they have not yet achieved a qualitative breakthrough. The main reasons are as follows (*1*): (*i*) focus has been on the thinking mode of mechanical reductionism theory with logical analysis and accurate demonstration, but ignores the thinking ways of ontology with the integrity and organic characteristics in TCM; (*ii*) they have not yet realized the conversion of TCM theory using modern or contemporary scientific theory and have not yet realized the establishment of a modern TCM theory system which has international recognition in the premise of self laws and the thinking ways of TCM theory; (*iii*) they have not yet found a detection indicator system with the characteristics of TCM. Furthermore, a technology system for experiments and quantitative diagnosis, which is suitable for the thinking model of TCM, has not been established. Therefore, how to break the old ideas and to realize the conversion of TCM theory into a scientific paradigm based on TCM's own laws and ways of thinking, and then to establish a technology system for the experiment and quantitative diagnosis of TCM, is an important task in the modernization of TCM.

2. Quantum TCM

Quantum theory reveals the basic laws of the microscopic physical world, and provides a new way of formulating and thinking about nature. Marked by quantum theory, the modern discipline whose philosophy is organic and holism coincides with the philosophy of TCM (*2*), so quantum theory may be used to explain the theory of TCM. Fortunately, the biophoton coherent theory in biological systems put forward by Popp (*3*) makes it possible to translate the theory of TCM using quantum theory. Based on this theory and combined with the common features of "Qi" and electromagnetic radiation, we propose a view that the electromagnetic radiation from the body can characterize the human "Qi" in TCM (*4*), and give the theory of TCM a new image - the Quantum TCM theory.

**Address correspondence to:*
Dr. Jinxiang Han, Shandong Academy of Medical Sciences, No. 18877 Jing-shi Road, Ji'nan, 250062, Shandong, China.
E-mail: samshjx@sina.com

Quantum TCM theory explains the connotation of TCM theory scientifically: (*i*) Meridian hypothesis (*5*): Electromagnetic radiation fields within biological organisms are characterized by non-local interference. With the occurrence of interference, interfering beams form a unitary tridimensional network, with striae (*i.e.*, beams) of varied intensity distributed on the organism surface similar to semi-reflectors. The striae carry bio-information of corresponding organs and integrate all tissues and organs of the organism. (*ii*) Viscera hypothesis (*6*): The electromagnetic radiation from the electromagnetic field within the human body is characterized by interference, and the quanta in them have a function of information transference, operating as non-molecular messengers of information communication in tissues, organs, cells, and biological macromolecules, *etc*. in the body, and play a key role in transferring information for life movements. Hence, the quanta in the human body are the "Qi" information for the regulation and adjustment of the viscera network in TCM. (*iii*) Heaven-human correspondence hypothesis (*7*): The lives on earth swim in a spatio-temporal electromagnetic field, which can be considered as the "Qi" of the universe. The "heaven-human correspondence" is a resonant interaction between human bodies' electromagnetic field ("Qi" of the human body) and the spatio-temporal electromagnetic field ("Qi" of the universe). (*iv*) Syndrome differentiation hypothesis (*8*): The symptom in TCM is the quantum superposition state formed with the body's electromagnetic radiation, and the syndrome differentiation adjusts quantum superposition states of electromagnetic radiation field to turn it into a healthy situation. Based on the above ideas, the concept of Quantum TCM is put forward (*1*): Guided by the holism and dialectical materialism thought of TCM, regarded by modern sciences, especially quantum theories, as the theoretical basis, and based on the view that the electromagnetic radiation from the body can characterize the human "Qi" in TCM, the Quantum TCM theory uses the quantum forms of electromagnetic radiation, photon (quantum) radiation, energy (caloric), *etc*. to study and explain the scientific principles within the TCM framework, which are concerned with the transformation rules of human health and diseases and their prevention, diagnosis, therapy, rehabilitation and healthcare.

The Quantum TCM converts the only qualitative "Qi" with a strong color of philosophy into the quantitative electromagnetic radiation at the science level by using the existing basic theory and technology. It makes the abstract concepts in TCM theory obvious, makes the fuzzy law clear, and defines the processes and details in the theory of TCM. Additionally, on the premise of the internal rules and thought processes of the TCM theory, the Quantum TCM frees the theory of TCM from heavy philosophy and gives it a modern scientific characteristic basis, including clarity, rigor and vindication. It makes a scientific paradigm transformation of TCM come true to a certain extent.

However, the realization of TCM modernization not only needs a scientific theoretical system, but also a strict and scientific experimental technology system for diagnosis. The establishment of a theoretical system for Quantum TCM lays the foundation for establishing an experimental technology system of Quantum TCM for diagnosis using the body's quantum electromagnetic radiation, light (quantum) radiation, and energy (heat) radiation in the microscopic state.

3. The exploration of an experimental technology system for diagnosis of the quantum TCM

The human swims in the space-time electromagnetic field formed by the celestial bodies and the earth, based on which the human magnetic fields are generated and maintained. The mechanism interacts with the organism and the biological effects are changeable with the variation of the field intensity, frequency and amplitude. According to the spectrum characteristics of electromagnetic waves and the features of biological effects, the electromagnetic spectrum can be separated into the ionization zone, visible zone, infrared and millimeter wave zone, radiation zone and low frequency region. However, there is a common characteristic, which is the presence of a "frequency window", in the interaction between the electromagnetic radiation and biology, that is to say, only when the frequency of the external electromagnetic wave is consistent with the natural vibration frequency of molecules or polymers in the organism and produce resonance between them, the biological macromolecules are enabled to absorb energy from the electromagnetic wave, and then result in significant biological effects (*9*). Consequently, the corresponding spectrum of the biological magnetic field with the spectrum of the space-time electromagnetic field must exist in the organism.

According to the difference of wavelengths, source and the analytic method of the electromagnetic wave from the electromagnetic field of the organism, the electromagnetic wave can be divided into different spectral intervals, including the ultraviolet-visible zone (ultraweak biophoton emission), infrared zone and other electromagnetic field zones, *etc*. All of these electromagnetic waves with different spectra can be regarded as the "Qi" information of the body, based on the view that the electromagnetic radiation from the body can characterize the human "Qi" in TCM. Besides, the TCM theory holds that "Qi" is the basic substance which constitutes the human body and maintains life activities of the body, and all occurrences and development of the various diseases come from the "Qi" of the body. The syndrome differentiation of TCM, in essence, is to distinguish the deficiency and excess of "Qi" of the main and collateral channels and viscera. Therefore, the

quantum state of the electromagnetic radiation field of the human body should be able to reflect the state of the body (health or disease) to a certain extent (*8*). Below, we will thoroughly analyze the quantitative detection technologies of electromagnetic waves in different bands and their ability to reflect the health status of the body, and then discuss the feasibility of these technologies in establishing the experimental technology system of Quantum TCM for diagnosis.

3.1. *The region of ultraviolet-visible (ultraweak biophoton emission)*

The ultraweak biophoton emission (UPE) is a common phenomenon of life, and comes from the transition of biological molecules from a high energy state to a low energy state, and the wavelength range of it is ultraviolet and visible light. Biologists have discovered that the bases of DNA molecules can form substances only existing in an excited state due to the heaps interaction, which may be one of the material bases of UPE (*10*). The UPEs radiated from the lives carry the original information about the lives, and this information is able to affect the human body mainly through the weak magnetic field, so as to correct the chaotic state of the magnetic field in the human body, and recover the life order of the atoms, molecules and cell. So the UPE, which can be used as a macro performance of a micro life activity, must be inevitably associated with various detailed life processes (*11*). Actually, many studies have found that UPE is closely related with a great deal of fundamental life processes, such as, growth regulation, oxidative metabolism, information transfer, cell division, cancer, death and so on. Also, any influence of internal change and external environment will cause changes at the microscopic energy level, which lead to changes of biophoton emission. Therefore, the biophoton, which carries a wealth of internal information about the human body, can act as the "Qi" information to synthetically reflect the health state of the host on the whole, and this is consistent with the diagnostic view of the TCM. Besides, during cell division of the organism, the double strands of DNA molecules are completely separated, and each separate strand synthesizes new double strands again using the surrounding material. In this process, it's easy to radiate an electromagnetic wave, but also easy to receive foreign electromagnetic waves. Hence, the intensity of UPE from the body also enables reflection of the active state of human cells, namely the division rate, and from this we can diagnose the human health state.

However, how can we get and analyze the UPE? Biophoton analytical technology (BPAT) is just the way. It can quantitatively detect, analyze and record the UPE which carries abundant inside information of the human body using the biophoton detector in order to get the health state of the body and achieve the early diagnosis of disease. The biophoton detector usually uses a photon counting system, and Figure 1 shows the biophoton detector in our laboratory and its schematic diagram. The core component of it is the photomultiplier tube (Hamamatsu Photonics K.K., Iwata City, Japan). During the measuring process, the photons radiated from a part of the body, arrive at the photocathode, and generate electrical pulses. Subsequently, the electric pulses are fed

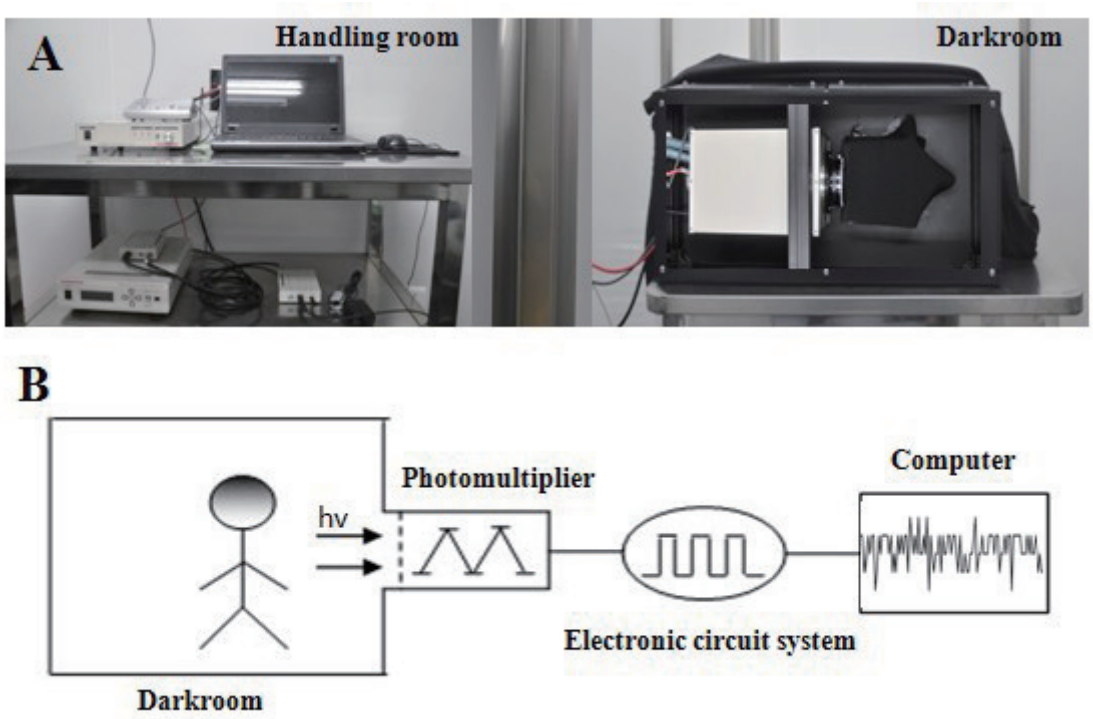

Figure 1. The biophoton detector (A) and the schematic diagram (B) used in the author's laboratory.

into the electronic circuit system, in which the electric pulses are amplified, screened, counted and so on. In the end, the measuring signals are displayed and stored by computer. Through the comparative analysis of the received signal, we can obtain the health state of the body.

At present, many research groups have obtained significant results: such as using the BPAT and uniting with the balance of the yin-yang theory in TCM theory, Joon-Mo Yang *et al*. found that the intensity of biophoton emission from the left hand was balanced with the right hand in the normal people, while in stroke patients the intensity of biophoton emission from the left hand was imbalanced with the right hand (*12*); Wen-Ying Yang *et al.* found that in bronchial asthma and chronic gastritis patients, there were significant differences in the intensity of biophoton emission from the corresponding acupoints on both sides of the body during the period of disease exacerbation, and displayed an imbalanced state, while there were no obvious differences in healthy control groups (*13*). Rong-Rong Zheng *et al*. detected the UPE of the index finger (large intestinal meridian passing from this finger) of simple constipation patients, and found that the luminescent value of left-right was obviously asymmetric, while the luminescent values of the healthy control groups showed symmetry (*14*). Also, some interesting phenomena has been found in the author's lab: the intensity of UPEs from the first finger (lung channel passing this finger) of the patient with Qi deficiency were obviously lower than that of healthy patients; and the same phenomena were also found in the middle finger (pericardium meridian passing this finger) and little finger (the heart channel of Hand-Shaoyin passing this finger) of the patient with insufficiency of the heart-Qi. However, further research is needed here.

These results directly or indirectly indicate that it is feasible to realize quantification of the diagnosis of Quantum TCM by using BPAT. BPAT not only is able to give holistic information of the internal state of the human body, but also has the ability to make information of life activity from microscopic to macroscopic in order to quantitatively analyze the holistic state of life which is called a symptom in TCM, and this is consistent with the diagnostic characteristics of TCM and can be used as a detection index system of Quantum TCM. In addition, the function of BPAT is collecting and analyzing the surface information of the human body so as to observe the inner healthy state, which is also in accord with the diagnostic ideas of TCM: analyze internal change through external appearance. Therefore, it is sufficient to use BPAT to establish the experimental technique system for diagnosis with TCM, which is suited for the thought model of TCM, and this technology has many merits for diagnosis, such as being rapid, sensitive, reliable, noninvasive and easy to be accepted by patients.

In addition to the application in TCM, BPAT has also been widely used in many other fields including food inspection, water quality analysis, environmental monitoring, drug development, gene technology, agricultural science and medical diagnosis *etc*.

However, BPAT also has some shortcomings. First, there are factors affecting the biophoton emission, such as change of the external environment or emotional fluctuations. Therefore, we must strictly control the experimental conditions and stabilize the emotion of volunteers when we detect the biophoton emission. Additionally, we must explain the results prudently considering all factors. Furthermore, before we apply this technique practically, we need to have a large number of systematic and standard detection techniques in the laboratory, to create a multi-level database corresponding to the various symptoms, to supply as well as perfect the base according to actual needs, and to set up a feasible "standard" finally, which requires considerable investment. Once a standard is setup, the advantages of BPAT can be sufficiently explored.

3.2. *Infrared region*

As we all know from physics, all objects above absolute zero can produce infrared radiation (thermal radiation), and this radiation energy depends on the temperature and the emissivity of the object's surface. The temperaturedistribution of normal humans is stable and symmetrical to some degree. However, change of subcutaneous blood circulation, local metabolism organization, or thermal conductivity of the skin *etc.* can result in a change of temperature distribution. When the human body gets ill or function is changed, blood flow and metabolism of the corresponding parts will be changed, which causes a local temperature change, which results in a change of infrared radiation.

From the perspective of molecular biology (*16*), the major source of infrared radiation is electromagnetic waves, generated by the transition of molecular vibration energy levels in proteins. The infrared energy or biological energy is transmitted along the protein molecular chain through dipole-dipole coupling interactions of the amide bond between adjacent protein molecules, which causes change of structure, configuration, and configuration of protein molecules, so as to promote growth and development of organisms. In this process, the bio-energy released by ATP hydrolysis has a similar effect. Once the ATP molecules or ATP enzymes or proteins conformational change goes wrong because of the effect of the internal or external environment, the bio-energy provided by the ATP hydrolysis will be insufficient or delivered abnormally. As a result, the biological tissues won't grow normally, which will lead to a change of infrared radiation on a large scale, and finally will cause diseases.

Therefore, both from a macro and micro perspective, infrared radiationplays a role to deliver information and energy, so it is closely related to the activities of the

human body, and can be used as the "Qi" information of the body. Through measuring and analyzing slight changes of infrared radiation in different parts, we can obtain the relevant internal state of the human body (the information of health or disease), so as to find the changes of thermal infrared radiationcorresponding to the variety of symptoms in TCM.

Thermal measurement technology, such as infrared thermography, was mainly used in clinical trials to measure the infrared radiation of the body surface. Figure 2 shows infrared thermography (Figure 2A) and the schematic diagram (Figure 2B) of it. It can filter, aggregate, and modulate the far infrared light waves radiated by humans through an optical electronic system and convert this wave into an electrical signal, which can be further converted into a digital signal. The temperature field of the human body will show up as an image through multimedia image processing. At the same time, special software was applied to analyze the difference in temperature quantitatively for judgment of lesion positions and nature for further diagnosis of disease.

From the general processes of occurrence and development of disease, the changes of human infrared radiation usually precedes variation of its structure, and shape, so that the medical infrared thermal imager can observe the early diagnosis of (*17*) disease in the human body, such as early prediction of cancer, differential diagnosis and screening of tumors (*18,19*), and early diagnosis of cardiovascular and cerebrovascular disease and various inflammation (*17*). Another study found that the degree of deficiency of Yin was proportional to the temperature of the tongue (*20*); and the surface temperature was positively associated with the Yang (*21*). Some researchers also found that the infrared radiation of the body's surface corresponding with the line of meridian circulation may change in the state of viscera lesions (*22,23*); *etc*.

The core of TCM theory is an overall concept, and TCM theory pays attention to the overall dialectics and dynamic balance, while the measurement technology of the infrared thermal imager can obtain continuous and dynamic information of the human body. Therefore, using thermal measurement techniques to study the dialectical theory of TCM is consistent with the methodology.

The thermal measurement technique is a new medical technology, which is different from traditional structure imaging. It reflects the functional state of the human body, and directly reflects the phenomenon of life, and is able to guide us to understand the pathogenesis of TCM. Additionally, it has the characteristics of no damage, no pain, no radiation and safety to the patients. With it, lesions can be found in advance of inspection results. The results are fast and easy to be accepted by volunteers. However, the infrared thermal imager diagnoses disease in the human body mainly through infrared thermography of surface temperature and the location and size of lesions within the human body are not clear and are unable to be located (*17*) accurately. Moreover, the disease reflected on the body surface is not only from the body, but the dysfunction of the surface itself. Thus, the infrared thermal imager has a limitation for diagnosis currently.

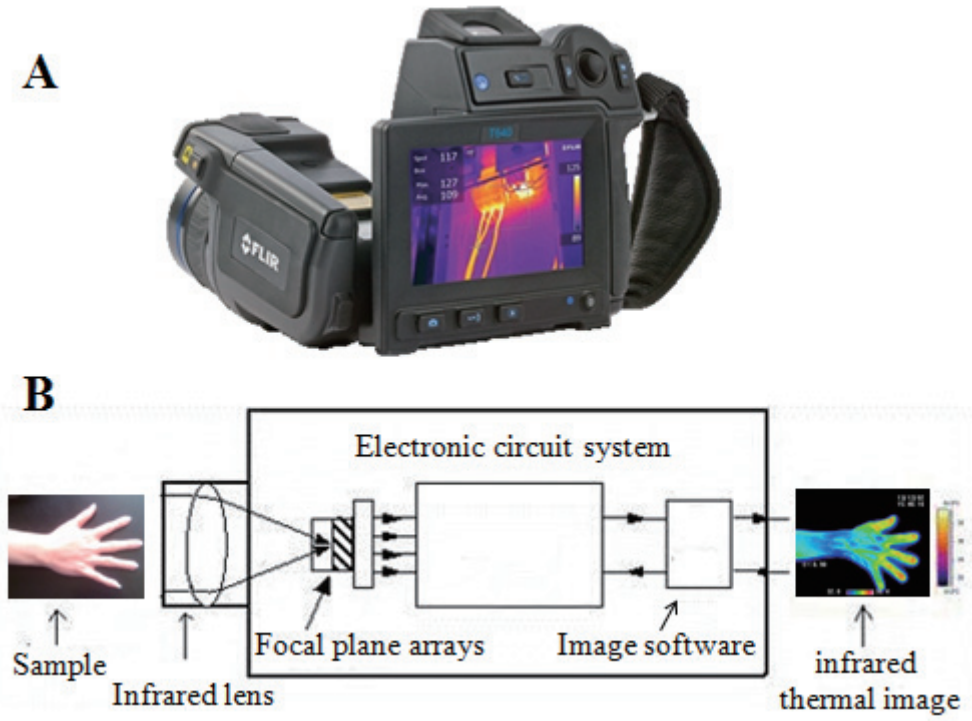

Figure 2. The infrared thermography (A) and the schematic diagram (B) of it.

3.3. *Other electromagnetic fields of the human body*

The same with UPE, which is an inherent attribute of biology, all substances (including lives) in nature have magnetisms which are either strong or weak. Each molecule, cell, tissue, organ, *etc*. in life have magnetic phenomena. There are two types of field sources in the human body concerning the biological magnetic field (*24*). One is the intrinsic magnetic field, which is formed by tissue *in vivo*. The physiological activities of the human body are accompanied by ion currents (Ion movement inside and outside the cell membrane), such as the bioelectricity in heart, brain, *etc.*, those currents have the ability to produce magnetic fields. In addition, paramagnetic materials (such as the Fe in hemoglobin, the Co in vitamin B12) in some biological materials within the human body are also important parts of the intrinsic magnetic field. The other type of magnetic field is formed by exogenous ferromagnetic substances. That is to say, the ferromagnetic substances, which are inhaled or eaten by the human body from nature, will be magnetized under the external magnetic field, and will form substances which are similar to magnets, so as to generate a magnetic field in vitro, such as the magnetic field generated by the stomach, liver and lungs.

It follows that the generation of the magnetic fields in the body are most associated with physiological activity. When the body is abnormal or diseased somewhere, the physiological activity will change inevitably, so as to lead to a variation of the magnetic field. Therefore, we can obtain information on the internal state of the human body by measuring and analyzing the slight changes of the magnetic field in the body, in order to find changes in the biological magnetic field corresponding to the various symptoms in TCM. So the measurement of the biological magnetic field can also serve as a means of quantification of Quantum TCM for diagnosis.

But it is very difficult to detect the biological magnetic field in an environment full of earth's magnetic field and magnetic field noise, because the biological magnetic field (generally 10-6 times in the magnetic field of the earth) of the human body is very weak. However, the superconducting quantum interferometer device (SQUID) with ultra-high sensitivity, successfully developed by the Massachusetts Institute of technology of the United States has solved the core issue of this problem (the schematic diagram of SQUID is shown in Figure 3). Although the research on SQUID is still in some dispute, this does not affect the enthusiasm of researchers studying it. At present, clinical medicine mainly uses the detection systems of the superconducting biomagnetometer, whose core component is the SQUID. This system consists of three basic parts: detection coil, SQUID and a low temperature container. The detection coils connecting with the input coils of SQUID can form a superconducting circuit, which enables the changes of magnetic flux to be transformed into changes of power consumption, so as to detect and quantify the weak magnetic signal of the human body. The cryogenic vessel filled with helium is a vacuum insulated container, in order to ensure the equipment working in the superconducting state (*25*). Coupled with the technologies of magnetic shielding and space identification, which are able to suppress the interference of the external magnetic field more efficiently, the detection system can get a more accurate determination of the biological magnetic field of the human body.

Presently, the measurement system of the superconducting biomagnetometer has achieved remarkable results for the diagnosis of disease. Typical

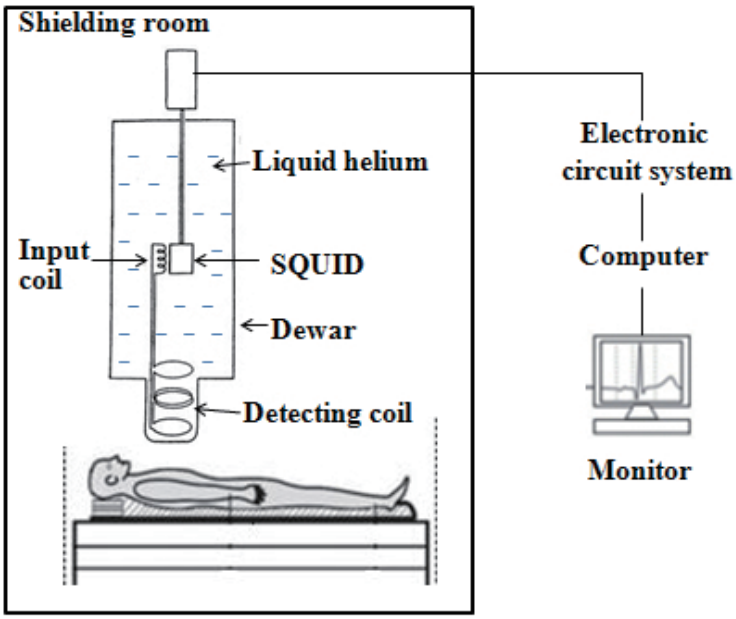

Figure 3. The schematic diagram of the superconducting quantum interferometer device (SQUID).

applications include magnetoencephalography (MEG), magnetocardiography (MCG), magnetopneumographic (MPG) and mechanomyography (MMG). MEG is mainly used for early diagnosis and lesion locations of brain disease, for example, the accurate localization and diagnosis of epilepsy (*26*). MCG is used for early diagnosis of heart disease, such as early diagnosis of arrhythmia (*27*). MPG is a method of measuring the dust content in lungs by detecting the residual magnetic field of the ferromagnetic dust, and is mainly used for diagnosing pneumoconiosis and defects of lung function (*28*). While the generation of MMG comes from the appearance of muscle current, which is generated during movement of skeletal muscle, and it is mainly used for diagnosing injuries of human muscle *et al.* (*29*). Also, the magnetic field in nerves, eye, retina, liver, abdomen, limbs and scalp are also detected. In spite of these fields, few studies have been examined on the diagnosis of TCM using the detection system of the superconducting biomagnetometer.

As seen above, further researchis needed for the diagnosis of TCM using the detection system of the superconducting biomagnetometer. We are able to get a basic understanding of the internal state of a human body through detecting and analyzing the biological magnetic field of all parts of the human body, so as to obtain valuable information for the quantification of symptoms. Additionally, the measurement of the human biological magnetic field is entirely noninvasive, with no contact, and has the characteristic of high sensitivity and accuracy. Consequently, it is more convenient to people than the measurement of human biological electricity. Furthermore, for some underlying diseases, biological electricity may not appear abnormal yet, as the electromagnetic map has shown. Therefore, the biological magnetic field of the human body can be used to study the "preventive treatment of disease" in TCM. However, the measurement of the biological magnetic field needs a large magnetic shielding room to eliminate the interference of the electromagnetic environment, and also needs a SQUID with high sensitivity at the temperature of liquid helium and a signal processing device. Thus, clinical application is less. In addition, in the detection of lungs, this method can only be used for the detection of dust containing ferromagnetic dust, and is invalid for the non-ferromagnetic dust.

4. Conclusion

From what we have been discussed above, the electromagnetic waves in three kinds of bands are significantly associated with the activities of the human body, so they can be used as the body's "Qi" information to reflect the overall state to some extent, and detection results of them are able to provide valuable information for the quantification of syndromes. However, compared with the detection technology of infrared light and other electromagnetic fields of the human body, the detection technology for the ultraviolet-visible range is more suitable as an experimental techniques system of Quantum TCM for diagnosis. The reasons are as follows: (*i*) The mechanism: The information contained in the ultraviolet-visible area partly comes from the accumulation of bases in the DNA molecules. It not only carries the information of the origin of life, but also controls the order of the human body's activities, so it is closely relative to the detailed process of life. Thus, when the state of the body is abnormal, the abnormal information must be reflected in this band first. While the electromagnetic waves in the infrared band mainly come from the thermal radiation produced in the energy level transition of various protein molecules, it is the lowest energy information, and is influenced by the external environment significantly. The electromagnetic waves from other electromagnetic fields mainly come from the ion current and magnetic substance within the body, so they can't reflect the body's state fundamentally. (*ii*)The detection technique: **a.** Although the detection technology of infrared thermal imaging can show the body's functional state, which can reflect the body's health status directly, it can't find the exact location and size of the lesions mainly through the infrared thermal imaging of the body's surface to diagnose disease within the human body. Besides, the disorders reflected by this mechanism may not come from the inside of the body entirely; they may also derive from the surface dysfunction of the body or the influence of the external environment, so the infrared thermography has certain limitations for diagnosis. **b.** Although the detection of SQUID on human bio-magnetism is much more convenient than the detection of human bio-electricity, the bio-magnetic fields are very weak, and may be influenced by the magnetic field in the environment. Thus, a large magnetic shielding room is needed to eliminate the environmental magnetic interference. Another drawback is that this device only be used to detect magnetic material. Therefore, it also has some limitations for diagnosis. **c.** Biophoton analytical technology (BPAT) is used to detect the intensity of photons from the non-localized coherent electromagnetic field in the human body, and the results can reflect the body's state directly. Additionally, biophotons are easier to detect than infrared and other electromagnetic waves, owing to the reason that most of the biophotons are in the visible spectra, and that the biophoton detector has the advantage of simple structure, so BPAT is more suitable for further study as an experimental techniquesystem for Quantum TCM for diagnosis.

References

1. Han JX. Try to discuss the modernization of TCM basic theory. Medical Innovation of China. 2011; 8:184-189. (in Chinese)
2. Han JX. The commensurability of Philosophy between the TCM theory and the quantum theory. TCM Res.

2011; 24:1-4. (in Chinese)
3 Popp FA. Principles of complementary medicine in terms of a suggested scientific basis. Indian J Exp Biol. 2008; 46:378-383.
4 Han JX, Han Y. The material basis of "Qi" in TCM is the electromagnetic (quantal) field of body. Journal of Shandong University of TCM. 2010; 34:474-477. (in Chinese)
5 Han JX. Meridian is a three-dimensional network from bio-electromagnetic radiation interference: An interference hypothesis of meridian. Cell Biochem Biophys. 2012; 62:297-303.
6 Han JX, Han Y. A viscera-state doctrine based on the physical and chemical perspective. Journal of Shandong University of TCM. 2011; 35:17-19. (in Chinese)
7 Han JX, Han Y. The scientific connotation of "heaven-human correspondence". Chinese Journal of Ethnomedicine and Ethnopharmacy. Academic Study. 2010; 19:63-65. (in Chinese)
8 Han JX, Huang JZ. Mathematical model of biological order state or syndrome in TCM: Based on electromagnetic radiation within the human body. Cell Biochem Biophys. 2012; 62:377-381.
9 Pang XF. Bioelectromagnetics. 2rd ed., National Defense Industry Press, Beijing, China. 2008; pp. 87-88, 174-175. (in Chinese)
10 Popp FA, Nagl W, Li KH, Scholz W, Weingärtner O, Wolf R. Biophoton emission new evidence for coherence and DNA as source. Cell biophysics. 1984; 6:33-52.
11 Han JX, Yang MN, Chen Y. Quantum: May be a new-found messenger in biological systems. Bisci Trends. 2011; 5:89-92.
12 Yang JM, Choi C, Hyun-hee, Woo WM, Yi SH, Soh KS, Yang JS, Choi C. Left-Right and Yin-Yang balance of biophoton emission from hands. Acupunct Eletrother Res. 2004; 29:197-211.
13 Yang WY, Zhou WX, Sun KX. Research on superweak luminescence of acupoints in a pathologic state. Shanghai Journal of Acupuncture and Moxibustion. 1998; 17:2-3. (in Chinese)
14 Zheng RR. The experimental research on the ultra-weak bioluminescence of human body and the relationship between physiological and pathological condition. Chinese journal of luminescence. 1986; 7:20-26. (in Chinese)
15 Kalikin LM, Schneider A, Thakur MA, Fridman Y, Griffin LB, Dunn RL, Rosol TJ, Shah RB, Rehemtulla A, McCauley LK, Pienta K. *In vivo* visualization of metastatic prostate cancer and quantitation of disease progression in immunocompromised mice. Cancer Biol Ther. 2003; 2:661.
16 Pang XF. Bioelectromagnetics. 2rd ed., National Defense Industry Press, Beijing, China, 2008; pp. 87-88, 215-219. (in Chinese)
17 Lahiri BB, Bagavathiappan S, Jayakumar T, Philip J. Medical applications of infrared thermography: A review. Infrared Physics & Technology. 2012; 55:221-235.
18 Kontos M, Wilson R, Fentiman I. Digital infrared thermal imaging (DITI) of breast lesions: Sensitivity and specificity of detection of primary breast cancers. Clinical Radiology. 2011; 66:536-539.
19 Bezerra LA, Oliveira MM, Rolim TL, Conci A, Santos FGS, Lyra PRM, Lima RCF. Estimation of breast tumor thermal properties using infrared images. Signal Processing. 2013; 93:2851-2863.
20 Zhang SQ, Xiao HS, Sheng YW. Observation on the tongue temperature of healthy persons and patients with yin deficiency by using thermal video. Chinese journal of integrated traditional and western medicine. 1990; 10:732-733. (in Chinese)
21 Zheng LS, Wang Y, Wu YR. Application of Thermal tomography imaging (TTM) technology in the medical. J Med Theor & Prac. 2011; 24:2592-2593. (in Chinese)
22 Zhang D, Zhu YG, Wang SY, Ma HM, Ye YY, Fu WX, Hu WG. Infrared thermoimages display of body surface temperature reaction in experimental cholecystitis. World J Gastroenterol. 2002; 8:323-327.
23 Ovechkin A, Lee SM, Kim KS. Thermovisual evaluation of acupuncture Points. Acupunct Electrother Res. 2001; 26:11-23.
24 Yan DJ, Li W, Qian CF. Measurement for body bio-magnetism and its clinical application. Progress in modern biomedicine. 2007; 7:425-428. (in Chinese)
25 Rose DF, Smith PD. Sato S. Magnetoencephalography and epilepsy research. Science. 1987; 238:329-335.
26 Manoharan A, Bowyer SM, Mason K, Tepley N, Elisevich K, Smith BJ, Barkley GL. Localizing value of MEG in refractory partial epilepsy: Surgical outcomes. International Congress Series. 2007; 1300:657-660.
27 Kwong JS, Leithäuser B, Park JW, Yu CM. Diagnostic value of magnetocardiography in coronary artery disease and cardiac arrhythmias: A review of clinical data. Int J Cardiol. 2013; 167:1835-1842.
28 Freedman AP, Robinson SE, Johnston RJ. Non-invasive magnetopneumographic estimation of lung dust loads and distribution in bituminous coal workers. J Occup Med. 1980; 22:613-618.
29 Marusiak J, Jaskólska A, Kisiel-Sajewicz K, Yue GH, Jaskólski A. EMG and MMG activities of agonist and antagonist muscles in Parkinson's disease patients during absolute submaximal load holding. J Electromyogr Kinesiol. 2009; 19:903-914.

(Received November 19, 2013; Revised December 16, 2013; Accepted December 19, 2013)

Review

DOI: 10.5582/ddt.2013.v7.6.233

HDAC6: Physiological function and its selective inhibitors for cancer treatment

Penghui Yang, Lei Zhang, Yingjie Zhang, Jian Zhang, Wenfang Xu*

Department of Medicinal Chemistry, School of Pharmaceutical Sciences, Shandong University, Ji'nan, Shandong, China.

ABSTRACT: Acetylation and deacetylation of histones are important in regulating gene expression and play a key role in modification of gene transcription. Specific HDACs isoforms can be regarded as a target for cancer therapy avoiding side-effects, HDAC6 with a unique physiological function and structure has become a hot issue recently. The unique isoform HDAC6 is involved in tumorigenesis, development and metastasis through tubulin, HSP90, invasin and ubiquitin-protein. Here we review the structure elements, biological function, and recent selective inhibitors of HDAC6, and study the structure-activity and structure-selectivity relationship.

Keywords: Histone deacetylases, HDAC6, cancer, inhibitor

1. Introduction

Histones are one of the important components which constitute the chromosome of eukaryotes. Acetylation and deacetylation of histones regulate gene expression through key transcriptional modifications (*1,2*). Histone acetyltransferases (HATS) and histone deacetylases (HDACS) regulate post-translational modifications by the acetylation and the decetylation of the ε-amino group of lysine residues in histone tails and some non-histone proteins (*3*). Relevant research shows that acetylation and deacetylation of histones are of significant importance in tumor genesis and progression. Inhibition of HDACS has become a promising direction for cancer therapy (*4*).

HDACS consist of four classes (I, II, III, and IV) based on their homology to yeast histone deacetylases. Class I consists of four different isoforms (HDAC1, 2, 3, and 8). Class II with six isoforms is grouped into two subclasses named Class IIa (HDAC4, 5, 7, and 9) and class IIb (HDAC6 and 10). Class IV consists of only one isoform, HDAC11. Seven isoforms, Sirt1-7, are referred to as class III. The enzymatic activity of HDACs plays its role by two mechanisms which include the Zn^{2+}-dependent mechanism of class I, II, and IV and the NAD^{+}-dependent mechanism of class III.

Most HDACS target histone proteins, as mentioned, some HDACS also target non-histone proteins with one important example, tubulin. To date, only HDAC6 (*5-7*) and Sirt2 (*8*) can use tubulin as a substrate and regulate the balance of tubulin acetylation and deacetylation. These effects play an important role in the microtubule network.

HDAC6, a unique cytoplasmic deacetylase, targets tubulin, HSP90 and cortactin, hence it can regulate cell adhesion, motility and chaperone function (*9*). Another uniqueness of HDAC6 is that it has two homologous tandem catalytic domains, DD1 and DD2 (*10*). Previous work shows that DD2 plays the greatest role for tubulin deacetylase rather than DD1 *in vitro*. The nuclear export signal (NES) and the Ser-Glu-containing tetrapeptide (SE14) (*11,12*) of the HDAC6 functional domains cause it to localize in the cytoplasm (Figure 1) (*14*). In the C-terminal region of HDAC6, there is a unique ubiquitin-binding zinc-finger domain named the ZnF-UBP domain or BUZ domain (*13*).

Some structurally diverse compounds have been considered as HDACS inhibitors, such as TSA (trichostatin A, **3**), SAHA (suberoylanilide hydroxamic acid, **4**), CHAP31 (**1**), TPXB (trapoxin B, **2**), and MS-275 (**5**) (Figure 2). Hydroxamates are usually pan-HDAC inhibitors, such as TSA, SAHA (*15*), and CHAP31 (*16*). Compounds, such as TPXB (*17*) and MS-275 (*18*), with other Zn^{2+} chelating groups are now being studied, and some of these types of HDACS inhibitors are class or even isoform selective.

**Address correspondence to:*
Dr. Wenfang Xu, Department of Medicinal Chemistry, School of Pharmaceutical Sciences, Shandong University, No. 44, West Wenhua Road, 250012, Jinan, Shandong, China.
E-mail: xuwenf@sdu.edu.cn

Figure 1. Structure of HDAC6.

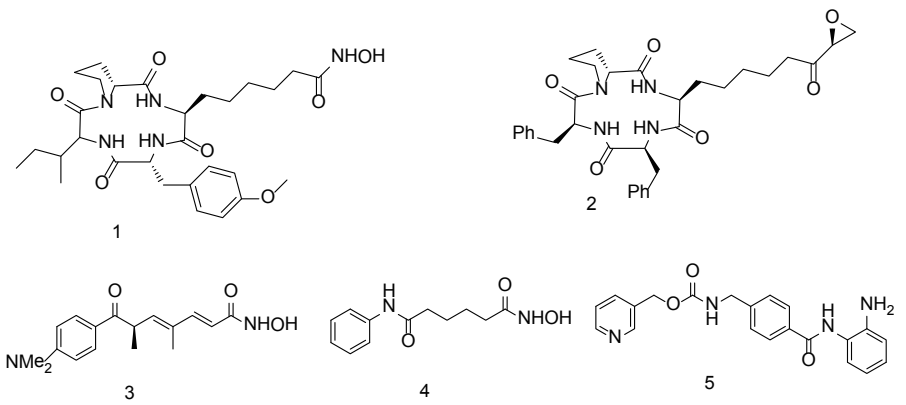

Figure 2. Structure of trichostatin A (TSA, 1), suberoylanilide hydroxamic acid (SAHA, 2), CHAP31 (3), trapoxin B (TPXB, 4), and MS-275 (5).

As pan-HDACS inhibitors often cause side effects, study of selective-inhibitors is necessary. HDAC6 is the only Zinc dependent isoform which deacetylates tubulin (*19*), because of the unique structure and function of HDAC6, there are some selective inhibitors for this subtype, and HDAC6 has been regarded as a therapeutic target for cancer without side effects. HDAC6-selective inhibitors with diverse structures are being studied by chemists.

2. Physiological function

HDAC6 regulates diverse important intracellular biological processes, it effects the growth, migration and death of cells. It also deacetylates HSP90 (heat shockprotein 90), tubulin and cortactin. A recent study found that HDAC6 can also deacetylate peroxiredoxin which is involed in regulation of redox reactions *in vivo* (*20*).

HDAC6 which plays a great role in misfolded protein degradation can be regarded as a target for protein conformational disorders (*21*). As a misfolded protein is harmful, cells can clear away it by the way of a molecular chaperon, ubiqutin-proteasomes system (UPS) and autophagy-lysosome pathway (ALP). For quite a long time, UPS and ALP have been regarded as two parallel degradation pathways, but recent research demonstrates that HDAC6 can form a tripolymer through the Znf-UBP combined with the ubiquitin-misfolded protein and dyneinmotor binding motif (*22*). The tripolymer can be degraded by ALP. So HDAC6 can control misfolded proteins through regulation of ALP and UPS.

HDAC6 is involved in neurological diseases, through some unclear mechanism. It is commonly accepted that HDAC6 affects the occurrence and development of neurological diseases by diverse pathways, such as the formation of aggresomes, autophagy increase, and clearing away misfolded protein.

Neurological diseases consist of Alzheimer disease, Huntingtons disease, Parkinsons disease (PD), and Oculopharyngeal muscular dystrophy which are familiar to us. Related work reveals that PD is related with graceful degradation and death of dopamine (DA) neurons, HDAC6 can promote the formation of α-synuclein complex, and the latter can prevent DA neurons from the damage of oligomers (*23*). Recent research demonstrates that aggresomes combined with misfolded protein is the mainly pathologic feature of neurological diseases. Now we review the definition and function of aggresomes and misfolded protein in neurological diseases. Misfolded protein (*24*) usually forms a poisonous polymerand is one of the elements causing the death of neurons. Aggresome (*25*), a temporary structure, is formed by the remaining misfolded protein without being cleared away. It can prevent cells from poisoning caused by misfolded protein through autophagy, and suspend the occurrence and development of neurological diseases. The formation of aggresome is a specific and active cellular protective response. HDAC6 can regulate either the formation of aggresome or autophagy as a component of aggresomes. Central nervous system (CNS) injury (*26*) is another neurological disease characterized by insufficient axonal regeneration and oxidative stress-induced neurodegeneration (*27,28*). Genetic and pharmacological approaches are employed to demonstrate the role of HDAC6 in CNS injury, and this fact reveals that inhibition of HDAC6 can promote regeneration of neurons in CNS injury (*29*). So HDAC6 can also be regarded as a target for a potential nontoxic therapy of CNS trauma.

Heart failure induced by pulmonary arterial hypertension has been studied recently. Catalytic activity of HDAC6 is consistently increased in myocardium and cultured cardiac myocytes and fibroblasts (*30*). This research describes a role in the heart for HDAC6, and HDAC6 can be regarded as a therapy for heart disease. In addition DNA damage caused by selective inhibition of HDAC6 was also reported recently.

3. Relationship with cancer

HDAC6 participates in tumorigenesis, development and metastasis by way of tubulin, HSP90, invasin and ubiquitin-protein (*14*). HDAC6 is mainly distributed in cytoplasm (*31*), and highly expressed in heart, liver, kidney, and pancreas (*32*).

Research demonstrates that intracellular ubiquitination and deubiquitination of HDAC6 are involved in tumorigenesis. Ubiquitin-HDAC6 with deacetylation activity disturbs normal gene transcription and protein expression in the course of chromosome condensation. So ubiquitination and deubiquitination of HDAC6 are of great importance in therapy of malignancy caused by a disorder of ubiquitination (*32*). HSP90 is an important regulator in cellular signal transduction, Aoyagi (*33*) and coworkers found that HSP90 is directly regulated by HDAC6. A decrease of HDAC6 expression induces acetylation of HSP90 and α-tubulin, then inhibits the combination with HSP90 and ATP, in this course the combination of chaperone and oncogene is reduced. Targeted inhibition of HDAC6 acetylates HSP90, and destroys the function of chaperone (*34*). It is of great importance in biological cancer treatment.

Inhibition of HDAC6 shows a synergistic role with known anticarcinogens in some cancers. Combined implication of bortezomib and tubocurarine chloride inhibiting proteasome and invasin can enhance the therapeutic effect on multiple myeloma (*32*). Estradiol can enhance the expression of mRNA and protein with respect to HDAC6, and remarkably enhance cell motility (*35*). While tamoxifen, a kind of antiestrogen, can obviously inhibit tubulin deacetylation, and consequently reduces cell motility which reveals the relationship of HDAC6 and tumor metastasis (*35*). HDAC6 can be regarded as one of the significant prognostic indicators through estrogen signaling. The therapeutic effect on malignancy can also be enhanced through the combination of Taxanes and endocrinotherapy.

Research shows that HDAC6 also plays a rolein ovarian cancer, ER+ breast cancer, esophageal cancer and gastric cancer. Consequently HDAC6 draws the attention of scientists for cancer therapy without cytotoxicity.

4. Selective inhibitors of HDAC6

To date, there are many structurally diverse HDACs inhibitors synthesized, such as hydroxamic acid derivatives, benzamides, carboxylates (short chain fatty acids), cyclic peptides, and electrophilic ketones. Most of them are pan-inhibitors without selectivity, such as SAHA, tri-chostatin A (TSA), trapoxin B, and MS-275 and are identified as the earliest inhibitors of HDACS. Cytotoxicity causing side-effects for patients is observed during cancer therapy, so isoform-selective inhibitors avoiding severe side-effects have been studied. With its unique physiological function and structure HDAC6 has been regarded as a new target for cancer therapy. With scientists' efforts, such structurally diverse selective inhibitors of HDAC6 have been described. According to the structure of the zinc binding group (ZBG), HDAC6 inhibitors are grouped into five types.

4.1. *Hydroxamic acid*

This type has been studied as the ZBG in the beginning, it is regarded as the most potent inhibitor for cancer therapy. Following the authorization of the first HDAC inhibitor SAHA by FDA, a number of structurally diverse inhibitors of this type have been described.

4.1.1. *Tubacin*

Tubacin (Figure 3) is identified as the first HDAC6 inhibitor which targets tubulin acetylation. It was screened by Haggarty *et al*. (*36,37*) through a high-throughput screening which is a multidimensional chemical genetic process. It is characterized by a 1,3-dioxane structure. To identify its tubulin acetylation and selectivity, Western blot analysis targeting tubulin and histone H3 was carried out with human A549 lung carcinoma cells. The study revealed that tubacin caused a dose-dependent increase of tubulin acetylation compared to H3 acetylation (*39*). It was also proved that tubacin decreased the level of cell motility in lymphocytes and showed (*39*) no effect on stability of microtubules.

A synergistic effect of tubacin and bortezomib was studied in multiple myeloma (MM) cell lines, cytotoxicity was not observed in normal noncancerous peripheral blood mononuclear cells. So a synergistic effect with tubacin and bortezomib is of great significance for cancer therapy.

4.1.2. *Isoxazole containing hydroxamic acids*

A series of new HDAC6 inhibitors characterized by

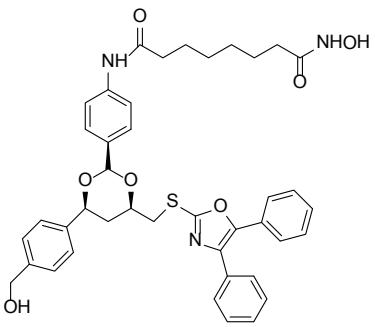

Figure 3. Structure of tubacin.

the CAP group with arylisoxazole (*38*) have been synthesized through the chemistry of nitrile oxide cycloaddition.

The typical compounds of this series consist of **3**, **4**, **7**, **8**, and **11** (Figure 4), the activity of such compounds has been evaluated in order to understand the structure-activity relationship and structure-selective relationship, and their activities have been tested with isolated enzymes and pancreatic cancer cell lines *in vitro* (*38*). The results showed that the best compound **7** displayed an IC_{50} value of 2 pM towards HDAC6 and high selectivity, and its antiproliferative activity is nearly 11-fold more potent than SAHA (*38*). Compound **7** is characterized by a linker of 6-methylene units and a Boc protected on arylisoxazole.

Compounds characterized by only the position of the BOC-protected group different from compound **7** also showed high potency and selectivity. Compound **11** synthesized by replacement of the BOC group with an acetyl group induced a considerable drop in enzyme inhibition activity (*38*). When we compared the activity of compound **4** and **8** with the relative compounds **3** and **7**, the same drop in potency was observed. Above all, the results demonstrate that the bulky lipophilic group and 6-methylene units are of great importance in enzyme assays.

As observed, compound **7** of this series is the most potent and selective for HDAC6 and more potent than SAHA, so it is highly potent for exploring HDAC6 biology and cancer treatment.

4.1.3. *Arylalanine acid*

Arylalanine containing hydroxamic acids have been identified as other HDAC6 selective inhibitors. In order to identify favorable structural elements of this type (*41*), structurally diverse arylalanine containing inhibitors have been synthesized from inhibitor SW55 (*39,40*). In the beginning compound **3** was synthesized, then series 4 (Figure 5) as the analoges of **3** were synthesized. *In vitro* selectivity and activity towards HDAC6 of the **4** series were tested through immunoprecipitated HDACD1 and HDAC6, and compound **4e** with a linker of 7 methylene spacers length and bromophenylalanine **4n** with a 6 methylene linker showed high potency and selectivity, and both compounds were also evaluated by Western blot through histone and tubulin acetylation (*42*). High selectivity of both compounds was revealed with hyperacetylation in the low micromolar range towards tubulin.

Pyridylalanines compound **8b** and phenylalanine compound **8c** (Figure 5) as analogues of compound **4n** have been synthesized for structural elements of this series. Activity and selectivity of them were also evaluated through immunoprecipitated HDACD1 and HDAC6 and Western blot (*42,43*). Both of them showed high selectivity and activity. Configuration of this series has also been studied in pyridylalanines compounds, and the research showed us a higher selectivity in compound **8b** with an S configuration (*42*). The spacer lengh of 6 methylenes was regarded as the best linker for pyridylalanines compounds.

Arylalanine diverse compounds have specific traits for highly potent selectivity towards HDAC6. Bromophenylalanine with a 6 methylene linker, pyridylalanines with a 6 methylene linker and phenylalanine with an 8 methylene linker are considered as the best selective HDAC6 inhibitors. The structure-activity relationship and structure-selectivity relationship have been identified. An azelaic acid spacer, with a 3-heteroaryl substituent were revealed as favorable structural elements. The research reveals a significative way of designing compounds with high potency and selectivity for HDAC6.

4.1.4. *Cyclic tetrapeptides*

Compounds containing cyclic peptides have been studied as inhibitors of HDACS, such as trapoxin B and CHAP31 containing different ZBG. Both of the compounds were tested for HDAC6 selectivity, but results were illusionary. However, research of cyclic peptides are still in the progress. With the effort of chemists, a cyclic tetrapeptide scaffold is used for selective HDAC6 inhibition (*44*). The compound containing the Tyr–Arg motif at aa3–aa4 positions was regared as a leading compound. Further study has been done on the modification of the aa2 position, and compounds **22** and **23** (Figure 6) with different ZBG were synthesized by introducing an Asp residue at the aa2 position, the latter containing hydroxamate is the most potent and selective for HDAC6 in *in vitro* enzyme assays (*44*). Confirmation of the *in vitro* activity of compound **23** was exhibited with the result of higher tubulin acetylation compared to histone 3 (*44*).

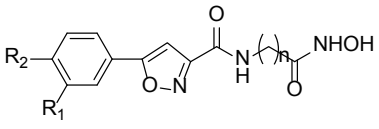

Figure 4. Structure of compounds containing isoxazole and triazole. 3: R1 = NHBOC, R2 = H, n = 6. **4**: R1 = NHBOC, R2 = H, n = 4. **7**: R1 = H, R2 = NHBOC, n = 6. **8**: R1 = H, R2 = NHBOC, n = 4. **11**: R1 = H, R2 = AcNH, n = 6.

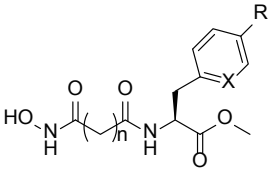

Figure 5. Structures of compounds 3 series and 4 series. Compound **3**: n = 6, R = phenyl, X = H; **4e**: n = 7, R = 3-thienyl, X = H; **4n**: n = 6, R = Br; **8b**: n = 6, X = N, R = -H; **8c**: n = 8, X = CH, R = -H.

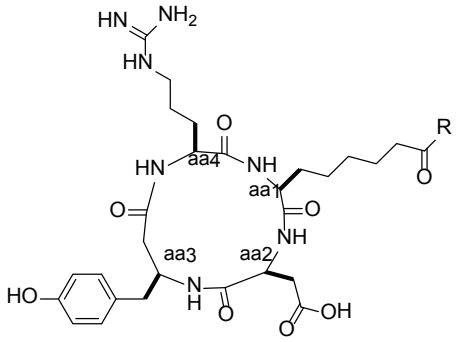

Figure 6. Structure of compound 22 and 23. Compound **22**: R = OH; **23**: R = NHOH.

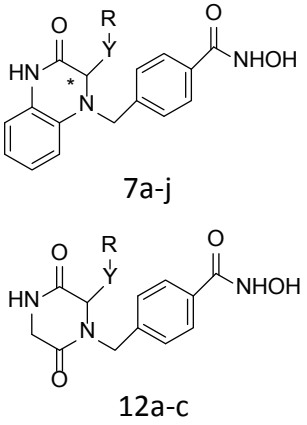

Figure 7. Structure of compounds 7 series and 12 series.

With the appearance of compound **23**, compounds with cyclic tetrapeptides are not non-selective any more. Modification at the aa2 position of the cyclic tetrapeptide structure displayed a promising improvement for HDAC6 selectivity.

4.1.5. *Chiral 3,4-dihydroquinoxalin-2(1H)-one and piperazine-2,5-dione aryl hydroxamates*

Novel 3,4-dihydroquinoxalin-2(1H)-one and piperazine-2,5-dione aryl hydroxamates displaying selectivity and potency for HDAC6 have been designed and synthesized, they are evaluated to have about a 40-fold selectivity for HDAC6 over HDAC1 (*45*). *In vitro* enzyme assays with compounds of the 7 series with dihydroquinoxalin displayed higher potency than the 12 series with piperazine (*45*), the result showed that cap dihydroquinoxalin had a performance increase for greater selectivity than that of series 12.

The structure-selectivity relationship of both series was studied. Achiral compound **7a** displayed no preferential a-tubulin acetylation over H3 acetylation than other chiral compounds (*45*), consequently the chiral center of such compounds is of great importance in selectivity and potency. By comparison with compounds **7b**, **7c**, **7d**, **7e**, **7i**, **7j** and **12a**, **12b**, **12c** (Figure 7), the conclusion is that the most selective and potent compounds with such structural elements are characterized by the configuration of the chiral centre rather than substituent 'R'.

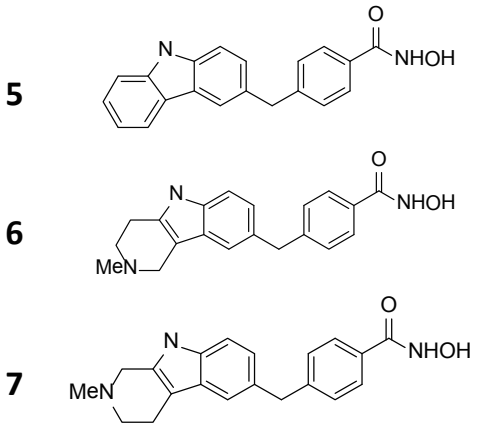

Figure 8. Structure of compound 5, 6, and 7.

Structural features of compounds **7b**, **7d**, **7i**, **7j**, and **12a** can be used for designing more potent selective inhibitors, as well as probing the biology of specific HDAC isoforms.

4.1.6. *The tricyclic inhibitors tubastatin A*

HDAC inhibitors containing a tricyclic structure were reported highly selective for HDAC6. Tubacin (Figure 3), the first HDAC6 selective inhibitor, was usually a probe for biology and selectivity for HDAC6 as a result of its high lipophilicity. A series of compounds with carbazole group and alkylaryl linker were synthesized based on the specificity of HDAC6 with a wider and shallower channel.

In order to find drug-like compounds, the lipophilicity should be decreased with regard to tubacin with high lipophilicity by introducing a tertiary amino on the carbazole of compound **5** (Figure 8), the tertiary amino moiety can form salts improving the solubility of compounds. Compound **6** and **7** respectively characterized with tetrahydro-γ-carboline and tetrahydro-β-carboline were obtained through modification of the tricyclic, both of the compounds displayed higher selectivity for HDAC6 over HDAC1 compared to tubacin (*46*). Compound **6** named tubastatin A displayed an IC_{50} value of 15 nM towards HDAC6 and about 1000-fold selectivity for HDAC6 over HDAC1 (*46*). Tubastatin displayed neuroprotective action in a cell model of oxidative stress and is the first HDAC6 inhibitor with neuroprotection (*46*).

Some brand-name drugs have already been demonstrated that have high selectivity and potency for HDAC6. Bufexamac (Figure 9) usually regarded as a nonsteroidal anti-inflammatory drug was found during a high-throughput adaptation of chemoproteomics for selective HDAC inhibitors. Selective HDAC6 inhibition of Bufexamac was confirmed through tubulin immunofluorescence and Western blot (*47*).

A series of compounds were synthesized through modification at the C3 position of SAHA, these analogues also demonstrated high selectivity for HDAC6 (*48*). Compound **1e** (Figure 9) with a methyl introduced at the C3 position is the most selective and potent of this series.

The existing compounds should never be ignored in probing HDAC6 selective inhibitors, as it may be highly potent for isoform selectivity.

4.2. *Thiol based inhibitors and their ester prodrugs*

Under the attention of selective HDAC6 inhibitors with little side-effects, many researchers devote themselves to finding better compounds for HDAC inhibition, and therefore structurally diverse groups were used for substituent groups for ZBG and CAP in order to study their structural elements required for HDAC6 selective inhibitors. With the effort of Itoh and Suzuk, a series of compounds with thiol (Figure 10) and diverse CAP groups were synthesized for HDAC6 inhibition (*49,50*). It was the first time that compounds containing thiol were used as selective HDAC6 inhibitors. These compounds were evaluated by HDAC1, HDAC4, and HADC6, and their selectivity for HDAC6 was better than tubacin. Compound **11a**, IC_{50} of 23 nM towards HDAC6, was the most potent, and compound **13a**, 46-fold selectivity for HDAC6/HDAC1 and 51-fold selectivity for HDAC6/HDAC4 (*49*), was the most selective. With comparison research, bulky alkyl and tert-butylcarbamate groups are structural elements for selectivity of HDAC6 (*49,50*). As thiol analogues **9b-13b** with thioesters can enhance stability and lipophilicity, compounds **9b-13b** were used for Western blots instead of **9a-13a** in order to confirm activity observed in *in vitro* enzyme assays, and the result showed an increased acetylation of tubulin acetylation rather than histone 4 (*49*).

In a recent study, compound **9a** was used for synthesizing a series of analoges characterized with five methylenes, diverse ZBG, and CAP. The structure-selectivity relationship was investigated for these analoges. Compound **16** (Figure 10) containing hydroxamate with an IC_{50} value of 26 nM towards HDAC6 and 55-fold selectivity for HDAC6/HDAC1 in *in vitro* enzyme assays was the most potent and selective for HDAC6 (*51*). Through comparing and analyzing with other analoges which were structurally different in the ZBG and N-terminus groups, Boc and cyclopentyl groups on CAP were necessary for selective HDAC6 inhibitors containing thiol, and a high affinity ZBG was discovered unfit for isoform selectivity compared with a compound containing carboxyl, thiol, and hydroxamate.

Compounds containing thiol can be converted into thioesters with high stability and lipophilicity, the latter with good pharmacokinetic properties can reduce the paclitaxel dosage in cancer treatment and with less cytotoxicity. All in all, thiol analoges have already been regarded as a new strategy for cancer therapy to avoid side effects.

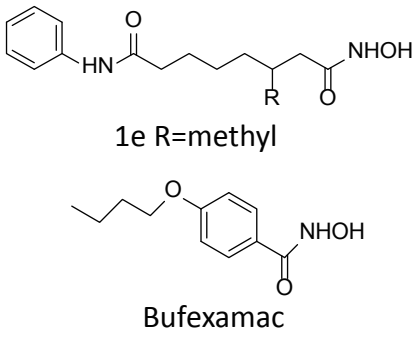

Figure 9. Structure of bufexamac and 1e.

4.3. *Sulfamides*

From the study of Jones *et al*. (*52,53*), we found a potent HDAC inhibitor with a methylketone ZBG. Based on their study, researchers tried to find if compounds with the sulfamide at the e-nitrogen are potent and selective for HDAC6 inhibition. Compounds **14a** and **14b** were synthesized with a lysine scaffold, while compounds **13e** and **13f** were synthesized by removal of the ZBG as linear long-chain-based analoges (Figure 11). Both of the two types of compounds were

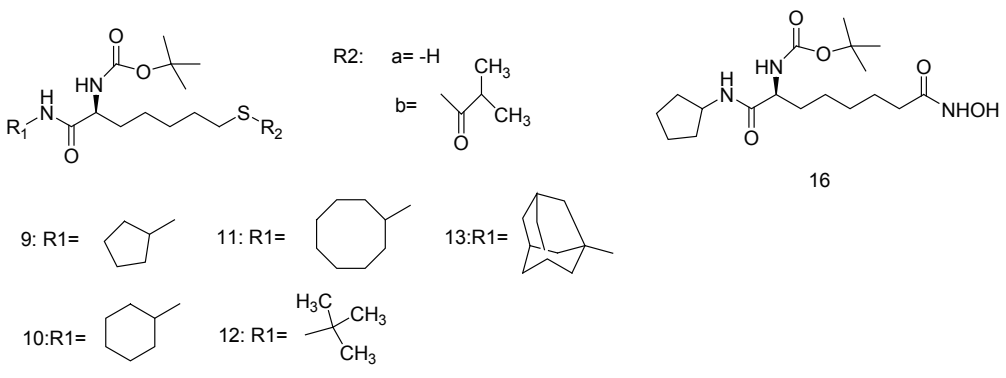

Figure 10. Structures of compounds with thiol.

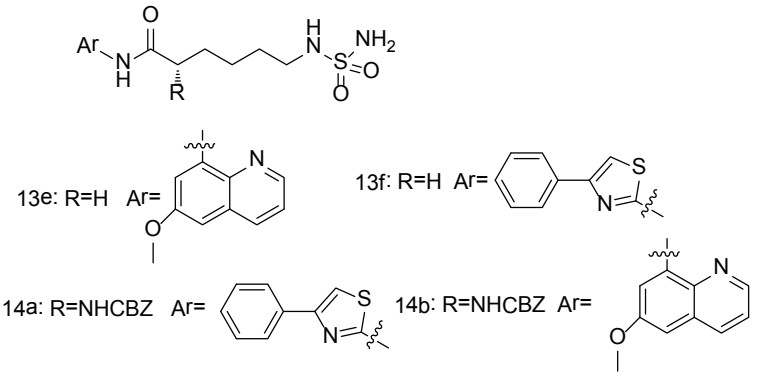

Figure 11. Structures of 13e, 13f, 14a, and 14b.

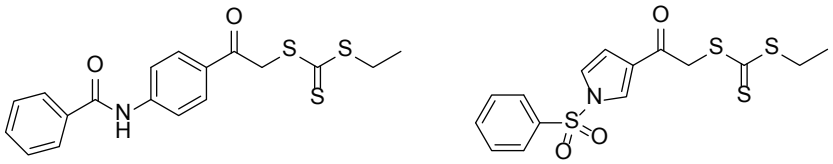

12ac 13

Figure 12. Structures of compounds 12ac and 13.

evaluated in *in vitro* enzyme assays with HDAC1 and HDAC6.

Compounds **13e** and **13f** showed higher potency for tubulin acetylation than histone 3 confirming enzyme assays for HDAC6 and HDAC1 (*54*). This suggested that compounds with linear long-chains showed obvious selectivity for HDAC6. The most potent compound **14b** exhibited an EC_{50} of 0.35 μM and 0.2 μM towards H3Ac and TubAc respectively (*54*), its activity is similar to that of SAHA.

The observed enzymatic potencies and cellular activities of compounds with a sulfamide moiety showed a new way for designing selective HDAC6 inhibitors which can be characterized with linear long-chains and sulfamide ZBG. Of course if you just want to increase the potency for HDAC6, synthesis of compounds with a lysine scaffold is a good choice.

4.4. *Trithiocarbonates*

As is mentioned above, thiol can be regarded as a ZBG in designing selective HDAC6 inhibitors. Because compounds displayed better activity *in vitro* rather than *in vivo*, scientists usually used thioesters which were analoges of relevant thiols to design more potent and selective HDAC6 inhibitors intracellularly. On that basis thioglycolamides, thiocarboxylates and thiol-substituted acetyls have been used as ZBGs for HDAC inhibitors. Through bioresearch and chemical study, trithiocarbonates are considered as a new ZBG for HDAC inhibitors.

Compound **12ac** (Figure 12) was described as a selective HDAC6 inhibitor of all compounds with trithiocarbonate, and compound **12ac** with a phenylacetyl moiety as the CAP group displayed better selectivity for HDAC6 (IC_{50} of 65 nm) over HDAC1(IC_{50} of 1.22 μM)in *in vitro* enzyme assays (*55*). The selective inhibition was also confirmed with the result that tubulin hyperacetylation (10 μM) was stronger than that of histone 3 (*55*). Compound **13** (Figure 13) structurally characterized with a pyrrole-N-sulfonamide displayed an IC_{50} of 9 nM for HDAC6 and an IC_{50} of 2.1 μM for HDAC1 (*55*).

Up to now such compounds were rarely studied, so compounds with trithiocarbonate as a new ZBG display a significant prospect for selective HDAC6 inhibitors.

4.5. *NQN naphthoquinone*

Recent research revealed an absolutely new selective HDAC inhibitor with a central naphthoquinone structure which didn't conform to the prototype of conventional HDAC inhibitors with CAP, linker and ZBG. The compound named NQN was screened by The Library of Pharmacologically Active Compounds (LOPAC, 1280 compounds) (*56*). As NQN is the central structure of vitamin K, analogues of vitamin K such as vitamin K3, NQN-1, NQN-2, and NQN-3 (Figure 13) were synthesized. In *in vitro* enzymeassays vitamin K3 was evaluated with an IC_{50} at low micromolar levels, NQN-1 was the most selective for HDAC6 with an IC_{50} of 5.54 μM, NQN-2 with one methylene extension of NQN-1 displayed an IC_{50} of 15.6 μM, NQN-3 with the carbonyl removed from NQN-1 was the least potent and selective for HDAC6 of this series of compounds with an IC_{50} > 180 μM (*56*). In AML MV4-11 cells, NQN-1 still induces hyperacetylation of tubulin rather than H3 and H4 (*56*). Interestingly NQN-1 can also induce

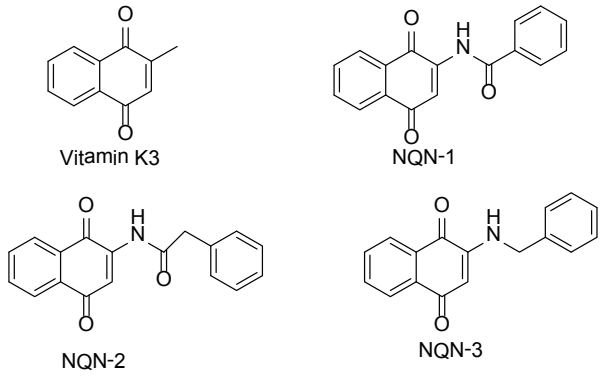

Figure 13. Structure of compounds vitamin K3, NQN-1, NQN-2, and NQN-3.

Hsp90 acetylation and FLT-3 and STAT5 depletions by comparison with SAHA, TSA, and tubastatin A (*56*).

It has been found that the carbonyl which links naphthoquinone and phenyl groups was necessary for HDAC6 inhibition through the inhibitory activity of vitamin K3 and NQN-3, and the larger phenyl group was not required for the NQN-2 result with a one carbon extension showing a less potent HDAC6 selectivity than NQN-1.

5. Summary and outlook

HDAC6 with specific structure and biological function plays a significant role in the carcinogenesis, progression and metastasis of tumors. HDACs inhibitors have been regarded as a new therapy for cancer and have also been used for neurological disorders. With the study of HDAC6 novel structurally diverse compounds were identified as HDAC6 inhibitors, and such new HDAC6 inhibitors didn't conform to the structure of typical HDAC inhibitors. The results show that we should break new ground in designing HDAC6 inhibitors, in the future more potent and selective HDAC6 inhibitors with absolutely new structures will be discovered. As the study of HDAC6 is in an initiation phase, HDAC6 will be a hot topic for cancer therapy.

Acknowledgements

This work was financially supported by national high technology research and development program of China (863 project; Grant No. 2007AA02Z314) and National Science and Technology Major Project (Grant No. 2009ZX09103-118). The statements in this paper reflect the reviews of the authors and we apologize for any unintended missed references in this review.

References

1. Biel M, Wascholowski V, Giannis A. Epigenetics an epicenter of gene regulation: Histones and histone-modifying enzymes. Angew Chem Int Ed Engl. 2005; 44:3186-3216.
2. Schafer S, Jung M. Chromatin modifications as targets for new anticancer drugs. Arch Pharm (Weinheim). 2005; 338:347-357.
3. Grunstein M. Histone acetylation in chromatin structure and transcription. Nature. 1997; 389:349-352.
4. Weidle UH, Grossmann A. Inhibition of histone deacetylases: A new strategy to target epigenetic modifications for anticancer treatment. Anticancer Res. 2000; 20:1471-1485.
5. Hubbert C, Guardiola A, Shao R, Kawaguchi Y, Ito A, Nixon A, Yoshida M, Wang XF, Yao TP. HDAC6 is a microtubule-associated deacetylase. Nature. 2002; 417:455-458.
6. Matsuyama A, Shimazu T, Sumida Y, Saito A, Yoshimatsu Y, Seigneurin-Berny D, Osada H, Komatsu Y, Nishino N, Khochbin S, Horinouchi S, Yoshida M. In vivo destabilization of dynamic microtubules by HDAC6-mediated deacetylation. EMBO J. 2002; 21:6820-6831.
7. Zhang Y, Li N, Caron C, Matthias G, Hess D, Khochbin S, Matthias P. HDAC-6 interacts with and deacetylates tubulin and microtubules in vivo. EMBO J. 2003; 22:1168-1179.
8. North BJ, Marshall BL, Borra MT, Denu JM, Verdin E. The human Sir2 ortholog, SIRT2, is an NAD+-dependent tubulin deacetylase. Mol Cell. 2003; 11:437-444.
9. Valenzuela-Fernandez A, Cabero JR, Serrador JM, Sanchez-Madrid F. HDAC6: A key regulator of cytoskeleton, cell migration and cell-cell interactions. Trends Cell Biol. 2008; 16:291-297.
10. Zhou H, Wu Y, Navre M, Sang BC. Characterization of the two catalytic domains in histone deacetylase 6. Biochem Biophys Res Commun. 2006; 341:45-50.
11. De Ruijter AJM, Van Gennip AH, Caron HN, Kemp S, and VanKuilenburg ABP. Histonedeacetylases (HDACs): Characterization of the classical HDAC family. Bioche mical Journal. 2003; 370:737-749.
12. Boyault C, Sadoul K, Pabion M, and hochbin SK. HDAC6, at the crossroads between cytoskeleton and cell signaling by acetylation and ubiquitination. Oncogene. 2007; 26:5468-5476.
13. Seigneurin-Berny D, Verdel A, Curtetetal S. Identification of components of the murine histone deacetylase 6 complex: Link between acetylation and ubiquitination signaling path-ways. Mol Cell Biol. 2001; 21:8035-8044.
14. Aldana-Masangkay GI, Sakamoto KM. The Role of HDAC6 in Cancer. J Biomed Biotechnol. 2011; 2011:875824.
15. Breslow R, Belvedere S, Gershell L. Development of cyto differentiating agents for cancer chemotherapy. Helv Chim Acta. 2000; 83:1685-1692.
16. Nishino N, Jose B, Okamura S, Ebisusaki S, Kato T, Sumida Y, Yoshida M. Cyclic tetrapeptides bearing a sulfhydryl group potently inhibit histone deacetylases. Org Lett. 2003; 5:5079-5082.
17. Itazaki H, Nagashima K, Sugita K, Yoshida H, Kawamura Y, Yasuda Y, Matsumoto K, Ishii K, Uotani N, Nakai H. Isolation and structural elucidation of new cyclotetrapeptides, trapoxins A and B, having detransformation activities as antitumor agents. J Antibiot (Tokyo). 1990; 43:1524-1532.
18. Suzuki T, Ando T, Tsuchiya K, Fukazawa N, Saito A, Mariko Y, Yamashita T, Nakanishi O. Synthesis and histone deacetylase inhibitory activity of new benzamide derivatives. J Med Chem. 1999; 42:3001-3003.

19. Haggarty SJ, Koeller KM, Wong JC, Grozinger CM, Schreiber SL. Domain-selective small-molecule inhibitor of histone deacetylase 6 (HDAC6)-mediated tubulin deacetylation. Proc Natl Acad Sci U S A. 2003; 100:4389-4394.
20. Parmigiani RB, Xu WS, Venta-Perez G, Erdigument-Bromage H, Yaneva M, Tempst P, Marks PA. HDAC6 is a specific deacetylase of peroxiredoxins and is involved in redox regulation. Proc Natl Acad Sci U S A. 2008; 105:9633-9638.
21. Rubinsztein DC. The rolesof intracellular protein-degradation pathways in neurodegeneration. Nature. 2006; 443:780-786.
22. Olzmann JA, Li L, Chudaev MV, Chen J, Perez FA, Palmiter RD, Chin LS. Parkin-mediated K63-linked polyubiquitination targets misfolded DJ-1 to aggresomes via binding to HDAC6. J Cell Biol. 2007; 178:1025-1038.
23. Du G, Liu X, Chen X, Song M, Yan Y, Jiao R, Wang CC. Drosophila histone deacetylase 6 protects dopaminergic neurons against {alpha}-synuclein toxicity by promoting inclusion formation. Mol Biol Cell. 2010; 21:2128-2137.
24. Hoozemans JJ, van Haastert ES, Eikelenboom P, de Vos RA, Rozemuller JM, Scheper W. Activation of the unfolded protein response in Parkinson's disease. Biochem Biophys Res Commun. 2007; 354:707-711.
25. Taylor JP, Tanaka F, Robitschek J, Sandoval CM, Taye A, Markovic-Plese S, Fischbeck KH. Aggresomes protect cells by enhancing the degradation of toxic polyglutamine-containing protein. Hum Mol Genet. 2003; 12:749-757.
26. Rivieccio MA, Brochier C, Willis DE, Walker BA, D'Annibale MA, McLaughlin K, Siddiq A, Kozikowski AP, Jaffrey SR, Twiss JL, Ratan RR, Langley B. HDAC6 is a target for protection and regeneration following injury in the nervous system. Proc Natl Acad Sci U S A. 2009; 106:19599-19604.
27. Anderson MF, Sims NR. The effects of focal ischemia and reperfusion on the glutathione content of mitochondria from rat brain subregions. J Neurochem. 2002; 81:541-549.
28. Young W. Secondary injury mechanisms in acute spinal cord injury. J Emerg Med. 1993; 11(Suppl 1):13-22.
29. Iwata A, Riley BE, Johnston JA, Kopito RR. HDAC6 and microtubules are required for autophagic degradation of aggregated huntingtin. J Biol Chem. 2005; 280:40282-40292.
30. Lemon DD, Horn TR, Cavasin MA, Jeong MY, Haubold KW, Long CS, Irwin DC, McCune SA, Chung E, Leinwand LA, McKinsey TA. Cardiac HDAC6 catalytic activity is induced in response to chronic hypertension. J Mol Cell Cardiol. 2011; 51:41-50.
31. Saji S, Kawakami M, Hayashi S, Yoshida N, Hirose M, Horiguchi S, Itoh A, Funata N, Schreiber SL, Yoshida M, Toi M. Significance of HDAC6 regulation via estrogen signaling for cell motility and prognosis in estrogen receptor-positive breast cancer. Oncogene. 2005; 24:4531-4539.
32. Hideshima T, Bradner JE, Wong J, Chauhan D, Richardson P, Schreiber SL, Anderson KC. Small-molecule inhibition of proteasome and aggresome function induces synergistic antitumor activity in multiple myeloma. Proc Natl Acad Sci U S A. 2005; 102:8567-8572.
33. Aoyagi S, Archer TK. Modulating molecular chaperone Hsp90 functions through reversible acetylation. Trends Cell Biol. 2005; 15:565-567.
34. Bali P, Pranpat M, Bradner J, Balasis M, Fiskus W, Guo F, Rocha K, Kumaraswamy S, Boyapalle S, Atadja P, Seto E, Bhalla K. Inhibition of histone deacetylase6 acetylates and disrupts the chaperone function of heat shockprotein90: A novel basis for antileukemia activity of histone deacetylase inhibitors. J Biol Chem. 2005; 280:26729- 26734.
35. Saji S, Kawakami M, Hayashi S, Yoshida N, Hirose M, Horiguchi S, Itoh A, Funata N, Schreiber SL, Yoshida M, Toi M. Significance of HDAC6 regulation via estrogen signaling for cell motility and prognosis in estrogen receptor-positive breast cancer. Oncogene. 2005; 24:4531-4539.
36. Haggarty SJ, Koeller KM, Wong JC, Butcher RA, Schreiber SL. Multidimensional chemical genetic analysis of diversity-oriented synthesis-derived deacetylase inhibitors using cell-based assays. Chem Biol. 2003; 10:383-396.
37. Haggarty SJ, Koeller KM, Wong JC, Grozinger CM, Schreiber SL. Domain-selective small-molecule inhibitor of histone deacetylase 6 (HDAC6)-mediated tubulin deacetylation. Proc Natl Acad Sci U S A. 2003; 100:4389-4394.
38. Kozikowski AP, Tapadar S, Luchini DN, Kim KH, Billadeau DD. Use of the nitrile oxide cycloaddition (NOC) reaction for molecular probe generation: A new class of enzyme selective histone deacetylase inhibitors (HDACIs) showing picomolar activity at HDAC6. J Med Chem. 2008; 51:4370-4373.
39. Wittich S, Scherf H, Xie C, Brosch G, Loidl P, Gerhauser C, Jung M. Structure-activity relationships on phenylalanine-containing inhibitors of histone deacetylase: In vitro enzyme inhibition, induction of differentiation, and inhibition of proliferation in friend leukemic cells. J Med Chem. 2002; 45:3296-3309.
40. Wittich S, Scherf H, Xie C, Heltweg B, Dequiedt F, Verdin E, Gerhauser C, Jung M. Effect of inhibitors of histone deacetylase on the induction of cell differentiation in murine and human erythroleukemia cell lines. Anticancer Drugs. 2005; 16:635-643.
41. Schafer S, Saunders L, Eliseeva E, Velena A, Jung M, Schwienhorst A, Strasser A, Dickmanns A, Ficner R, Schlimme S, Sippl W, Verdin E. Phenylalanine-containing hydroxamic acids as selective inhibitors of class IIb histone deacetylases (HDACs). Bioorg Med Chem. 2008; 16:2011-2033.
42. Schäfer S, Saunders L, Schlimme S, Valkov V, Wagner JM, Kratz F, Sippl W, Verdin E, Jung M. Pyridylalanine-containing hydroxamic acids as selective HDAC6 inhibitors. Chem Med Chem. 2009; 4:283-290.
43. Scott GK, Marx C, Berger CE, Saunders LR, Verdin E, Schäfer S, Jung M, Benz CC. Destabilization of ERBB2 transcripts by targeting 3' UTR mRNA associated HuR and histone deacetylase-6 (HDAC6). Mol Cancer Res. 2008; 6:1250-1258.
44. Olsen CA, Ghadiri MR. Discovery of potent and selective histone deacetylase inhibitors via focused combinatorial libraries of cyclic α3β-tetrapeptides. J Med Chem. 2009; 52:7836-7846.
45. Smil DV, Manku S, Chantigny YA, et al. Novel HDAC6 isoform selective chiral small molecule histone deacetylase inhibitors. Bioorg Med Chem Lett. 2009; 19:688-692.
46. Butler KV, Kalin J, Brochier C, Vistoli G, Langley B, Kozikowski AP. Rational design and simple chemistry yield a superior, neuroprotective HDAC6 inhibitor, tubastatin A. J Am Chem Soc. 2010; 132:10842-10846.
47. Bantscheff M, Hopf C, Savitski MM, et al.

Chemoproteomics profiling of HDAC inhibitors reveals selective targeting of HDAC complexes. Nat Biotechnol. 2011; 29:255-265.
48. Choi SE, Weerasinghe SV, Pflum MK. The structural requirements of histone deacetylase inhibitors: Suberoylanilide hydroxamic acid analogs modified at the C3 position display isoform selectivity. Bioorg Med Chem Lett. 2011; 21:6139-6142.
49. Itoh Y, Suzuki T, Kouketsu A, Suzuki N, Maeda S, Yoshida M, Nakagawa H, Miyata N. Design, synthesis, structure–selectivity relationship, and effect on human cancer cells of a novel series of histone deacetylase6-selective inhibitors. J Med Chem. 2007; 50:5425-5438.
50. Suzuki T, Kouketsu A, Itoh Y, Hisakawa S, Maeda S, Yoshida M, Nakagawa H, Miyata N. Highly potent and selective histone deacetylase 6 inhibitors designed based on a small-molecular substrate. J Med Chem. 2006; 49:4809-4812.
51. Gupta PK, Reid RC, Liu L, Lucke AJ, Broomfield SA, Andrews MR, Sweet MJ, Fairlie DP. Inhibitors selective for HDAC6 in enzymes and cells. Bioorg Med Chem Lett. 2010; 20:7067-7070.
52. Jones P, Altamura S, Chakravarty PK, Cecchetti O, De Francesco R, Gallinari P, Ingenito R, Meinke PT, Petrocchi A, Rowley M, Scarpelli R, Serafini S, Steinkühler C. A series of novel, potent, and selective histone deacetylase inhibitors. Bioorg Med Chem Lett. 2006; 16:5948-5952.
53. Jones P, Altamura S, De Francesco R, Paz OG, Kinzel O, Mesiti G, Monteagudo E, Pescatore G, Rowley M, Verdirame M, Steinkühler C. A novel series of potent and selective ketone histone deacetylase inhibitors with antitumor activity in vivo. J Med Chem. 2008; 51:2350-2353.
54. Wahhab A, Smil D, Ajamian A, et al. Sulfamides as novel histone deacetylase inhibitors. Bioorg Med Chem Lett. 2009; 19:336-340.
55. Dehmel F, Weinbrenner S, Julius H, Ciossek T, Maier T, Stengel T, Fettis K, Burkhardt C, Wieland H, Beckers T. Trithiocarbonates as a novel class of HDAC inhibitors: SAR studies, isoenzyme selectivity, and pharmacological profiles. J Med Chem. 2008; 51:3985-4001.
56. Inks ES, Josey BJ, Jesinkey SR, Chou CJ. A novel class of small molecule inhibitors of HDAC6. ACS Chem Biol. 2012; 7:331-339.

(Received February 13, 2012; Accepted March 12, 2012)

Brief Report

DOI: 10.5582/ddt.2013.v7.6.243

Oxoprothracarcin, a novel pyrrolo[1,4]benzodiazepine antibiotic from marine *Streptomyces* sp. M10946

Yong Han[1], Yaoyao Li[1], Yan Shen[1], Jie Li[2], Wenjun Li[2], Yuemao Shen[1,*]

[1] *Key Laboratory of Chemical Biology (Ministry of Education), School of Pharmaceutical Sciences, Shandong University, Ji'nan, Shandong, China;*
[2] *Yunnan Institute of Microbiology, Yunnan University, Kunming, Yunnan, China.*

ABSTRACT: A novel pyrrolo[1,4]benzodiazepine antibiotic, designated oxoprothracarcin (3), was isolated from the marine strain *Streptomyces* sp. M10946 along with three known secondary metabolites, cyclo(D)-Pro-(D)-Val (1), cyclo(D)-Pro-(D)-Leu (2), and limazepine A (4). The chemical structures of these substances were elucidated by spectroscopic analyses, including 1D- and 2D-NMR and ESI-MS. Antitumor and antibacterial assays indicated that compounds 1-4 weakly inhibit the growth of MDA-MB-231 and A549 cells. The isolation of compound 3 with a high yield (36 mg/10 L) indicated that this marine *S.* sp. M10946 may provide new lead compounds for structural modification and drug screening.

Keywords: Marine Streptomyces, cyclo(D)-Pro-(D)-Val, cyclo(D)-Pro-(D)-Leu, oxoprothracarcin, limazepine A

1. Introduction

Traditionally, secondary metabolites produced by microorganisms, and especially terrestrial actinomycetes, are remarkable sources of lead compounds for drug discovery (*1*). However, the rate at which new metabolites from terrestrial actinomycetes are discovered has decreased, and the rate of re-isolation of known compounds has increased due to the replication of isolating microbial strains (*2*). Compared to terrestrial actinomycetes, marine actinomycetes are relatively unexploited sources (*3*). The fact that marine *Streptomyces* in particular are rich in novel bioactive metabolites is just becoming apparent (*4-6*). Moreover, genetic analysis has indicated that some marine-derived *Streptomyces* form an independent clade (*7*). The present study obtained four metabolites, i.e. cyclo(D)-Pro-(D)-Val (**1**) (*8*), cyclo(D)-Pro-(D)-Leu (**2**) (*8*), oxoprothracarcin (**3**) (*9-11*), and limazepine A (**4**) (*12*) (Figure 1), from the metabolites of marine *Streptomyces* sp. M10946. Reported here are the isolation, structural determination, and antitumor and antibacterial activities of compounds **1-4**.

**Address correspondence to:*
Dr. Yuemao Shen, School of Pharmaceutical Sciences of Shandong University, No. 44 West Wenhua Road, Ji'nan, Shandong 250012, China.
E-mail: yshen@sdu.edu.cn

2. Materials and Methods

2.1. *General*

NMR spectra were recorded on a Bruker Advance 600 spectrometer (Bruker, Fällanden, Switzerland) at 600/150 MHz. Mass spectra were obtained on ABI-4000 mass spectrometers (AB SCIEX, Framingham, MA, USA). An Agilent 1260 HPLC system (Agilent, Santa Clara, CA, USA) with a C-18 column (9.4 × 250 mm, 5 μm) was also used. Column chromatography included a RP-18 (Merck, Darmstadt, Germany) column and a Sephadex LH-20 column (GE healthcare, Uppsala, Sweden). TLC analyses were performed with precoated silica gel GF254 plates (0.20-0.25 mm, Qingdao Marine Chemical Factory, Qingdao, China). All general chemical reagents were purchased from Sinopharm Chemical Reagent Company (Beijing, China).

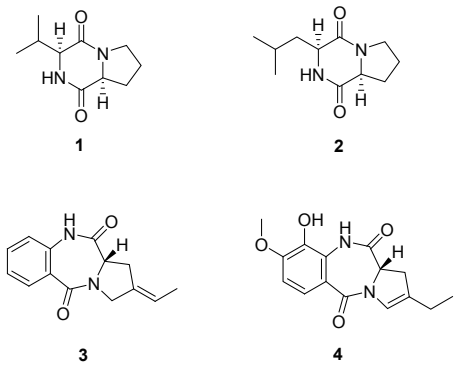

Figure 1. Chemical structures of compounds 1–4.

2.2. *Microorganism sample*

The strain *Streptomyces* sp. M10946 was isolated from mangrove sediment collected from Hut Bay and grown on medium containing trehalose as the sole carbon source [trehalose 10g, $(NH_4)_2SO_4$ 2.64 g, KH_2PO_4 2.38 g, K_2HPO_4 5.65 g, $MgSO_4 \cdot 7H_2O$ 1.0 g, $CuSO_4 \cdot 5H_2O$ 0.0064 g, $FeSO_4 \cdot 7H_2O$ 0.0011 g, $MnCl_2 \cdot 4H_2O$ 0.0079 g, $ZnSO_4 \cdot 7H_2O$ 0.0015 g, distilled water 1 L, pH 7.2-7.4] at 28ºC. This strain was identified as *Streptomyces* sp. by partial 16S rRNA gene sequencing analysis.

2.3. *Tumor cell lines*

The MDA-MB-231 human breast cancer cell line and A549 human lung cancer cell line were purchased from the American Type Culture Collection (ATCC). All cells were maintained in DMEM with 10% fetal bovine serum (FBS, Gibco) in a humidified CO_2 incubator in 5% CO_2 at 37°C.

2.4. *Fermentation and isolation*

Fermentation took place for 14 d on YMG (10 L) agar plates at 28°C. The culture was diced and extracted with AcOEt/MeOH/AcOH (80:15:5). The organic solution was collected through filtration and the remaining agar residue was extracted exhaustively with the same solvent until the filtrate was colorless. Upon evaporation, the combined filtrate yielded a crude extract. The crude extract was partitioned between water and EtOAc (1:1, v/v) until the EtOAc layer was colorless. The EtOAc extract was partitioned between MeOH and petroleum ether. The MeOH layer was concentrated in a vacuum to yield a brown syrupy extract (1.4 g). The extract was subjected to MPLC (30 g RP-18 silica gel; 30%, 50%, 70%, and 100% MeOH, 1 L for each gradient) to yield 4 fractions, Fr. a–d.

Fraction a (192 mg) was separated by column chromatography (CC) over Sephadex LH-20 (in MeOH) to yield one subfraction (Fr.a.1). Fr.a.1 (33 mg) was subjected to HPLC (C-18 column, 9.4 × 250 mm, 5 μm; 30% MeOH) to yield 1 (3 mg) and 2 (9 mg). Fraction b (240 mg) was subjected to CC over Sephadex LH-20 (in MeOH) to yield two subfractions (Fr.b.1 and Fr.b.2). Fr.b.1 (53mg) was purified by Sephadex LH-20 (in MeOH) to yield 3 (36 mg). Fr.b.2 (28 mg) was purified by recrystallization (MeOH) to yield 4 (20 mg).

2.5. *Biological study*

The cytotoxicity of compounds **1**-**4** was assessed using a 3-(4,5-dimethylthiazol-2-yl) –2,5-diphenyltetrazolium bromide (MTT) cell survival assay (*13*), Briefly, 3000 - 5000 MDA-MB-231 and A549 cells were seeded in 96-well plates overnight and treated three times with increasing concentrations of compounds. After the cells were treated for 72 h, a 10-μL of aliquot of MTT solution (5 mg/mL) was added and cells were incubated for 4 h at 37°C. Two hundred μL of DMSO was then added to dissolve formazan crystals. The color density was measured with a microplate reader (M-3350, Bio-Rad) at 570 nm. Growth inhibition rates were calculated as follows: $(A570_{\text{control cells}} - A570_{\text{treated cells}})/A570_{\text{control cells}} \times 100\%$.

The antibacterial activity of compounds **1** - **4** was tested against *Bacillus subtilis* (CMCC (B) 63501), *Bacillus pumilus* (CMCC (B) 63202), and *Penicillium avellaneum* (UC 4376) using the filter paper method. Growth inhibition was calculated as the radius of the inhibition zone.

3. Results and Discussion

3.1 *Elucidation of the structures of compounds*

ESI-MS revealed the molecular weight of compound **1** to be 196 Da. The ^{13}C-NMR spectrum of **1** (Table 1) displayed 10 signals. The ^{1}H-NMR spectrum of **1** (Table 1) displayed 15 signals. ^{1}H-NMR signals at δH 4.19 (t, 7.3 Hz, 1H) and 4.04 (s, 1H) and ^{13}C-NMR signals at δC 172.6 and 167.6 revealed the presence of two acylamino groups, indicating that **1** is a cyclic dipeptide. ^{1}H-NMR signals at δH 2.47-2.52 (m, 1H), 1.09 (d, J = 7.3, 3H), and 0.93 (d, J = 6.9, 3H) and ^{13}C-NMR signals at δC 29.5, 18.8, and 16.7 indicated the presence of an isopropyl group. The HMBC correlation from CH(10) to C(1), along with the ^{1}H-^{1}H COSY correlation between CH(9)↔CH_2(10)↔CH_3(11), indicated the presence of fragment **1A** (Figure 2), which was a valine residue. ^{1}H-NMR signals at δH 3.43-3.58 (m, 2H), 1.95-1.96 (m, 2H), 2.01-2.06 (m, 1H), and 2.31-2.34 (m, 1H) and ^{13}C-NMR signals at δ 46.2, 23.3,

Table 1. ^{1}H-NMR and ^{13}C-NMR spectroscopic data for compounds 1 and 2 (MeOD).

	Compound **1**		Compound **2**	
	Proton	Carbon	Proton	Carbon
	Pro		Pro	
3	3.43-3.58 (m, 2H)	46.2t	3.50-3.52 (m, 2H)	46.4t
4	1.95-1.96 (m, 2H)	23.3t	1.93-1.96 (m)	23.6t
			1.99-2.06 (m)	
5	2.01-2.06 (m)	29.9t	1.99-2.06 (m)	29.1t
	2.31-2.34 (m)		2.28-2.33 (m)	
6	4.04 (m)	60.0d	4.27 (t, J = 7.5)	60.3d
7		172.6s		172.8s
8	Val		Leu	
9	4.21 (t, J = 7.3)	61.5d	4.13-4.16 (m)	54.6d
10	2.47-2.52 (m)	29.5d	1.87-1.92 (m, 2H)	39.4t
11	1.09 (d, J = 7.3, 3H)	18.8q	1.60-1.64 (m)	25.8d
12	0.93 (d, J = 6.9, 3H)	16.7q	0.96 (d, J = 4.3, 3H)	23.3q
13			0.97 (d, J = 4.2, 3H)	22.2q
1		167.6s		168.9s

δ in ppm. J in Hz.

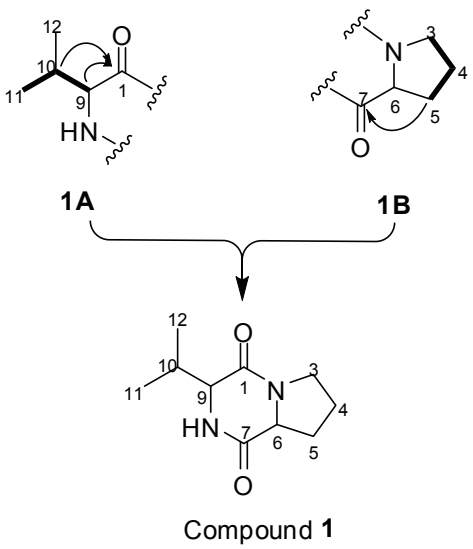

Figure 2. Selected HMBC (H→C) and ^{1}H-^{1}H COSY (—) correlations, and the structures of fragments 1A and 1B of compound 1.

and 29.9 indicated the presence of three CH_2 groups. Furthermore, the HMBC spectrum showed that CH_2(5) was correlated with C(7). In combination with the ^{1}H-^{1}H COSY correlation between CH_2(3)↔CH(4)↔CH(5), these findings indicated the presence of fragment **1B** (Figure 2), which was a proline residue (Figure 2). The spectral data for **1** were consistent with those reported in the literature (*8*). Thus, compound 1 was determined to be cyclo(D)-Pro-(D)-Val.

ESI-MS revealed the molecular weight of compound **2** to be 210 Da. The chemical structure of **2** was determined by comparing NMR data for **2** with those for **1**. Both compounds had similar spectroscopic data (Table 1), except for C(11), C(12), and C(13). ^{1}H-NMR signals at δH 1.87-1.92 (m, 2H), 1.60-1.64 (m, 1H), 0.96 (d, J = 4.3, 3H), and 0.97 (d, J = 4.2, 3H) and ^{13}C-NMR signals at δC 39.4, 25.8, 23.3, and 22.2 indicated the presence of an isobutyl group. The HMBC spectrum showed that CH(9) was correlated with C(1). Along with the ^{1}H-^{1}H COSY correlation between CH(9)↔CH_2(10)↔CH(11)↔CH_3(12), these findings indicated that **2** had a leucine residue. The spectral data of **2** were consistent with those reported in the literature (*8*). Therefore, compound **2** was determined to be cyclo(D)-Pro-(D)-Leu.

ESI-MS data revealed the molecular weight of compound **3** to be 242 Da. The ^{1}H-NMR spectrum of **3** (Table 2) displayed 14 signals. The ^{13}C-NMR spectrum of **3** (Table 2) displayed 14 signals for one methyl, two methylenes, six methines, and five quaternary carbon atoms, including two carbonyl groups (with one at δC 172.2 C(11) and the other at δC 167.7 C(5)). This suggested the presence of two acylamino groups as in compounds **1** and **2**. The ^{1}H-NMR signal at δH 5.50 (1H, m) and ^{13}C-NMR signals at δC 119.1 and 134.5 suggested a trisubstituted

Table 2. ^{1}H-NMR and ^{13}C-NMR spectroscopic data for compounds 3 and 6 (DMSO-d_6).

Position	Compound **3**		Compound **4**	
	Proton	Carbon	Proton	Carbon
1	2.59-2.63 (m)	28.2t	2.71-2.76 (m)	33.0t
	3.26-3.28 (m)		3.26-3.28 (m)	
2		134.5s		129.3s
3	4.03 (d, J = 15.8)	52.5t	6.61 (s)	121.1d
	4.24 (d, J = 15.7)			
4				
5		167.7s		161.5s
5a		127.7s		120.8s
6	7.79 (d, *J* = 7.8)	131.4d	7.30 (d, *J* = 8.7)	121.2d
7	7.16 (t, *J* = 8.1)	125.8d	6.97 (d, *J* = 8.8)	108.7d
8	7.26 (t, *J* = 7.6)	133.9d		150.4s
9	7.64 (d, *J* = 7.7)	122.5d		137.1s
9a		137.8s		125.1s
NH/OH	10.64 (s)		9.43 (s, 2H)	
11		172.2s		169.0s
11a	4.34 (dd, *J* = 9.3, 2.4)	58.4d	4.66 (dd, *J* = 10.8, 3.7)	56.6d
12	5.49-5.50 (m)	119.1d	2.16 (q, *J* = 7.3, 2H)	21.5t
13	1.68 (d, *J* = 6.7, 3H)	14.5q	1.08 (t, *J* = 7.4, 3H)	12.5q
MeO			3.87 (s, 3H)	56.5q

δ in ppm. J in Hz.

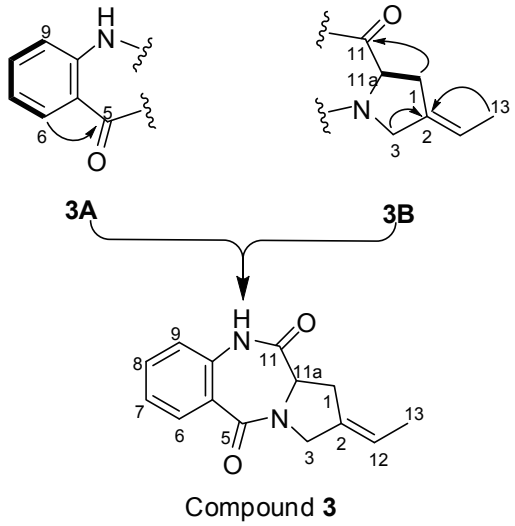

Figure 3. Selected HMBC (H→C) and 1H-1H COSY (—) correlations, and the structures of fragments 3A and 3B of compound 3.

double bond. The ^{1}H-^{1}H COSY correlation between CH(6)↔CH(7)↔CH(8)↔CH(9) indicated that **3** had a disubstituted benzene. Next, the HMBC correlation from CH(6) to C(5) indicated the presence of fragment **3A** (Figure 3). The double bond was assigned at C(2) and CH(12) in accordance with the HMBC correlation (Figure 3) of δH 1.68 CH_3(13) with δC 127.5 CH(12) and δH 2.59, δH 3.28 CH_2(1) and that of δH 4.03, δH 4.24 CH_2(3) with δC 134.5 C(2). The HMBC correlation from CH(11a) and CH_2(1) to C(5), in combination with the ^{1}H-^{1}H COSY correlation between CH_2(1)↔CH(11a), indicated the presence of fragment **3B** (Figure 3). Therefore, compound **3** was determined

to be (S,E)-2-ethylidene-2,3-dihydro-1H-benzo[e] pyrrolo[1,2-a][1,4]diazepine-5,11(10H,11aH)-dione, a new natural product that has been registered (CAS No.: 1052219-35-8). After consulting the names of reported analogues (*9-11*), compound **3** was designated oxoprothracarcin.

ESI-MS data revealed the molecular weight of compound **4** to be 288 Da. The ^{1}H-NMR and ^{13}C-NMR spectral data for **4** (Table 2) were similar to those for **3**. The ^{1}H-NMR spectrum of **4** (Table 2) displayed 16 signals. The ^{13}C-NMR spectrum of **4** (Table 2) displayed 15 signals for two methyls, two methylenes, four methines, and seven quaternary carbon atoms, including two carbonyl groups (with one at δC 169.0 C(11) and the other at δC 161.5 C(5)). The ^{1}H-NMR signal at δH 6.61 (1H, s) and ^{13}C-NMR signals at δC 121.1 and 129.3 suggested a trisubstituted double bond like that in compound **3**. However, the HMBC correlation from CH_2(1), CH_2(3), CH(11a), CH_2(12), and CH_3(13) to C(2) and the ^{1}H-^{1}H COSY correlation between CH_2(12)↔CH_3(13) and CH_2(1)↔CH(11a) indicated a C=C bond between C(2) and C(3). The ^{1}H-^{1}H COSY correlation between CH(6)↔CH(7), and the ^{13}C-NMR signals at δC 150.4 C(8) and 137.1 C(9) indicated the presence of a methoxyl group at C(8) and a hydroxyl group at C(9). The spectral data for compound **4** were identical to those of limazepine A reported in the literature (*8*).

3.2. *Biological study*

At a concentration of 10 μM, compounds **1** - **4** inhibited the growth of MDA-MB-231 cells at rates of 5.2%, 6.3%, 10.2%, and 3.8%, and they inhibited the growth of A549 cells at rates of 18.4%, 19.6%, 7.3%, and 0.7%. The antibacterial activity of compounds **1** - **4** was tested against *Bacillus subtilis* (CMCC (B) 63501), *Bacillus pumilus* (CMCC (B) 63202), and *Penicillium avellaneum* (UC 4376) using the filter paper method. Activity of each compound was tested twice at a concentration of 1.0 mg/mL with a loading volume of 20 μL. Results indicated that compounds **1** - **4** had no effect on the growth of the bacteria tested at 20 μg/disc.

3.3. *Conclusions and perspectives*

Genetic analysis indicated that some marine *Streptomyces* form an independent clade (*7*), so marine *Streptomyces* was surmised to potentially be rich in novel secondary metabolites. The present study succeeded in isolating only one new compound, which suggests that fermentation medium screening and/or genetic manipulation are needed to encourage the production of secondary metabolites in marine *Streptomyces*. However, compound **3** was isolated with a high yield (36 mg/10 L) and could be used as a lead compound for structural modifications.

Acknowledgement

This work was financially supported by the 973 Program (the National Basic Research Program of China, grant no. 2010CB833802).

References

1. Zheng Y, Shen Y. Clavicorolides A and B, sesquiterpenoids from the fermentation products of edible fungus *Clavicorona pyxidata*. Org Lett. 2008; 11:109-112.
2. Fenical W, Jensen PR. Developing a new resource for drug discovery: marine actinomycete bacteria. Nature Chem Bio. 2006; 2:666-673.
3. Bull AT, Stach JEM. Marine actinobacteria: New opportunities for natural product search and discovery. Trends Microbiol. 2007; 15:491-499.
4. Williams DE, Dalisay DS, Patrick BO, Matainaho T, Andrusiak K, Deshpande R, Myers CL, Piotrowski JS, Boone C, Yoshida M. Padanamides A and B, highly modified linear tetrapeptides produced in culture by a *Streptomyces* sp. isolated from a marine sediment. Org Lett. 2011; 13:3936-3939.
5. Sun P, Maloney KN, Nam SJ, Haste NM, Raju R, Aalbersberg W, Jensen PR, Nizet V, Hensler ME, Fenical W. Fijimycins A-C, three antibacterial etamycin-class depsipeptides from a marine-derived *Streptomyces* sp. Bioorg Med Chem. 2011; 19:6557-6562.
6. Matsuo Y, Kanoh K, Jang JH, Adachi K, Matsuda S, Miki O, Kato T, Shizuri Y. Streptobactin, a tricatechol-type siderophore from marine-derived *Streptomyces* sp. YM5-799. J Nat Prod. 2011; 74:2371-2376.
7. Xu Y, He J, Tian XP, Li J, Yang LL, Xie Q, Tang SK, Chen YG, Zhang S, Li WJ. Streptomyces glycovorans sp. nov., Streptomyces xishensis sp. nov. and Streptomyces abyssalis sp. nov. isolated from marine sediments. Int J Syst Evol Microbiol. 2012; 62:2371-2377.
8. Fdhila F, Vázquez V, Sánchez JL, Riguera R. dd-Diketopiperazines: Antibiotics active against *Vibrio anguillarum* isolated from marine bacteria associated with cultures of *Pecten maximus*. J Nat Prod. 2003; 66:1299-1301.
9. Shimizu K, Kawamoto I, Tomita F, Morimoto M, Fujimoto K. Prothracarcin, a novel antitumor antibiotic. J Antibiotics. 1982; 35:972.
10. Arima K, Kosaka M, Tamura G, Imanaka H, Sakai H. Studies on tomaymycin, a new antibiotic. I. Isolation and properties of tomaymycin. J Antibiotics. 1972; 25:437.
11. Kariyone K, Yazawa H, Kohsaka M. The structure of tomaymycin and oxotomaymycin. Chem Pharm Bull. 1971; 19:2289-2293.
12. Fotso S, Zabriskie TM, Proteau PJ, Flatt PM, Santosa DA, Mahmud T. Limazepines A− F, pyrrolo [1, 4] benzodiazepine antibiotics from an Indonesian Micrococcus sp. J Nat Prod. 2009; 72:690-695.
13. Mosmann T. Rapid colorimetric assay for cellular growth and survival: Application to proliferation and cytotoxicity assays. J Immunol Methods. 1983; 65:55-63.

(Received March 26, 2013; Revised December 20, 2013; Accepted December 23, 2013)

Appendix

Cyclo[Val-Pro] (**1**). Colorless crystal. ^{1}H- and ^{13}C-NMR spectral data: see Table 1. ESI-MS: m/z = 197.5 ([M + H]$^{+}$) and m/z = 219.5([M + Na]$^{+}$).

Cyclo[Leu-Pro] (**2**). Colorless crystal. ^{1}H- and ^{13}C-NMR spectral data: see Table 1. ESI-MS: m/z = 211.4 ([M + H]$^{+}$) and m/z = 233.4([M + Na]$^{+}$).

Oxoprothracarcin (2-ethylidene-2,3-dihydro-1H-benzo[e]pyrrolo[1,2-a][1,4]diazepine-5,11(10H,11aH)-dione, **3**). White crystal. ^{1}H- and ^{13}C-NMR spectral data: see Table 2. ESI-MS: m/z = 243.5 ([M + H]$^{+}$) and m/z = 265.4([M + Na]$^{+}$).

Limazepine A (**4**). White crystal. ^{1}H- and ^{13}C-NMR spectral data: see Table 2. ESI-MS: m/z = 289.4 ([M + H]$^{+}$) and m/z = 311.5 ([M + Na]$^{+}$).

Original Article

DOI: 10.5582/ddt.2013.v7.6.248

Synthesis of peptides of Carapax Trionycis and their inhibitory effects on TGF-β1–induced hepatic stellate cells

Chunling Hu, Xiaozhi Peng, Yinpin Tang, Yanwen Liu*

School of Pharmacy, Hubei University of Traditional Chinese Medicine, Hubei, China.

ABSTRACT: We previous identified the anti-fibrotic active ingredients from Carapax Trionycis as two peptides. Here, we synthesized these two peptides (peptide 1 and peptide 2) by a solid phase method and examined their effects on proliferation and activation of cultured hepatic stellate cells (HSC) which are the main ECM (extracellular matrix)-producing cells in fibrosis progression. We demonstrated that peptide 1 and peptide 2 significantly reduced HSC proliferation and activation in a dose dependent manner. Further, peptide 1 and peptide 2 could interfere with TGF-signaling by down-regulating Smad 3 phosphorylation. Thus, these synthetic peptides of Carapax Trionycis could inhibit proliferation and activation of HSC and might be used as a candidate for treatment of liver fibrosis.

Keywords: Synthesis of peptides of Carapax Trionycis, hepatic stellate cells, extracellular matrix (ECM), TGF-β/Smad

1. Introduction

Liver fibrosis is characterized by the accumulation of excess extracelluar matrix (ECM), including collagens (*1*). Hepatic stellate cells (HSCs) play a pivotal role in liver fibrogenesis (*2*). HSCs survival is a hallmark of liver fibrosis. The major event in hepatic fibrogenesis is the transdifferentiation of quiescent HSCs to a myofibroblastic cell type. This process is driven by a variety of compounds, including growth factors (*3*). Hepatic fibrosis is a dynamic process caused by chronic liver injury induced by various etiological factors, such as viral, toxic, metabolic and auto-immune agents, eventually leading to cirrhosis. The HSC-T_6 cell line has been widely used in fibrosis research because it retains all the features of activated stellate cells, including the expression of collagen I, collagen III, alpha-smooth-muscle actin (α-SMA), matrix metalloproteinase (MMP) and tissue inhibitor of metalloproteinase (TIMP) (*4*). HSCs are responsible for collagen deposition in liver fibrosis. Therefore, in the present study we used HSC-T_6 cells to test the effect of two synthetic peptides.

Carapax Trionycis, as a traditional Chinese medicine, originated from the shell of *Trionyx sinensis* Wiegmann. Clinical experience indicated that traditional Chinese medicine Compounds containing Carapax Trionycis showed a curative effect when used for the treatment of liver fibrosis (*5-7*). Previous studies had demonstrated that extracts of Carapax Trionycis were able to protect liver against fibrosis in CCl_4 animal models (*8,9*), synthesized an extract of Carapax Trionycis and verified that it could inhibit activation and induce early apoptosis of HSC-T_6 (*10,11*). Our group isolated two active ingredients from Carapax Trionycis and proved their anti-fibrotic activity (*12,13*). Further we identified the active ingredients are two peptides with sequences of N-D-D-Y (526.2) and N-P-N-P-T (542.16) respectively (*14*). The Carapax Trionycis natural source is very limited and extractive procedures are very costly, which widely restricts the application of these active peptides. Here, we synthesized peptides 1 and 2 based on the sequences of active ingredients by a solid phase method. However, how the synthetic peptides inhibit activated HSC-T_6 proliferation and its exact mechanism remains unknown.

The aim of this study was to determine whether synthetic peptides 1 and 2 affect the survival of cultured HSC-T_6 cells and collagen I, collagen III, MMP-1, and TIMP-1 content, and to examine whether the protein expression of cultured HSC-T_6 cells changes following administration of the synthetic peptides. Also, for the mechanism study, we identified whether synthetic peptides show anti-fibrotic effects by decreasing p-Smad 3 expression, at least in part, *via* the TGF-β_1/Smad pathway as well as by the elimination of the extracellular matrix.

**Address correspondence to:*
Dr. Yanwen Liu, School of Pharmacy, Hubei University of Traditional Chinese Medicine, 1 Huangjia River West Road, Wuhan, Hubei 430065, China.
E-mail: huchunling2007@126.com

2. Materials and Methods

2.1. *Materials*

Fmoc-AA-OH, Wang resin, and TBTU were acquired from Gil (Shanghai, China). MALDI-TOF MS was supplied by Shimadzu Co. (Tokyo, Japan). The HSC-T_6 cell line was purchased from Fuxiang Biological Co., Ltd (Shanghai, China). Fetal calf serum was purchased from Sanli Biological Co., Ltd (Wuhan, China). Trypsin and High-DMEM were purchased from Gibco (Gibco, NY, USA). TGF-β_1 and MTS were acquired from Sigma (Sigma-Aldrich, USA). Collagen I, collagen III, MMP-1, and TIMP-1 ELISA kits were obtained from R&D (Minneapolis, MN, USA). Monoclonal anti- collagen I, collagen III, Smad 3, p-Smad 3, TIMP-1, and MMP-1 antibodies and horseradish-peroxidase (HRP)-conjugated goat anti-rabbit Ig G secondary antibody were purchased from Santa Cruz (Santa Cruz Biotechnology, CA, USA). The SuperSignal Substrate Chemiluminescence Kit was from Pierce (Rockford, USA).

2.2. *Solid-phase synthesis of active peptides of Carapax Trionycis*

The introduction of solid phase peptide synthesis (SPPS) in 1963 by Bruce Merrifield opened the door for researchers to prepare structurally diverse peptides. In this study, SPPS was used with Wang resin as the carrier and *N*-Fmoc protected α-amino acids as the materials based on the sequences of the active ingredients from Carapax Trionycis. After condensation with the reagentmix of TBTU/NMM, and deprotection with 20% piperidine, the synthetic peptide crude products were removed from the Wang resin by the cleavage reagents TFA/TIS/H_2O. By analysis and purification with RP-HPLC, we finally obtained two bioactive peptides 1 and 2. Synthetic peptides of Carapax Trionycis were determined by MALDI-TOF MS analysis. The sample was obtained in a volume of 0.5 μL on the target board of MALDI. After natural drying at room temperature, the sample was obtained from a mixed solution of 0.1% TFA and 50% ACN again, and a blank control was set up at the same time.

2.3. *Cell culture and MTS assay*

HSC-T_6 cells were maintained in Dulbecco's modified Eagle's medium plus 10% fetal calf serum and incubated at 37°C in a 5% CO_2 humidified atmosphere. HSCs were digested with 0.25% trypsin and adjusted to 6×10^4 cells/mL when the HSCs were in the exponential growth phase. The cells were planted into 96-well plates, 0.2 mL/well, 4-wells/group and incubated overnight.

Several studies have provided ample evidence that TGF-β_1 is a strong stimulant of hepatic stellate cell proliferation (*15*). Therefore, we used TGF-β_1 to stimulate HSC-T_6 cells. Cells were pre-treated with TGF-β_1 (800 pg/mL) in each well for 2 h and then treated separately with serum containing synthetic peptides 1 and 2.

Control group cells were cultured in only serum medium. The stimulant group cells were cultured in TGF-β_1 medium. The experimental group cells were treated with synthetic peptides 1 and 2 at different concentrations (0.01, 0.05, 0.1, and 0.5 mg/mL) in TGF-β_1 medium. After cells were incubated for 72 h, the culture medium was removed, and 20 μL MTS/PMS was added in each well for 1 h. OD values were analyzed by one-way ANOVA test. The rate of inhibition was calculated as follows:

IR (%) = [(control value – blank) – (test value – blank)]/(control value – blank) × 100.

2.4. *Emzyme-linked immunosorbent assay (ELISA)*

HSC-T_6 cells were trypsinized and seeded in triplicate at a density of 6×10^4 cells/mL in six-well plates for 24 h. Before experiments, the medium was changed to serum-free medium and the cells were incubated for 24 h. They were pre-treated with TGF-β_1 (800 pg/mL) for 2 h and then treated with peptides 1 and 2 (0.01, 0.05, 0.10 mg/mL) for 72 h before analysis by ELISA assay. Cell culture supernatants were collected. Collagen I, collagen III, MMP-1, and TIMP-1 were measured using ELISA kits according to the procedure recommended by the manufacturer.

2.5. *Western blot analysis*

HSC-T_6 cells were treated as described for ELISA. Western blot analysis was then performed with antibodies directed against collagen I, collagen III, Smad 3, p-Smad 3, TIMP-1, and MMP-1 to detect the expression of these proteins. Control, TGF-β_1-treated and TGF-β_1 + synthetic peptides–treated (0.01, 0.05, 0.10 mg/mL) HSC-T_6 cells were lysed with RIPA buffer (containing 1% Nonidet P-40, 0.5% sodium deoxycholate, 0.1% sodium dodecyl sulfate [SDS], and 50 μg/mL aprotinin), to which 200 μg/mL phenylmethylsulfonyl fluoride was added immediately after addition of the lysis buffer. Protein samples (30 μg each) were separated electrophoretically on 10% SDS polyacrylamide gels, and electroblotted onto polyvinylidene difluoride membranes. The membranes were blocked with 5% skim milk in Tris-buffered saline for 1 h at room temperature and incubated overnight at 4°C with primary anti-rat antibodies. After washing, the membranes were incubated for 1 h at room temperature with HRP-conjugated secondary goat anti-rabbit IgG. The bands were visualized using a SuperSignal Substrate Chemiluminescence Kit.

2.6. *Statistical analysis*

Each experiment was repeated a minimum of three times. Results were expressed as Mean ± SD. Statistical analysis was performed by one-way ANOVA test. *p* values less than 0.05 were considered statistically significant.

3. Results

3.1. *Analysis and identification of synthetic peptides of Carapax Trionycis*

Two peptides of Carapax Trionycis 1 and 2 were synthesized using a classical solid phase method from right to left based on the sequence (sequence 1 is NDDY; sequence 2 is NPNPT) of active ingredients from Carapax Trionycis. By the analysis and purification from RP-HPLC, the purity of synthetic peptides was over 98%, chromatographic analysis is shown in Figure 1.

Synthetic peptides of Carapax Trionycis were determined by MALDI-TOF MS analysis. The molecular weight of synthetic pepetide 1 was 525.981 (Figure 2), which was identical with primary active ingredient (NDDY, molecular weight: 526.2) from Carapax Trionycis. The molecular weight of synthetic pepetide 2 was 542.083 (Figure 2), which was identical with primary active ingredient (NPNPT, molecular weight: 542.16) from Carapax Trionycis. The results suggested that synthetic peptides 1 and 2 had the same sequence structure as the corresponding ingredients from Carapax Trionycis.

3.2. *Effect of synthetic peptides on HCS-T_6 cells proliferation*

To test if our synthetic peptides could inhibit proliferation of cultured hepatic stellate cells, we first treated HSC-T_6 cells with synthetic peptides at various concentrations, then we monitored cell proliferation by cell number quantification. As shown in Figure 3, after treatment with synthetic peptides 1and 2 (0.01 ~ 0.60 mg/mL) for 72 h, HSC-T_6 proliferation was significantly inhibited in a dose dependence manner. The IC_{50} values of synthetic peptides 1and 2 for HSC-T_6 cells at 72 h were 0.53 mg/mL and 0.52 mg/mL respectively. Therefore, we chose concentrations of 0.01, 0.05, and 0.10 mg/mL for further analysis.

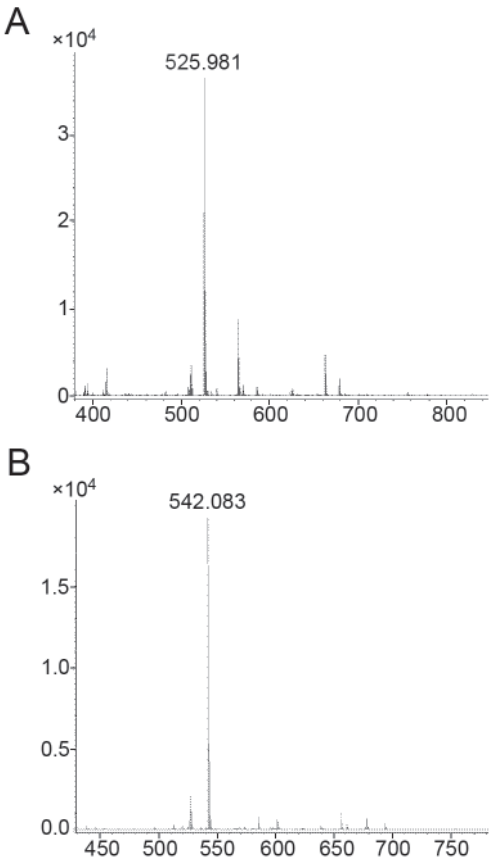

Figure 2. Identification of the synthetic peptides by mass spectrometry analysis. MS/MS spectrum indicated that the major peaks were molecular ion peaks. The m/z 525.981 signal was the molecular ion with loss of a hydrogen ion of synthetic peptide 1 **(A)** and the m/z 542.083 signal was the molecular ion with loss of a hydrogen ion of synthetic peptide 2 **(B)**. Mass to charge ratio is denoted, m/z.

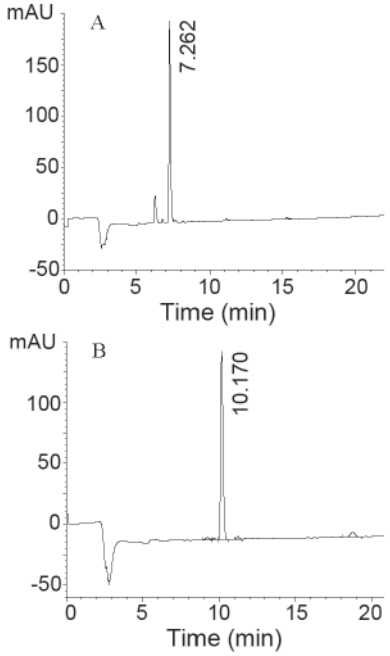

Figure 1. RP-HPLC chromatograms of synthetic peptide 1 (A) and peptide 2 (B). Column: Zorbox Eclipse XDB-C18 (250 × 4.6 mm, 5 μm); mobile phase: acetonitrile (0.05% TFA)- water (0.05% TFA) (acetonitrile: 10-50% in 30 min); flow rate: 1.0 mL/min; detection wavelength: 220 nm.

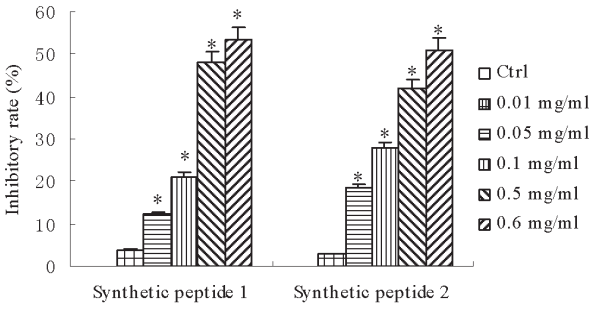

Figure 3. Effect of synthetic peptides on HSC-T_6 proliferation. The inhibitory rate (%) of synthetic peptides 1 and 2 on HSC-T_6 proliferation increased significantly following increase in the synthetic peptides 1 and 2 concentration. * $p < 0.01$ compared with control group ($n = 4$).

3.3. *Effect of synthetic peptides on profibrotic mediators and ECM degradation modulators*

The extent of liver fibrosis depends on rates of hepatic collagen synthesis and degradation. Collagens are the main components of ECM. Matrix degradation is catalyzed by the activity of MMPs. The activities of MMPs are inhibited by TIMPs (*16*). So next, we examined the collagen I, collagen III, and TIMP-1 expression levels in the cell culture supernatant after peptide 1 and peptide 2 treatment. As show in Figure 4, their contents were significantly decreased in a dose dependent manner except for MMP-1. Further analyses indicated that the change of content was greater for 0.05 and 0.10 mg/mL synthetic peptides than for control group and for TGF-β_1 group. Differences among the various concentration groups were notable.

To further test whether the change of collagens was related to the content of MMP-1 and TIMP-1, we determined the protein expression of these fibrogenic genes and found that the levels of collagen I, collagen III, TIMP-1, and α-SMA proteins were lower in the TGF-β_1 + synthetic peptides groups than in the TGF-β_1 groups except for MMP-1 (Figure 5) by Western blot.

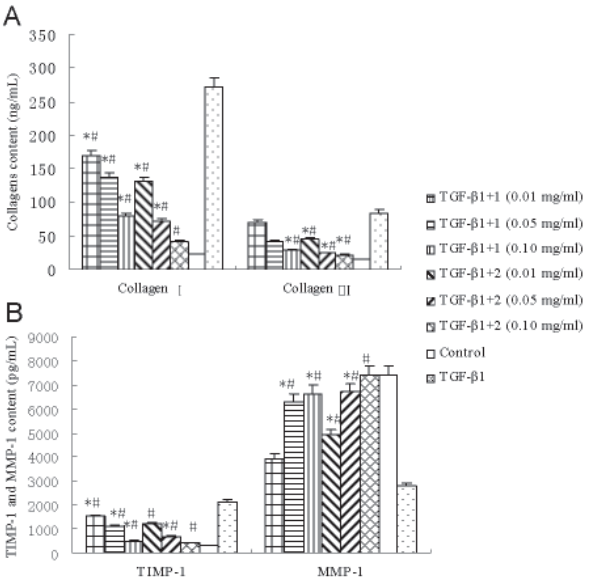

Figure 4. Effects of synthetic peptides 1 and 2 on the content of collagen I, collagen III, TIMP-1, and MMP-1 in HSC-T_6 cells. The cells were maintained in Dulbecco's modified Eagle's medium plus 10% fetal calf serum and were pre-treated with TGF-β1 (800 pg/mL) in each well for 2 h, and then treated separately with serum containing synthetic peptides 1 and 2 for 72 h before analysis with ELISA assay. Cell culture supernatants were collected. * $p < 0.01$ compared with the control group, # $p < 0.01$ compared with the TGF-β1 group ($n = 4$).

4. Discussion

During fibrosis progression, the main ECM-producing cells are activated HSCs, which secrete ECM proteins including collagen I and III (*17*). Cross-remodeling of the ECM in the fibrotic liver is likely to be regulated by the synthesis and enzymatic degradation of the ECM. Expression of MMP-1 can be important in mediating HSC proliferation, potentially by regulating ECM turnover (*18*) and is one of the major causes of liver fibrosis (*19,20*). Also, the activities of MMPs are

3.4. *Inhibitory effect of synthetic peptides on TGF-β_1–induced hepatic stellate cells was associated with TGF-β_1/Smad activation*

TGF-β_1 is the most potent fibrogenic cytokine described for HSCs and can stimulate HSCs activation and ECM production. We next examined whether the TGF-β_1/Smad signaling pathway is involved in activated HSC-T_6 cells. As demonstrated by Western blot, TGF-β_1 stimulation caused marked increases in expression of p-Smad 3 when compared to the control group, but co-treatment with synthetic peptides 1 and 2 eliminated these changes (Figure 6B). However, the level of Smad 3 protein did not differ significantly in the various groups (Figure 6A).

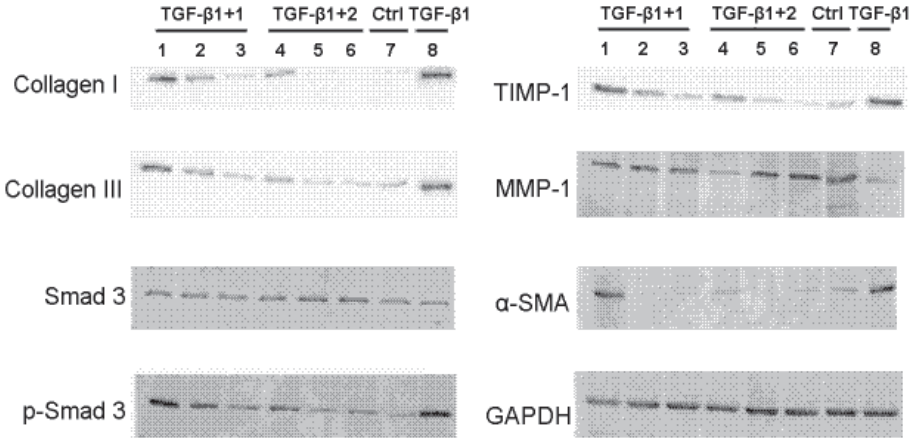

Figure 5. The protein bands for collagen I, collagen III, Smad 3, p-Smad 3, TIMP-1, MMP-1, and α-SMA. The expression levels of above proteins were normalized by an internal control of GAPDH.

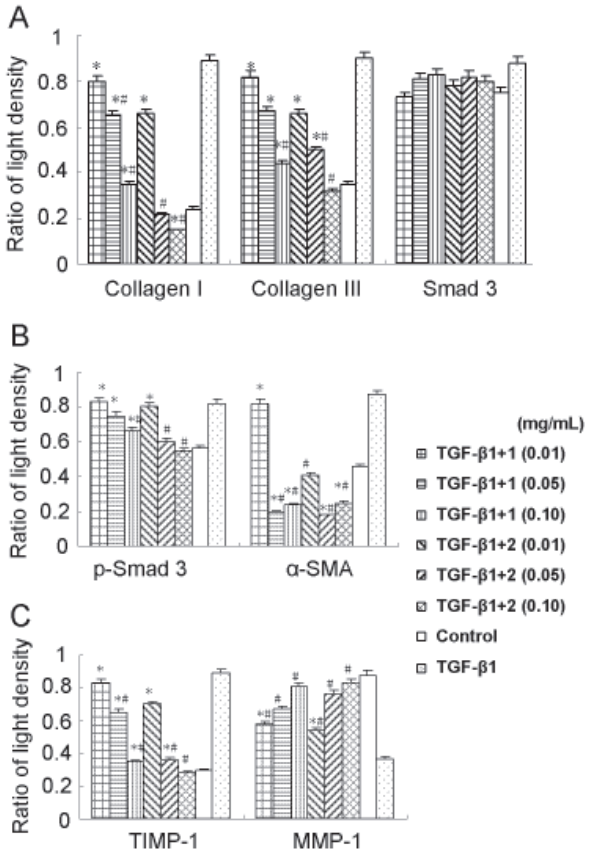

Figure 6. Western blot analysis of collagen I, collagen III, Smad 3, p-Smad 3, TIMP-1, MMP-1, and α-SMA. Panels A-C shows the levels of collagen I, collagen III, p-Smad 3, α-SMA, TIMP-1, and MMP-1 proteins. A drastic difference in protein expression between the TGF-β1 + synthetic peptides groups and TGF-β1 groups was observed. * $p < 0.01$ compared with the control group, # $p < 0.01$ compared with the TGF-β1 group ($n = 4$).

inhibited by TIMPs. Especially, TIMP-1 increases early following liver injury and persists as fibrosis develops (*21*). Our *in vitro* study showed that synthetic peptides 1 and 2 promoted recovery from liver fibrosis not only by the removal of collagens (Figure 4A), but also by the reduction of TIMP-1 content and the improvement of MMP-1 content (Figure 4B).

A previous study reported that α-SMA occurs in vascular smooth muscle, the luminal portions of bile ducts, and the periphery of hepatocytes, but not in lobules and rarely in HSCs in normal rat liver. However, α-SMA-immunopositive cells are increased in number and reactivity in injured livers. Therefore, α-SMA is accepted as a typical marker of activated HSCs during the fibrotic process and acute liver injury. To evaluate HSCs activation, we performed Western blots for α-SMA. The results indicated that expression of α-SMA protein was reduced in the TGF-β_1 + synthetic peptides groups compared with the TGF-β_1 groups (Figure 6B). Besides, TIMP-1, collagen I and collagen III expression were decreased concurrently with decreased α-SMA expression in cultured HSC-T_6 cells (Figures 6A and 6C).

TGF-β_1 is the most potent fibrogenic cytokine described for HSCs (*22,23*), and can stimulate HSCs activation and ECM production. Disruption of TGF-β_1/Smad signaling markedly reduces fibrosis in experimental models (*24,25*). In our study, we examined the phosphorylation levels of Smad 3 and found that TGF-β_1 stimulation led to elevated levels of Smad 3 phosphorylation in cultured HSC-T_6 cells, whereas co-treatment with synthetic peptides 1and 2 eliminated these changes (Figure 6B). Interestingly, the level of Smad 3 protein wasn't significantly different (Figure 6A). These results suggested TGF-β_1/Smad signaling may be associated with the therapeutic benefits of the peptides. Therefore, it is likely that inhibition of p-Smad 3 expression plays a major role in the down regulation of collagenproduction in HSCs (*26,27*).

In summary, our data indicated that synthetic peptides 1and 2 efficiently inhibited cultured HSC-T_6 cell activation and proliferation by decreasing p-Smad3 expression, at least in part, via the TGF-β_1/Smad pathway as well as by the elimination of the extracellular matrix. The present study provides a foundation for the prevention and treatment of liver fibrosis.

Acknowledgments

ELISA and Western blot analysis were performed at the Center for liver disease research in the first affiliated hospital of Zhejiang University, and we thank Dr. H. P. Yao for his excellent technical assistance.

References

1. Latella G, Vetuschi A, Sferra R, Catitti V, Dangelo A, Zanninelli G. Targeted disruption of Smad3 confers resistance to the development of dimethylnitrosamine-induced hepatic fibrosis in mice. Liver Int. 2009; 29:997-1009.
2. Friedman SL. Stellate cells: A moving target in hepatic fibrogenesis. Hepatology. 2004; 40:1041-1043.
3. Friedman SL. Liver fibrosis from bench to bedside. J. Hepatol. 2003; 38 (Suppl 1): s38-s53.
4. Lee JH, Lee H. The use of low molecular weight heparin-pluronic nanogels to impede liver fibrosis by inhibition of the TGF-β/Smad signaling pathway. Biomaterials. 2011; 32:1438-1445.
5. Tan Y, Lv ZP, Bai XC. Traditional Chinese medicine Bao Gan Ning increase phosphorylation of CREB in liver fibrosis *in vivo* and *in vitro*. J Enthopharm. 2006; 105:69-75.
6. Zhao ZJ, Qiu Q, Zhang XX. Effect of Compound Biejia Ruangan tablet on expressions of connective tissue growth factor mRNA and protein in kidney tissue of rats with adriamycin-induced nephropathy. J Chin Integr Med. 2007; 5:651-655.
7. Chen JM, Yang YP, Chen DY. Efficacy and safety of Fufang Biejia Ruangan tablet in patients with chronic hepatitis B complicated with hepatic fibrosis. Chin J Exp Clin Virol. 2007; 21:358-360.
8. Gao JR, Zhang CZ, Liu YW. Experimental study of

Amydase Carapax decoction on prevention & treatment of liver fibrosis in rats induced by two different causes. Chin Arch TCM. 2009; 27:1727-1733.
9. Tang YP, Liu YW, Xu LY. The research of extract of Carapax Trionycis on anti-hepatic fibrosis effects. Journal of Hubei University of Chinese Medicine. 2011; 13:44-46.
10. Hu CL, Tang YP, Liu YW. Peptide synthesis of Carapax Trionycis and its effect on hepatic stellate cells. Herald of Medicine. 2011; 30:1724-1726.
11. Hu CL, Tang YP, Liu YW. Synthesis of an active peptide from Carapax Trionycis and its inhibitory effect on the proliferation of hepatic stellate cells. J Chin Pharm Sci. 2012; 21:132-135.
12. Tang YP, Hu CL, Shi JN, Gao JR, Yao HP, Liu YW. Study on anti-fibrotic active components from Carapax Trionycis. J Chin Mod TCM. 2010; 6:262-265.
13. Gao JR, Tao J, Zhang CZ, Liu YW, Shao ZH, Cai WM, Xu HL. Experimental study of Amydase Carapax on prevention & treatment of liver fibrosis. Chin Arch TCM. 2008; 26:2462-2471.
14. Gao JR, Liu YW, Li CY, Yao HP, Zhang CZ, Chen JW. Screening, isolation and identification of active substance from Amydase Carapax on anti-hepatic fibrosis. Chin J Hepatol. 2010; 18:346-352.
15. Gressner AM, Weiskirchen R. Modern pathogenetic concepts of liver fibrosis suggest stellate cells and TGF-β as major players and therapeutic targets. J Cell Mol Med. 2006; 10:76-99.
16. Yoshiji H, Kuriyama S, Miyamoto Y, Thorgeirsson UP, Gomez DE, Kawata M, Yoshii J, Ikenaka Y, Noguchi R, Tsujinoue H. Tissue inhibitor of metalloproteinases-1 promotes liver fibrosis development in a transgenic mouse model. Hepatology. 2000; 32:1248-1254.
17. Fallowfield JA. Therapeutic targets in liver fibrosis. Am J Physiol Gastrointest Liver Physiol. 2011; 300:G709-G715.
18. Iredale JP. Models of liver fibrosis: Exploring the dynamic nature of inflammation and repair in a solid organ. J Clin Invest. 2007; 322:539-548.
19. Hemmann S, Graf J. Expression of MMPs and TIMPs in liver fibrosis – A systematic review with special emphasis on anti-fibrotic strategies. J Hepatol. 2007; 46:955-975.
20. Liu J, Tan H. The preventive effects of heparin-superoxide dismutase on carbon tetrachloride-induced acute liver failure and hepatic fibrosis in mice. Mol Cell Biochem. 2009; 327:219-228.
21. Knittel T, Mehde M. Expression of matrix metalloproteinases and their inhibitors during hepatic tissue repair in the rat. Histochem. Cell Biol. 2000; 113:443-453.
22. Bataller R, Brenner DA. Liver fibrosis. J Clin Invest. 2005; 115:209-218.
23. Inagaki Y, Okazaki I. Emerging insights into transforming growth factor beta Smad signal in hepatic fibrogenesis. Gut. 2007; 56:284-292.
24. Breitkopt K, Haas S, Wiercinska E. Anti-TGF-β strategies for the treatment of chronic liver disease. Alcohol Clir Exp Res. 2005; 29:121s-131s.
25. Dooley S, Hamzavi J, Breitkopf K. Smad7 prevents activation of hepatic stellate cells and liver fibrosis in rats. Gastroenterology. 2003; 125:178-191.
26. Prosser CC, Yen RD, Wu J. Molecular therapy for hepatic injury and fibrosis: Where are we? World J Gastroenterol. 2006; 12:509-515.
27. Shi Y, Massague J. Mechanisms of TGF-β signaling from cell membrane to the nucleus. Cell. 2003; 113:685-700.

(Received December 10, 2013; Revised December 26, 2013; Accepted December 28, 2013)

Original Article

DOI: 10.5582/ddt.2013.v7.6.254

Evaluation of antiviral activity of Oligonol, an extract of *Litchi chinensis*, against betanodavirus

Toru Ichinose[1,*], Thommas Mutemi Musyoka[1,*], Ken Watanabe[1], Nobuyuki Kobayashi[1,2,]**

[1] *Laboratory of Molecular Biology of Infectious Agents, Graduate School of Biomedical Sciences, Nagasaki University, Nagasaki, Japan;*
[2] *Central Research Center, AVSS Corporation, Nagasaki, Japan.*

ABSTRACT: Betanodaviruses, members of the family Nodaviridae, are the causal agents of viral nervous necrosis (VNN) in many species of marine farmed fish. In the aquaculture industry, outbreaks of betanodavirus infection result in devastating damage and heavy economic losses. Although an urgent need exists to develop drugs against betanodavirus infection, there have been few reports about anti-betanodavirus drugs. In this study, we examined the inhibitory effect of Oligonol, a purified phenolic extract from lychee fruit, on betanodavirus infection in fish cells. Oligonol significantly inhibited replication of betanodavirus (EC_{50} = 0.9-1.8 μg/mL) as shown by the reduction of the virus-induced cytopathogenic effect (CPE) and the protection of cells in the crystal violet staining assay. The inhibition was dose dependent. A time-of-addition assay indicated that Oligonol's action takes place at an early stage of the viral infection. According to an attachment inhibition assay, it is possible that Oligonol partially inhibits attachment of the virion to the cell. Our data show that Oligonol could serve as an antiviral agent against betanodavirus.

Keywords: Nervous necrosis virus, fish nodavirus, polyphenol, antiviral drugs

1. Introduction

The family Nodaviridae is composed of the genera *Alphanodavirus* and *Betanodavirus*, which predominantly infect insects and fish, respectively. Nodaviruses are small (25-30 nm in diameter), spherical, non-enveloped viruses with a genome consisting of two single-stranded positive-sense RNA molecules, RNA1 and RNA2 (*1*).

Betanodavirus is the causative agent of a highly destructive disease of marine fish: viral encephalopathy and retinopathy, also known as viral nervous necrosis (VNN). VNN devastates many species of marine fish culture worldwide (*2*). Vaccination has shown promising results in many kinds of fish viral infections but not in VNN because this disease occurs primarily in larval and juvenile fish. The developing fish are difficult to vaccinate because of their small size and immature immune system (*3*). Currently, there is no commercially available drug or vaccine against betanodavirus infection. Selection of putative virus-free spawners and disinfection procedures are used as the major control strategies to prevent the spread of the virus. Inhibitors of endosomal acidification (*4*) and gymnemagenol, a triterpene glycoside saponin (*5*), inhibit betanodavirus infection. These observations underscore the need for novel antiviral drugs, albeit with an alternative mode of action.

Several attempts have been made to use plant phytochemicals as antiviral agents against fish viral diseases (*6,7*). Numerous plant-derived polyphenols have antiviral activity (*8*). Oligonol has an anti-influenza viral activity (*9*). It is an optimized, purified, natural phenolic product from Lychee, containing catechin-type monomers and oligomers of proanthocyanidin (*10,11*), which has been approved by the Food and Drug Administration (USFDA) as a new dietary supplement. Oligonol has biological effects including antidiabetic (*12*), anticancer (*13*), and immunoregulatory properties (*14,15*). In the present study, we investigated the antiviral activity and a possible mechanism(s) of action of Oligonol against betanodavirus using an *in vitro* cell-based system.

2. Materials and Methods

2.1. *Cells, viruses, and antibodies*

E-11 cells, cloned from the striped snakehead (*Ophicephalus striatus*) cell line (SSN-1) (*16*), were

*Authors with equal contributions
***Address correspondence to:*
Dr. Nobuyuki Kobayashi, Laboratory of Molecular Biology of Infectious Agents, Graduate School of Biomedical Sciences, Nagasaki University, 1-14 Bunkyo-machi, Nagasaki City, Nagasaki 852-8521, Japan.
E-mail: nobnob@nagasaki-u.ac.jp

grown at 25°C in Leibovitz's L-15 medium (Sigma-Aldrich, MO, USA) supplemented with 5% fetal bovine serum (FBS), 300 μg/mL L-glutamine, and 100 μg/mL penicillin/streptomycin. A betanodavirus, redspotted grouper nervous necrosis virus (RGNNV), used in this study was isolated and characterized as described previously (*4*). Stock viruses were prepared by harvesting the supernatant of the infected E-11 cell culture; the viruses were titrated and stored at −80°C until use. The virus titer was determined by the tissue culture infectious dose of 50% ($TCID_{50}$) assay. Anti-RGNNV coat protein antiserum was produced by immunizing a guinea pig with purified coat protein with Freund's complete adjuvant (Becton, Dickinson and Company, NJ, USA) (*17*).

2.2. *Reagents*

Oligonol (> 95% purity) was purchased from Amino Up Chemical Co., Ltd. (Sapporo, Japan), dissolved in 100% dimethyl sulfoxide (DMSO, Wako Pure Chemical Industries, Osaka, Japan) at a concentration of 100 mg/mL, and stored at 4°C. Bafilomycin A1 (Sigma-Aldrich) was dissolved in 100% DMSO and stored at − 20°C.

2.3. *Determination of cytotoxicity and antiviral activity*

To determine cytotoxicity of Oligonol, E-11 cells (4×10^4 cells/well) were seeded on 48-well plates and grown for 36 h. The medium was replaced with 2-fold serial dilutions of Oligonol (0.63-40 μg/mL) in the L-15 medium supplemented with 2% FBS. After incubation for 96 h, cell viability was assessed by crystal violet staining. Briefly, the cells were fixed with 70% EtOH for 5 min and then stained with 0.5% crystal violet for 6 h. After a wash with water, absorbance was measured at 560 nm using an Infinite M200 plate reader (Tecan Group Ltd., Switzerland). Cytotoxicity percentage values were calculated by the following formula: $[(A_{control} - A_{sample})/A_{control}] \times 100$, where $A_{control}$ is the absorbance corresponding to untreated cells and A_{sample} is the absorbance corresponding to the cells that were treated with Oligonol. The 50% cytotoxic concentration (CC_{50}) was calculated from the dose-response curve by linear regression analysis. To determine the antiviral activity, a cytopathogenic effect (CPE) reduction assay and virus titer reduction assay were performed on the supernatants as described previously (*4*). E-11 cells (4×10^4 cells/well) were seeded on 48-well plates and cultured for 96 h with 2-fold serial dilutions of Oligonol (0.63-40 μg/mL) and an equal volume of a virus suspension (0.01, 0.1, or 1.0 $TCID_{50}$/cell). The development of virus-induced CPE was observed under a microscope (Axiovert 25, Carl Zeiss, Germany), and culture supernatants were collected for measurements of virus yield. Viability of the cells was determined by crystal violet staining and calculated by the following formula: Survival rate (%) = $[(A_{virus + sample} - A_{virus})/(A_{control} - A_{virus})] \times 100$, where $A_{control}$ is the absorbance corresponding to uninfected untreated cells, A_{virus} is the absorbance corresponding to infected untreated cells, and $A_{virus + sample}$ is the absorbance corresponding to virus-infected cells that were treated with a given concentration of Oligonol. The 50% effective concentration (EC_{50}) was calculated from the dose-response curve by linear regression analysis. The selectivity index (SI) for Oligonol was calculated by the formula: CC_{50}/EC_{50}.

2.4. *Detection of the viral coat protein by Western blotting*

E-11 cells (4×10^4 cells/well) were seeded on 48-well plates and infected with RGNNV (1.0 $TCID_{50}$/cell) in the presence of Oligonol (0.63-40 μg/mL). At 96 h post-infection (h.p.i), the cells were washed twice with ice-cold phosphate buffer saline (PBS) and lysed in a buffer consisting of 4% SDS, 100 mM Tris-HCl (pH 6.8), 2.5% β-mercaptoethanol, 20% glycerol, and 0.4% bromophenol blue. The cell lysate was analyzed by a 10% SDS-polyacrylamide gel electrophoresis (SDS-PAGE) and transferred to a polyvinylidene fluoride (PVDF) membrane (Merck Millipore, MA, USA). The membrane was incubated with a 1:3,000 dilution of a polyclonal antibody against the RGNNV coat protein, followed by a 1:30,000 dilution of a biotinylated anti-guinea pig IgG F(c) antibody (Rockland, PA, USA), and finally with a 1:3,000 dilution of a streptavidin-alkaline phosphatase conjugate (GE Healthcare, UK). The results were visualized in 0.0125% BCIP (Nacalai Tesque, Kyoto, Japan) and 0.0125% NBT (Wako Pure Chemical Industries, Osaka, Japan) in a 0.1 M diethanolamine solution (pH 9.5) containing 5 mM $MgCl_2$. As an internal control, actin was measured using a 1:2,000 dilution of a rabbit anti-actin antibody (Sigma-Aldrich) followed by a 1:5,000 dilution of a biotinylated anti-rabbit Ig antibody.

2.5. *The time-of-addition assay*

E-11 cells (4×10^4 cells/well) were seeded on 48-well plates and infected with the virus at 1.5 $TCID_{50}$/cell, nearly equal to multiplicity of infection (M.O.I) of 1.0, for 1 h (viral adsorption). Following that, the cells were washed twice with the L-15 medium without FBS to remove any unbound virus. The cells were incubated with the L-15 medium containing Oligonol (10 μg/mL) and 2% FBS from − 3 h to 0 h (*Pre-adsorption*), 0 h to 1 h (*Co-adsorption*), or 0 h to 96 h (*During infection*). For virus treatment, the virus (6×10^6 $TCID_{50}$) was incubated with 10 μg/mL of Oligonol at 25°C for 3 h. Following this, the mixture of virus and Oligonol was diluted 1:25 with the L-15 medium and then added to the cells and incubated at 25°C for 1 h. The cells were then washed twice and cultured in a fresh medium for 96 h (*Pre-treatment of virus*). The supernatants were harvested at 96 h.p.i, and the viral titers were determined by the $TCID_{50}$ assay.

2.6. *The attachment inhibition assay*

E-11 cells (5×10^5 cells) were seeded on 35-mm culture dishes and then pretreated with Oligonol (2.5 and 10 μg/mL) in the L-15 medium free of FBS at 25°C for 3 h. Following this, the cells were infected with the virus at an M.O.I of 1.0 in a medium containing various concentrations of Oligonol at 4°C for 1 h. After washing twice with the medium containing the same concentration of Oligonol, and twice with ice-cold PBS, the cells were lysed by TRIzol reagent (Life Technologies Corporation, CA, USA), total RNA was isolated as described previously (*4*), and analyzed by reverse transcription PCR (RT-PCR).

2.7. *Detection of viral RNA by RT-PCR*

RT-PCR was performed as described previously (*4*) with some modifications. Briefly, for the detection of (+) RNA1 and 18S ribosomal RNA (rRNA), the RNA samples extracted from the infected cells (5×10^4 and 5×10^2 cells, respectively) were used as a template. For the detection of (+) RNA1, the RNA samples were reverse transcribed with M-MLV reverse transcriptase (Life Technologies Corporation) using a primer, RGRNA1-2490R, (5′-GTCAGTGTAGTCTGCATACTG-3′) at 37°C for 50 min. Aliquots (one-tenth volume) of the reverse-transcribed samples were used for PCR amplification. PCR was performed using Pfu polymerase (Bio Academia, Inc., Osaka, Japan) and primers RGRNA1-2490R and RGRNA1-1868F (5′-TGCGTGAGTTCGTCGAGTTT-3′) with 30 cycles of denaturation at 94°C for 30 s, annealing at 57°C for 30 s, and extension at 72°C for 1 min. For the detection of 18S rRNA, 18S rRNA-R primer (5′-GCTGGAATTACCGCGGCT-3′) and 18S rRNA-F primer (5′-CGGCTACCACATCCAAGGAA-3′) were used. Reverse transcription and PCR amplification for 15 cycles were performed as described above. The PCR products were analyzed by agarose gel electrophoresis and visualized by ethidium bromide staining. Intensity of the bands was quantitated using the Image J software (National Institutes of Health, MD, USA).

3. Results

3.1. *Oligonol inhibits betanodavirus replication*

To determine the cytotoxicity of Oligonol, serial concentrations of Oligonol (0.63-40 μg/mL) were added to near-confluent E-11 cells (monolayer). In the viability assay, the cells treated with Oligonol concentrations lower than 10 μg/mL did not show any significant morphological changes (Figure 1A). The CC_{50} value of Oligonol was 27.0 ± 1.0 μg/mL.

To evaluate the antiviral potency of Oligonol against RGNNV, E-11 cells were treated with various concentrations of Oligonol and inoculated with RGNNV (0.01, 0.1, or 1.0 $TCID_{50}$/cell) for 96 h. Cell morphology was observed under a microscope (Figure 1A), and the cells were stained with crystal violet to calculate the EC_{50} value (Figure 1B and Table 1). We used bafilomycin A1 as a positive control drug. In the presence of bafilomycin A1 (10 nM), CPE development was completely suppressed, as reported previously (*4*). Similarly, CPE development was completely suppressed in the presence of 10 μg/mL (1.0 $TCID_{50}$/cell) as well as 2.5 μg/mL (0.01 $TCID_{50}$/cell) of Oligonol. The relative survival rate of the cells was calculated from the absorbance of the culture plates stained with crystal violet (Figure 1B). At the concentration of 10 μg/mL, almost a 100% survival rate was observed. As shown in Table 1, EC_{50} and SI of Oligonol depend on the amount of the virus used during inoculation. The effect of Oligonol on virus production was evaluated by the $TCID_{50}$ assay (Figure 1C). Oligonol treatment significantly inhibited virus production in a dose-dependent manner. The influence of Oligonol on expression of the viral coat protein was determined by Western blotting (Figure 1D). Ninety-six hours after the infection, cell lysates were prepared and subjected to Western blotting using an anti-coat protein antibody. The intensity of coat protein bands was significantly decreased by Oligonol (> 1.25 μg/mL). These results suggest that Oligonol inhibits betanodavirus replication in a dose-dependent manner with minimal cytotoxicity.

3.2. *The mode of action of Oligonol against betanodavirus*

To investigate the mode of action of Oligonol, the time-of-addition assay was performed (Figure 2A). Either Oligonol (10 μg/mL) or DMSO (0.04%) was added to E-11 cells before or during viral infection at an M.O.I of 1.0. Compared with DMSO treatment, pre-treatment of the virus with Oligonol showed no significant inhibitory effect on virus yield, suggesting that Oligonol lacks a virucidal activity (Figure 2A, right). On the other hand, a significant reduction (over 99%) in virus yield was observed when the cells were pre-incubated with Oligonol before virus adsorption (*Pre-adsorption*). Similarly, during the analysis of cell morphology (Figure 2B), pre-treatment of the virus with Oligonol did not significantly inhibit CPE development. In contrast, CPE development was substantially suppressed when the cells were pre-incubated with Oligonol before virus adsorption. When Oligonol was present during the full replication cycle (*During infection*), the titers of the progeny virus and CPE development were strongly reduced. In fact, substantial inhibition of virus yield and CPE development were observed when the cells were incubated with Oligonol before and during virus adsorption (*Pre-adsorption* and *Co-adsorption*). In summary, Oligonol showed significant antiviral activity against RGNNV when added before or during viral adsorption. These results suggest that Oligonol may interfere with the viral adsorption.

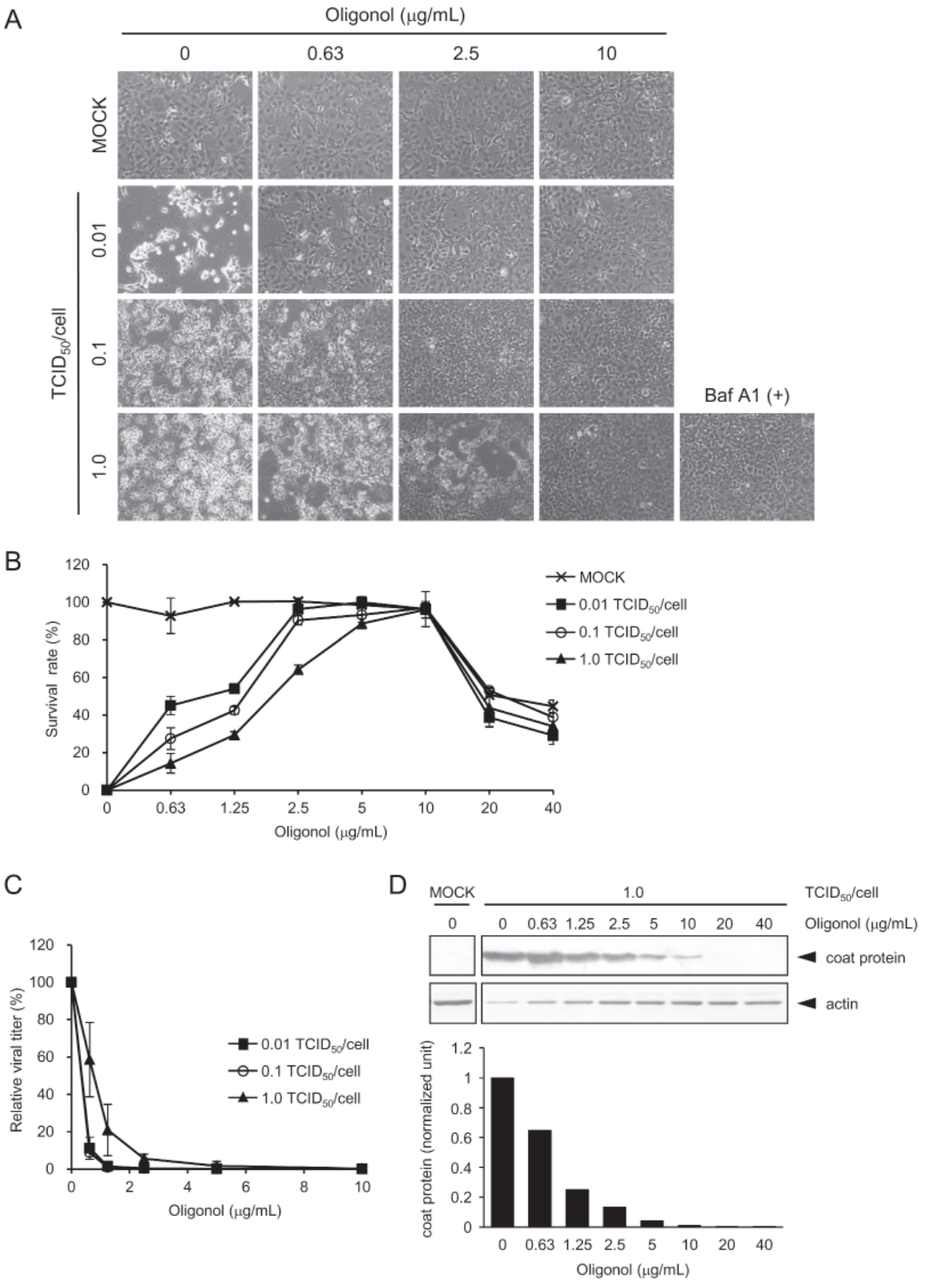

Figure 1. Anti-betanodavirus effects of Oligonol. E-11 cells infected with RGNNV (0.01, 0.1, and 1.0 $TCID_{50}$/cell) were treated with Oligonol for 96 h. **(A)** Effect of Oligonol on betanodavirus-induced CPE development observed under a phase-contrast microscope. Baf A1 (+): bafilomycin A1 (10 nM). **(B)** Effect of Oligonol on the cell survival rate. After staining with crystal violet, absorbance at 560 nm was determined and the percentage of survival rate was calculated. **(C)** Effect of Oligonol on betanodavirus production. Culture supernatants were collected and a viral titer was measured by the $TCID_{50}$ assay. The relative viral titer was calculated as the percentage of the viral titer to that of the cells infected in the absence of Oligonol. The data represents the mean of three independent experiments, and the error bars show standard deviation. **(D)** Effect of Oligonol on viral coat protein expression. Total cell lysates were prepared with lysis buffer and subjected to SDS-PAGE, and Western blotting was carried out using an anti-RGNNV coat protein antibody. Band intensity of the coat protein was normalized to actin and expressed as a ratio of the amount of coat protein in the treated cells to that in untreated cells.

3.3. *Oligonol partially inhibits attachment of betanodavirus to the cell*

To investigate the mechanism of the inhibitory effect of Oligonol on betanodavirus infection, we examined the influence of Oligonol on the attachment of betanodavirus to E-11 cells by the attachment inhibition assay. It has been reported that endocytosis of betanodavirus does not occur at 4°C (*18*). Cells were inoculated with the virus at an M.O.I = 1.0 in the presence of either 2.5 or 10 μg/mL of Oligonol for 1 h at 4°C. When E-11 cells were infected with the virus in the absence of Oligonol, the viral (+) RNA1 band was detected (Figure 3A). However, when the cells were treated with either 2.5 or 10 μg/mL of Oligonol, the intensity of these bands decreased. Relative band intensity of (+) RNA1 was calculated in normalized units (Figure 3B). In the presence of either 2.5 or 10 μg/mL of Oligonol, the relative band intensity decreased. These results suggest that Oligonol may inhibit the attachment of betanodavirus to the cell.

Table 1. *In vitro* cytotoxicity and anti-betanodavirus activity of Oligonol [a]

$TCID_{50}$/cell	EC_{50} (μg/mL)[b]	CC_{50} (μg/mL)[c]	Selectivity index (SI)[d]
0.01	0.87 ± 0.07	27.0 ± 1.0	31.1 ± 3.1
0.1	1.17 ± 0.06	27.0 ± 1.0	23.2 ± 2.0
1.0	1.81 ± 0.09	27.0 ± 1.0	15.0 ± 1.3

The values represent mean ± standard deviation of three independent experiments. [a] Evaluation after 96 h of treatment [b] 50% effective concentration [c] 50% cytotoxicity concentration [d] Selectivity index = CC_{50}/EC_{50}.

4. Discussion

In this study, we investigated the antiviral activity and the possible mode of action of Oligonol against betanodavirus replication. The results indicate that Oligonol effectively inhibits betanodavirus replication

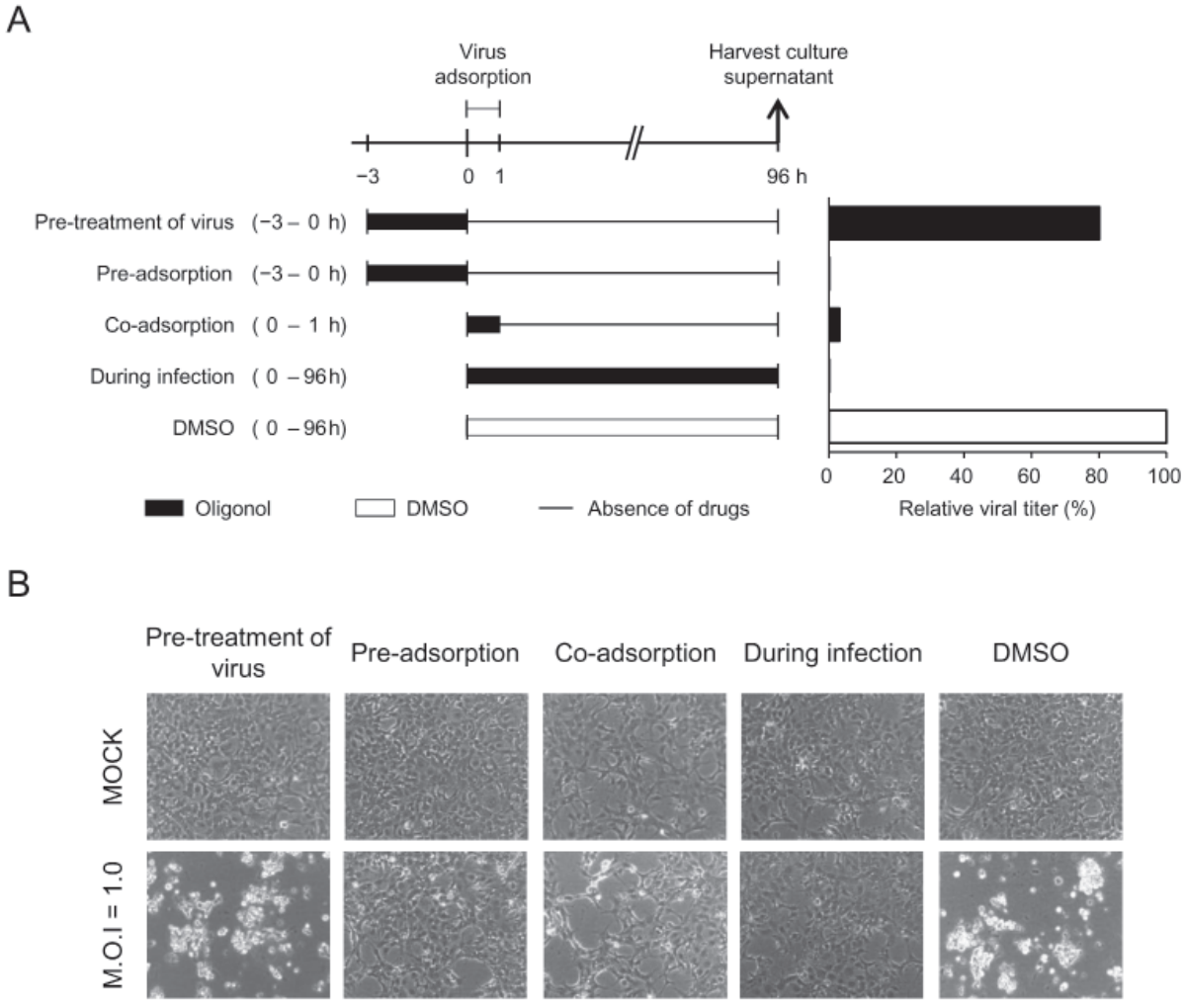

Figure 2. The time-of-addition assay for the effect of Oligonol on betanodavirus production. (A) Oligonol treatment protocols and the effect on betanodavirus production. E-11 cells were infected with RGNNV (1.5 $TCID_{50}$/cell corresponding approximately to an M.O.I of 1.0) and treated with Oligonol (10 μg/mL) or 0.04% (v/v) DMSO at the indicated periods. In the experiment with the pre-treatment of the virus, betanodavirus was incubated with Oligonol for 3 h and then diluted to achieve an M.O.I of 1.0 before viral adsorption. The culture supernatant was collected at 96 h.p.i, and virus yield was determined by the $TCID_{50}$ assay. The ratio of viral titers is presented as a mean of two independent experiments. **(B)** Effect of different Oligonol treatment protocols on the betanodavirus-induced CPE development. Pictures were taken using a phase-contrast microscope at 96 h.p.i.

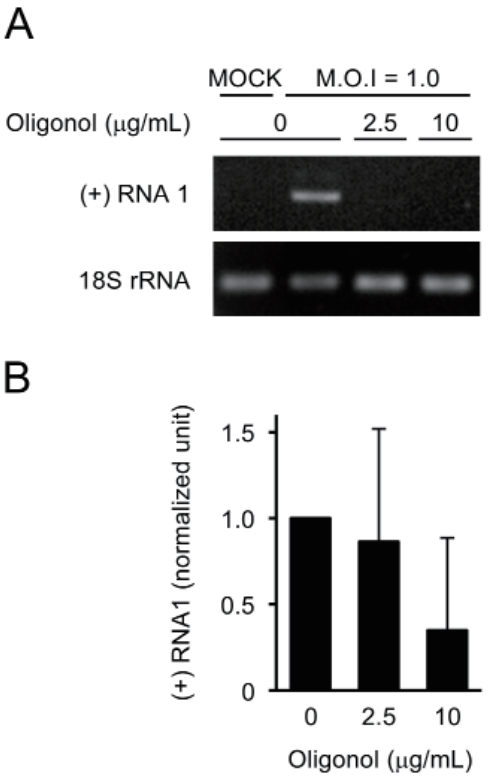

Figure 3. Effect of Oligonol on attachment of betanodavirus to the cells. (A) The attachment inhibition assay. E-11 cells were infected with RGNNV at an M.O.I of 1.0 in the presence of Oligonol (2.5 or 10 μg/mL) at 4°C for 1 h. Total RNA was isolated and (+) RNA1 and 18S ribosomal RNA (rRNA) were analyzed by RT-PCR. The data are representative of three independent experiments. **(B)** Quantification of relative band intensity of (+) RNA1. Intensity of (+) RNA1 and 18S rRNA bands was quantified, normalized to cellular 18S rRNA, and expressed as a ratio of the amount of (+) RNA1 in the treated cells to that in untreated cells. The data represents a mean of three independent experiments, and error bars show standard deviation.

in a dose-dependent manner as shown by the reduction of virus-induced CPE, virus production, and viral protein expression (Figure 1). The time-of-addition assays (Figure 2) suggested that the inhibition of betanodavirus replication by Oligonol primarily occurs at the virus adsorption step. Pre-treatment of cells before virus adsorption or treatment of cells during virus adsorption greatly reduced virus yield. However, pre-treatment of RGNNV virions prior to infection showed no inhibitory effect. These results indicate that Oligonol does not directly react with the virion.

The specific functional cell receptors for betanodavirus have not been identified yet, although it has been demonstrated that sialic acid is involved in RGNNV's binding to cells (*18*). A previous study on the antiviral effect of Oligonol on influenza A virus (*9*) showed that Oligonol affects viral surface molecules, thus interfering with the attachment step of this virus. Based on the results of the attachment inhibition assay (Figure 3), it can be concluded that Oligonol possibly inhibits attachment of the virion to the cell by interacting with cellular molecules.

Catechin, the polyphenolic compound from green tea, exhibits antiviral activity against influenza virus (*19*) and hepatitis C virus (*20*) by targeting the attachment and entry steps of the viral replication cycle. This phenomenon may be explained by the similarity of chemical structure of the different polyphenols in both Oligonol (*9*) and green tea (*19*). This observation suggests that the primary target of polyphenolic compounds is likely to be some membrane components.

In conclusion, this study demonstrated that Oligonol possesses suppressive properties against RGNNV replication. Oligonol targets an early step of RGNNV replication in E-11 cells, most likely by inhibiting the attachment of virions to cells. This inhibitory effect is accompanied by low toxicity. These results suggest that Oligonol can be considered as an anti-betanodavirus candidate drug.

References

1. Tan C, Huang B, Chang SF, Ngoh GH, Munday B, Chen SC, Kwang J. Determination of the complete nucleotide sequences of RNA1 and RNA2 from greasy grouper (*Epinephelus tauvina*) nervous necrosis virus, Singapore strain. J Gen Virol. 2001; 82:647-653.
2. Ikenaga T, Tatecho Y, Nakai T, Uematsu K. Betanodavirus as a novel transneuronal tracer for fish. Neurosci Lett. 2002; 331:55-59.
3. Samuelsen OB, Nerland AH, Jorgensen T, Schroder MB, Svasand T, Bergh O. Viral and bacterial diseases of Atlantic cod *Gadus morhua*, their prophylaxis and treatment: a review. Dis Aquat Organ. 2006; 71:239-254.
4. Adachi K, Ichinose T, Takizawa N, Watanabe K, Kitazato K, Kobayashi N. Inhibition of betanodavirus infection by inhibitors of endosomal acidification. Arch Virol. 2007; 152:2217-2224.
5. Gopiesh Khanna V, Kannabiran K, Sarath Babu V, Sahul Hameed A. Inhibition of fish nodavirus by gymnemagenol extracted from *Gymnema sylvestre*. J Ocean Univ China (English Edition). 2011; 10:402-408.
6. Balasubramanian G, Sarathi M, Venkatesan C, Thomas J, Sahul Hameed AS. Oral administration of antiviral plant extract of *Cynodon dactylon* on a large scale production against White spot syndrome virus (WSSV) in *Penaeus monodon*. Aquaculture. 2008; 279:2-5.
7. Kang SY, Kang JY, Oh MJ. Antiviral activities of flavonoids isolated from the bark of *Rhus verniciflua* stokes against fish pathogenic viruses *In Vitro*. J Microbiol. 2012; 50:293-300.
8. Saladino R, Gualandi G, Farina A, Crestini C, Nencioni L, Palamara AT. Advances and challenges in the synthesis of highly oxidised natural phenols with antiviral, antioxidant and cytotoxic activities. Curr Med Chem. 2008; 15:1500-1519.
9. Gangehei L, Ali M, Zhang W, Chen Z, Wakame K, Haidari M. Oligonol a low molecular weight polyphenol of lychee fruit extract inhibits proliferation of influenza virus by blocking reactive oxygen species-dependent ERK phosphorylation. Phytomedicine. 2010; 17:1047-1056.
10. Sakurai T, Nishioka H, Fujii H, Nakano N, Kizaki T, Radak Z, Izawa T, Haga S, Ohno H. Antioxidative effects of a new lychee fruit-derived polyphenol mixture, oligonol,

converted into a low-molecular form in adipocytes. Biosci Biotechnol Biochem. 2008; 72:463-476.
11. Fujii H, Sun B, Nishioka H, Hirose A, Aruoma OI. Evaluation of the safety and toxicity of the oligomerized polyphenol Oligonol. Food Chem Toxicol. 2007; 45:378-387.
12. Devalaraja S, Jain S, Yadav H. Exotic fruits as therapeutic complements for diabetes, obesity and metabolic syndrome. Food Res Int. 2011; 44:1856-1865.
13. Kundu JK, Hwang DM, Lee JC, Chang EJ, Shin YK, Fujii H, Sun B, Surh YJ. Inhibitory effects of oligonol on phorbol ester-induced tumor promotion and COX-2 expression in mouse skin: NF-kappaB and C/EBP as potential targets. Cancer Lett. 2009; 273:86-97.
14. Sung YY, Yang WK, Kim HK. Antiplatelet, anticoagulant and fibrinolytic effects of Litchi chinensis Sonn. extract. Mol Med Rep. 2012; 5:721-724.
15. Fujii H, Nishioka H, Wakame K, Magnuson BA, Roberts A. Acute, subchronic and genotoxicity studies conducted with Oligonol, an oligomerized polyphenol formulated from lychee and green tea extracts. Food Chem Toxicol. 2008; 46:3553-3562.
16. Iwamoto T, Nakai T, Mori K, Arimoto M, Furusawa I. Cloning of the fish cell line SSN-1 for piscine nodaviruses. Dis Aquat Organ. 2000; 43:81-89.
17. Adachi K, Ichinose T, Watanabe K, Kitazato K, Kobayashi N. Potential for the replication of the betanodavirus redspotted grouper nervous necrosis virus in human cell lines. Arch Virol. 2008; 153:15-24.
18. Liu W, Hsu CH, Hong YR, Wu SC, Wang CH, Wu YM, Chao CB, Lin CS. Early endocytosis pathways in SSN-1 cells infected by dragon grouper nervous necrosis virus. J Gen Virol. 2005; 86:2553-2561.
19. Song JM, Lee KH, Seong BL. Antiviral effect of catechins in green tea on influenza virus. Antiviral Res. 2005; 68:66-74.
20. Ciesek S, von Hahn T, Colpitts CC, Schang LM, Friesland M, Steinmann J, Manns MP, Ott M, Wedemeyer H, Meuleman P, Pietschmann T, Steinmann E. The green tea polyphenol, epigallocatechin-3-gallate, inhibits hepatitis C virus entry. Hepatology. 2011; 54:1947-1955.

(Received October 7, 2013; Revised November 12, 2013; Accepted November 25, 2013)

Original Article

DOI: 10.5582/ddt.2013.v7.6.261

Cerebrolysin attenuates cerebral and hepatic injury due to lipopolysaccharide in rats

Omar M. E. Abdel-Salam[1,*], Enayat A. Omara[2], Nadia A. Mohammed[3], Eman R. Youness[3], Yasser A. Khadrawy[4], Amany A. Sleem[5]

[1] *Department of Toxicology and Narcotics, National Research Centre, Cairo, Egypt;*
[2] *Department of Pathology, National Research Centre, Cairo, Egypt;*
[3] *Department of Medical Biochemistry, National Research Centre, Cairo, Egypt;*
[4] *Department of Medical Physiology, National Research Centre, Cairo, Egypt;*
[5] *Department of Pharmacology, National Research Centre, Cairo, Egypt.*

ABSTRACT: This study aimed to investigate the effect of cerebrolysin on oxidative stress in the brain and liver during systemic inflammation. Rats were intraperitoneally challenged with a single subseptic dose of lipopolysaccharide (LPS; 300 µg/kg) without or with cerebrolysin at doses of 21.5, 43 or 86 mg/kg. After 4 h, rats were euthanized and the brain and liver tissues were subjected to biochemical and histopathological analyses. Cerebrolysin revealed inhibitory effects on the elevation of lipid peroxidation and nitric oxide induced by LPS. In contrast, the decrease in reduced glutathione level and paraoxonase activity induced by LPS was attenuated by an injection of cerebrolysin in a dose-dependent manner. Moreover, cerebrolysin reduced LPS-induced activation of brain NF-κB and reversed LPS-induced decline of brain butyrylcholinesterase and acetylcholinesterase activities in a dose-dependent manner. Histopathological analyses revealed that neuronal damage and liver necrosis induced by LPS were ameliorated by cerebrolysin dose-dependently. Cerebrolysin treatment dose-dependently attenuated LPS-induced expressions in cyclooxygenase 2, inducible nitric oxide synthase, and caspase-3 in the cortex or striatum as well as the liver. These results suggest that cerebrolysin treatment might have beneficial therapeutic effects in cerebral inflammation. Cerebrolysin might also prove of value in liver disease and this possibility requires further exploration.

Keywords: Cerebrolysin, cholinesterases, lipopolysaccharide, NF-κB, oxidative stress

**Address correspondence to:*
Dr. Omar M. E. Abdel Salam, Department of Toxicology and Narcotics, National Research Centre, Tahrir St., Dokki, Cairo, Egypt.
E-mail: omasalam@hotmail.com

1. Introduction

Cerebrolysin is a brain derived peptide preparation produced by the biotechnologically standardized enzymatic breakdown of purified porcine brain proteins. It consists of a mixture of approximately 25% low molecular weight biologically active peptides (< 10 kDa) and 75% free amino acids, based on total nitrogen (*1*,*2*). The solution is free of proteins, lipids, and antigenic properties. Cerebrolysin has been shown to exert neurotrophic and neuroprotective actions, increasing the viability of cortical neurons and promoting their growth (*3*), increasing the tolerance of neurons to ischemic damage and slowing the execution of the cell death (*4*). The drug also has been shown to rescue the alterations in neurogenesis in amyloid precursor protein (APP) transgenic (tg) mice by protecting neural precursor cells and decreasing their rate of apoptosis (*5*) and to enhance neurogenesis in the ischemic brain (*6*). Cerebrolysin treatment resulted in significant improvements in the memory and global score and delayed progression in patients with Alzheimer's disease and vascular dementia (*1*,*7*) and improved the outcome after moderate and severe head injury (*2*) having only mild and transient adverse reactions. The efficacy of cerebrolysin persisted for up to several months after treatment, suggesting that cerebrolysin has not merely symptomatic benefits, but a disease-delaying potential (*7*).

Oxidative stress and increased inflammatory response have been implicated in the pathogenesis of neurological disorders such as stroke and ischemia/reperfusion injury (*8*) and in neurodegenerative diseases such as Parkinson's disease, Alzheimer's disease, Huntington's disease, amyotrophic lateral sclerosis, and multiple sclerosis (*9*). The brain is highly susceptible to oxidative stress in view of the high rate of oxygen utilization, its high content of polyunsaturated fatty acids, the presence of redox-active transition metals such as Cu^{2+} and Fe^{2+} and the paucity of antioxidant enzymes (*10*). The presence of systemic

inflammation also has profound effects on brain functions (*9*). The systemic injection of lipopolysaccharide (LPS), a product of the gram negative bacterial cell wall causes increased brain oxidative stress and neuroinflammation and thus represents a useful model for studying the effect of systemic inflammation on brain function (*11,12*). The mammalian Toll-like receptor 4 (TLR4) on immune cells is the signal-transducing receptor that when activated by the bacterial LPS triggers the acute inflammatory cascade (*13*). When administered peripherally at subseptic doses, LPS results in impaired antioxidant mechanisms and mitochondrial redox activity, increased lipid peroxidation (*11*,*12*), induction of cyclooxygenase 2 (COX-2) mRNA in the rat brain (*14*) and an up-regulation of cytokines such as tumor necrosis factor-alpha (TNF-α), interleukin (IL)-1β, and IL-6 in brain as well as in peripheral tissues and plasma (*15*). Studies also indicated that short-term systemic inflammation produced *in vivo* by administration of LPS can result in neuronal damage by itself (*16*) or exacerbates damage in an existing cerebral pathological state (*17*).

The aim of this study was therefore to investigate the effect of cerebrolysin on oxidative stress in the brain during systemic inflammation caused by intraperitoneal injection of LPS in rats. We also examined the effect of cerebrolysin on brain acetylcholinesterase (AChE) and butyrylcholinesterase (BChE) activities and on nuclear factor-kappaB (NF-κB), a multisubunit transcription factor that is critical for inducible expression of multiple genes involved in inflammatory responses (*18*). Moreover, the effect of cerebrolysin on oxidative stress and liver tissue damage caused by LPS was examined.

2. Materials and Methods

2.1. *Animals*

Sprague Dawley rats of either sex weighing (130 ± 10 g) were used. Animals were obtained from the Animal House Colony of the National Research Centre (Cairo, Egypt) and housed in stainless steel wire meshed suspended rodent cages under environmentally controlled conditions (25 ± 2°C and the light/dark cycle of 12/12 hours). Standard laboratory food and water were provided *ad libitum*. Animals received human care in compliance with guidelines of the Ethical Committee of National Research Centre and followed the recommendations of the National Institutes of Health Guide for Care and Use of Laboratory Animals (Publication No. 85-23, revised 1985).

2.2. *Drugs and chemicals*

LPS derived from *Escherichia coli* (Serotype 055: B5, Sigma-Aldrich, St Louis, MO, USA) was used and dissolved in sterile saline, aliquoted, and frozen at −20°C. Cerebrolysin (EVER Neuro Pharma GmbH, Unterach, Austria) was used and dissolved in isotonic (0.9% NaCl) saline solution immediately before use. The doses of cerebrolysin in the study were based upon the human dose after conversion to that of rat according to Paget and Barnes (*19*) conversion tables.

2.3. *Study design*

Rats were randomly divided into 5 groups of 6 animals each. Group I (normal control) received saline intraperitoneally (0.1 mL). Groups 2-5 were intraperitoneally (*i.p.*) injected with LPS in a dose of 300 μg/kg for induction of endotoxemia. Following LPS injection, group 2 was given *i.p.* saline and kept as positive control, while groups 3-5 were administered *i.p.* cerebrolysin at doses of 21.5, 43, and 86 mg/kg, respectively. Rats were euthanized 4 h after LPS injection by decapitation under ether anaesthesia, brains and livers were then removed, washed with ice-cold saline solution (0.9% NaCl), weighed and stored at –80ºC for the biochemical analyses. The tissues were homogenized with 0.1 M phosphate buffered saline at pH 7.4, to give a final concentration of 10% (w/v) for the biochemical assays. The time selected for tissue sampling (4 h after *i.p.* administration of LPS) was based on previous studies that indicated the rise in plasma and tissue cytokines and inflammatory mediators after LPS administration (*20*).

2.4. *Biochemical analyses*

2.4.1. *Determination of lipid peroxidation*

Lipid peroxidation was assayed by measuring the level of malondialdehyde (MDA). Malondialdehyde forms a 1:2 adduct with thiobarbituric acid which can be measured by spectrophotometry. Malondialdehyde was determined by measuring thiobarbituric reactive species using the method of Ruiz-Larrea *et al.* (*21*), in which the thiobarbituric acid reactive substances react with thiobarbituric acid to produce a red colored complex having peak absorbance at 532 nm.

2.4.2. *Determination of reduced glutathione (GSH)*

GSH was determined by Ellman's method (*22*). The procedure is based on the reduction of Ellman's reagent by –SH groups of GSH to form 2-nitro-s-mercaptobenzoic acid. The nitromercaptobenzoic acid anion has an intense yellow color which can be determined spectrophotometrically.

2.4.3. *Determination of nitric oxide*

Nitric oxide measured as nitrite was determined by using Griess reagent, according to the method of Moshage *et al.* (*23*) where nitrite, stable end product of nitric oxide radical, is mostly used as indicator for the production of nitric oxide.

2.4.4. *Determination of paraoxonase activity*

Arylesterase activity of paraoxonase (PON1) was measured spectrophotometrically in supernatants using phenyl acetate as a substrate (*24*). In this assay, arylesterase/paraoxonase catalyzes the cleavage of phenyl acetate resulting in phenol formation. The rate of formation of phenol was measured by monitoring the increase in absorbance at 270 nm at 25ºC. The working reagent consisted of 20 mM Tris-HCl buffer, pH 8.0, containing 1 mM calcium chloride and 4 mM phenyl acetate as the substrate. Samples diluted 1:3 in buffer were added and the change in absorbance was recorded following a 20 sec lag time. Absorbance at 270 nm was taken every 15 sec for 120 sec using a UV-VI8 Recording Spectrophotometer (Shimadzu, Kyoto, Japan). One unit of arylesterase activity is equal to 1 µM of phenol formed per minute. The activity was expressed in kU/L, based on the extinction coefficient of phenol of 1,310 M/cm at 270 nm, pH 8.0, and 25ºC. Blank samples containing water were used to correct for the spontaneous hydrolysis of phenylacetate.

2.4.5. *Determination of brain NF-κB*

NF-κB was measured in supernatants using commercially available ELISA kit (Glory Science Co., Ltd, Del Rio, TX, USA) using a double antibody sandwich enzyme-linked immunosorbent assay (ELISA) to assay the level of NF-κB.

2.4.6. *Determination of brain AChE activity*

AChE activity in the cortex was determined according to Gorun *et al*. (*25*). The principle of the method is the measurement of the thiocholine produced as acetylthiocholine is hydrolyzed. The color was read immediately at 412 nm.

2.4.7. *Determination of brain BChE activity*

BChE activity was measured spectrophotometrically in supernatants using commercially available kit (Ben S.r.l., Milano, Italy). In this assay cholinesterase catalyzes the hydrolysis of butyrilthiocholine, forming butyrate and thiocholine. The thiocholine reacts with 5,5'-dithiobis-2-nitrobenzoic acid (DTNB) forming a colored compound. The increase in absorbance in the unit time at 405 nm is proportional at the activity of the cholinesterase in the sample.

2.5. *Histopathological examination*

The brain and liver tissue from different groups were collected and fixed in 10% formalin, dehydrated in graduated ethanol 50-100%, cleared in xylene, and embedded in paraffin. Sections 4-5 µm thick were prepared, stained with haematoxylin and eosin (H & E) stain, and examined for histopathological changes under light microscope.

2.6. *Immunohistochemical analysis*

For immunohistochemistry, 4 µm thick deparaffinized brain and liver tissue sections were used. Briefly, deparaffinized slices were incubated overnight with the antibodies against COX-2 diluted 1:100, inducible nitric oxide synthase (iNOS) diluted 1:100, and cleaved caspase-3 diluted 1:1,000. Endogenous peroxidase activity was blocked by incubation in 0.075% hydrogen peroxide in PBS. For antibody detection DAKO EnVision+ System, Peroxidase/DAB kit was employed. The sections were then counterstained with haematoxylin, dehydrated using graded alcohols and xylene, and mounted with Entelan. The immunostaining intensity and cellular localization of, COX-2, iNOS, and cleaved caspase-3 were analyzed by light microscopy.

2.7. *Statistical analysis*

Data were expressed as mean ± SEM. The data were analyzed by one-way ANOVA followed by Duncan's multiple range test, using SPSS software (SAS Institute Inc., Cary, NC, USA). A probability value of less than 0.05 was considered statistically significant.

3. Results

3.1. *Biochemical results*

3.1.1. *Lipid peroxidation*

The administration of LPS resulted in a significant increase in the level of MDA in brain and liver by 40.1% (36.48 ± 1.58 *vs*. 26.04 ± 1.92 nmol/g) and 73.8% (48.33 ± 1.3 *vs*. 27.8 ± 0.65 nmol/g), respectively, compared with the saline control group. Brain MDA significantly decreased by 19.8% following treatment with cerebrolysin at 86 mg/kg, compared with the LPS control group (29.24 ± 2.0 *vs*. 36.48 ± 1.58 nmol/g). Meanwhile, in the liver, MDA significantly decreased by 38.5, 44.5, and 45.6% after cerebrolysin doses of 24.5, 43, and 86 mg/kg, respectively (Table 1).

3.1.2. *GSH*

Following LPS challenge, GSH decreased by 42.8% (3.49 ± 0.08 *vs*. 6.10 ± 0.58 µmol/g) and 36.6% (5.20 ± 0.39 *vs*. 8.20 ± 0.33 µmol/g) in brain and liver, respectively, compared with the saline control group. A significant increase by 17.5% was observed in brain GSH after the highest dose of cerebrolysin (4.10 ± 0.14 *vs*. 3.49 ± 0.08 µmol/g). Meanwhile, the level of GSH in liver was not significantly altered by treatment with cerebrolysin (Table 1).

3.1.3. *Nitric oxide*

A significant increase in the level of nitric oxide by 56.7 and 102.6% was observed in brain (29.52 ± 0.72 *vs*. 18.84 ± 0.52 µmol/g) and liver (30.75 ± 1.22 *vs*. 15.18 ± 1.62 µmol/g), respectively. Cerebrolysin inhibited the rise in brain nitric oxide in a dose dependent manner by 22.4, 27.2, and 42.7% in brain. Similarly, cerebrolysin treatment resulted in decreased nitric oxide levels in the liver by 28.3, 32.0, and 34.5% (Table 1).

3.1.4. *Paraoxonase*

The activity of the enzyme was significantly decreased in both the brain and liver by LPS injection. In the brain PON1 activity decreased by 42.5% (7.46 ± 0.44 *vs*. 12.97 ± 0.77 kU/L). In the liver PON1 activity decreased by 36.9% (24.42 ± 0.80 *vs*. 38.67 ± 2.1 kU/L). Cerebrolysin inhibited the decline in PON1 activity in both brain and liver tissue in a dose-dependent manner. In brain PON1 activity increased by 59.7, 92.1, and 104.6% by cerebrolysin doses of 24.5, 43, and 86 mg/kg as compared to LPS control. In the liver, PON1 activity increased by 24.5, 34.6 and 38.2% by cerebrolysin as compared to LPS control (Table 1).

3.1.5. *NF-κB*

NF-κB in the brain was markedly increased following endotoxin administration (16.90 ± 0.12 *vs*. 2.20 ± 0.08 U/L). Treatment with cerebrolysin resulted in a significant and dose-dependent reduction in brain NF-κB by 15.7, 39.1, and 59.3% (14.25 ± 0.62, 10.30 ± 0.28, 6.88 ± 0.26 U/L) by cerebrolysin given at 24.5, 43 and 86 mg/kg as compared to LPS control (16.90 ± 0.12 U/L) (Table 2).

3.1.6. *AChE*

The administration of LPS was followed by a significant decrease in brain AChE activity by 26.5% (5.68 ± 0.24 *vs*. 7.73 ± 0.32 µmol SH/g/min). The decline in AChE was reversed by cerebrolysin given at 43 and 86 mg/kg which increased AChE activity by 23.6 and 29.2%, respectively, as compared to the LPS control (7.02 ± 0.54 and 7.34 ± 0.56 *vs*. 5.68 ± 0.24 µmol SH/g/min) (Table 2).

3.1.7. *BChE*

Following LPS challenge, a significant decrease in brain BChE activity by 23.9% was observed as compared to saline control (217.6 ± 8.9 *vs*. 285.8 ± 15.6 U/L). Cerebrolysin (24.5, 43 and 86 mg/kg) given to LPS-treated rats resulted in a significant and dose-dependent elevation in brain BChE activity by 26.7, 128.9, and 239.5% (275.7 ± 14.9, 498.1 ± 17.1, 738.8 ± 25.6 U/L) as compared to LPS control (217.6 ± 8.9 U/L). BChE activity increased by 74.3 and 158.5% by 43 and 86 mg/kg cerebrolysin as compared to the saline control (Table 2).

Table 1. Effect of cerebrolysin on malondialdehyde (MDA), reduced glutathione (GSH), nitric oxide (NO) levels and paraoxonase (PON1) activity in brain and liver of rats treated with lipopolysaccharide

	Saline	LPS	LPS + cerebrolysin 24.5 mg/kg	LPS + cerebrolysin 43 mg/kg	LPS + cerebrolysin 86 mg/kg
Brain					
MDA (nmol/g.tissue)	26.04 ± 1.92	36.48 ± 1.58*	32.00 ± 1.08*	31.92 ± 1.13*	29.24 ± 2.0+
GSH (µmol/g.tissue)	6.10 ± 0.58	3.49 ± 0.08*	3.39 ± 0.12*	3.83 ± 0.06*	4.10 ± 0.14*
NO (µmol/g.tissue)	18.84 ± 0.52	29.52 ± 0.72*	22.90 ± 0.66*,+	21.48 ± 1.42+	16.92 ± 0.84+
PON1 (kU/L)	12.97 ± 0.77	7.46 ± 0.44*	11.91 ± 0.86+	14.33 ± 0.65+	15.26 ± 0.72+
Liver					
MDA (nmol/g.tissue)	27.80 ± 0.65	48.33 ± 1.30*	29.74 ± 1.70+	26.80 ± 1.42+	26.30 ± 1.27+
GSH (µmol/g.tissue)	8.20 ± 0.33	5.20 ± 0.39*	5.66 ± 0.18+	5.54 ± 0.21*	5.40 ± 0.36*
NO (µmol/g.tissue)	15.18 ± 1.62	30.75 ± 1.22*	22.05 ± 1.79*,+	20.90 ± 1.36*,+	20.14 ± 1.30*,+
PON1 (kU/L)	38.67 ± 2.10	24.42 ± 0.80*	30.40 ± 2.10*,+	32.86 ± 1.51+	33.74 ± 1.98+

Results are mean ± S.E. Six rats were used per each group. Data were analyzed by one-way ANOVA and means of different groups were compared by Duncan's multiple range test. $p < 0.05$ was considered statistically significant. * $p < 0.05$ *vs.* saline group. + $p < 0.05$ *vs*. LPS control group.

Table 2. Effect of cerebrolysin on NF-κB, acetylcholinesterase (AChE) activity and butyrylcholinesterase (BChE) activity in rat brain tissues after lipopolysaccharide (LPS) in rats

	Saline	LPS	LPS + cerebrolysin 24.5 mg/kg	LPS + cerebrolysin 43 mg/kg	LPS + cerebrolysin 86 mg/kg
NF-κB (U/L)	2.20 ± 0.08	16.90 ± 0.12*	14.25 ± 0.62*,+,#	10.30 ± 0.28*,+	6.88 ± 0.26*,+,#
AChE (µmol SH/g/min)	7.73 ± 0.32	5.68 ± 0.24*	6.15 ± 0.61*	7.02 ± 0.54+	7.34 ± 0.56+
BChE (U/L)	285.8 ± 15.6	217.6 ± 8.9*	275.7 ± 14.9+,#	498.1 ± 17.1*,+	738.8 ± 25.6*,+,#

Results are mean ± S.E. Six rats were used per each group. Data were analyzed by one-way ANOVA and means of different groups were compared by Duncan's multiple range test. $p < 0.05$ was considered statistically significant. * $p < 0.05$ *vs*. saline group. + $p < 0.05$ *vs*. LPS control group. # $p < 0.05$ *vs*. LPS + cerebrolysin at 43 mg/kg-treated group.

3.2. *Brain histopathology*

Sections from the cortex and striatum in saline-treated rats showed normal cytoplasm and nucleus in neurons (Figures 1A and E). Microscopic examination of sections from the cortex and striatum of LPS only treated rats revealed neuronal damage indicated by necrosis, gliosis, vacuolation of neuropil, and degenerative changes with shrunken, darkly stained pyknotic nuclei. Inflammatory cell infiltration was observed in cerebral cortex and striatum. In brain parenchyma vacuoles with hemorrhage were also noticed (Figures 1B and F). Examined brain sections of rats treated with LPS and cerebrolysin at 43 mg/kg showed no histopathological changes except for pyknosis of some nuclei (Figures 1C and G). Brain sections of rats treated with LPS and cerebrolysin at 86 mg/kg showed almost normal architecture and normal neuron cells similar to those of the control (Figures 1D and H).

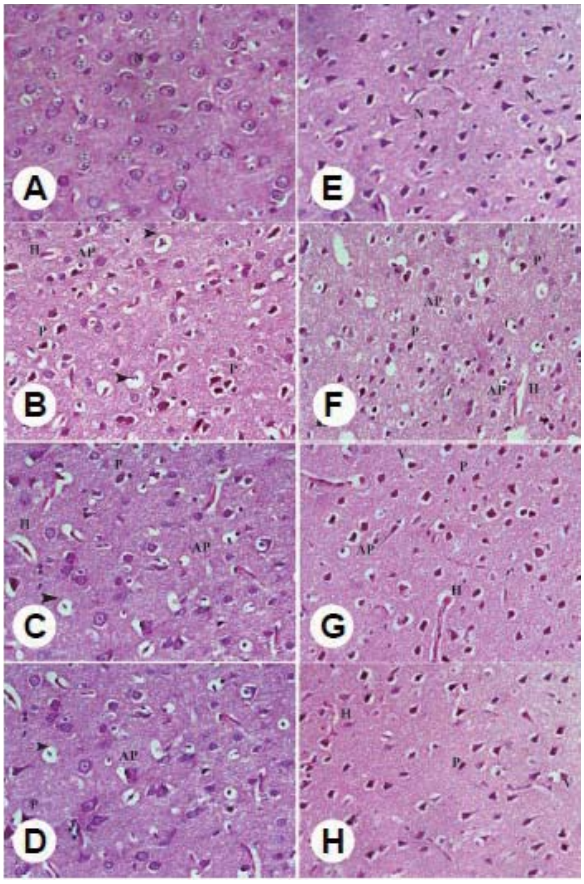

Figure 1. H & E stained sections from the rat cortex and striatum. (**A**) normal rat cortex showing the normal neurons (N); (**B**) cortex after LPS injection showing cytoplasmic vacuolation (arrow head), haemorrhage (H) and pyknotic darkly stained nuclei (P) with apoptotic cells (AP); (**C**) cortex after injection of LPS and cerebrolysin at 43 mg/kg showing moderate amelioration of damage with cytoplasmic vacuolations (arrow head), and pyknotic darkly stained nuclei (P) with apoptotic cells (AP); these changes were less as compared with LPS only treated group; (**D**) cortex after injection of LPS and cerebrolysin at 86 mg/kg marked amelioration of damage and recovery of the brain cells with few cytoplasmic vacuolations (arrow head) and pyknotic darkly stained nuclei (P) with apoptotic cells (AP); (**E**) normal rat striatum showing the neuron with the surrounding supporting cells with normal nuclei which showed dispersed chromatin and prominent nucleoli. The cytoplasm of these cells was basophilic; (**F**) striatum after LPS injection showing shrunken neurons with vacuolation of neuropil (V) and haemorrhage. Pyknotic (P) darkly stained and apoptotic nuclei (AP) were seen; (**G**) striatum after injection of LPS and cerebrolysin at 43 mg/kg showing amelioration of damage with less vacuolation of neuropil (V), hemorrhage, pyknotic (P) darkly stained and apoptotic nuclei (AP); (**H**) striatum after injection of LPS and cerebrolysin at 86 mg/kg: evidence of neuroprotection with markedly reduced number of damaged cells with few vacuolation of neuropil (V), hemorrhage, pyknotic (P) darkly stained and apoptotic nuclei (AP) (H & E, ×400).

3.3. *Brain immunohistochemistry*

3.3.1. *COX-2 expression*

Negligible COX-2-immunopositive neurons were seen in cortex and striatum of saline control group (Figures 2A and E, respectively). COX-2 expression in the cortex and

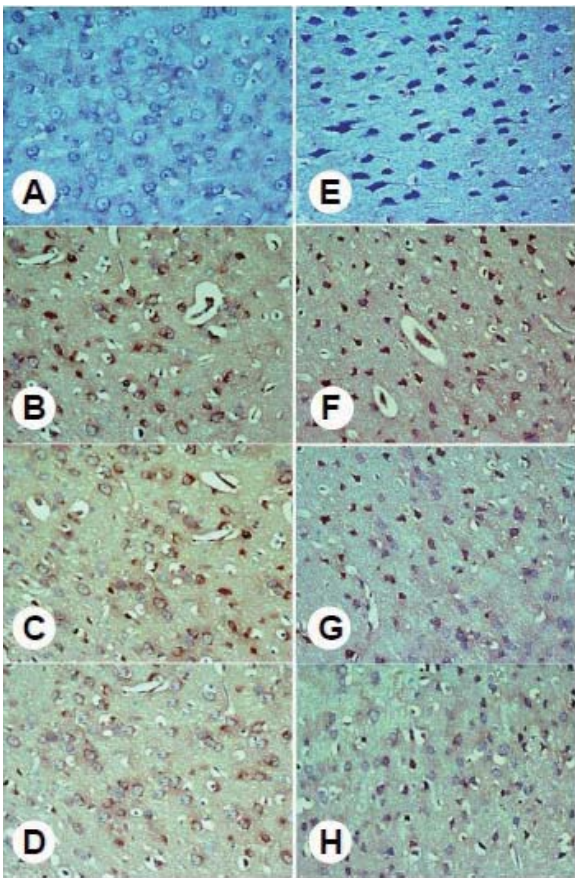

Figure 2. COX-2 immunohistochemistry of rat cortex and striatum. (**A**) negligible positive immunostaining in normal rat cortex; (**B**) strong COX-2 expression in cortex after LPS injection; (**C**) cortex after injection of LPS and cerebrolysin at 43 mg/kg: markedly decreased COX-2 expression; (**D**) cortex injection of LPS and cerebrolysin at 86 mg/kg: markedly decreased COX-2 expression. (**E**) striatum of control rat: negligible positive immunostaining; (**F**) strong COX-2 expression in striatum after LPS injection; (**G**) striatum after injection of LPS and cerebrolysin at 43 mg/kg: markedly reduced COX-2 expression; (**H**) striatum after injection of LPS and cerebrolysin at 86 mg/kg: almost normal COX-2 expression (COX-2 immunohistochemistry, haematoxylin counterstain, ×400). Brown color indicates positive.

striatum increased after LPS administration (Figures 2B and F, respectively). Sections from rats treated with LPS and cerebrolysin showed moderate to normal staining of COX-2 expression in the cortex (Figures 2C and D) and striatum (Figures 2G and H).

3.3.2. *iNOS immunoreactivity*

No iNOS immunoreactivity was observed in the cytoplasm of neurons in cortex and striatum of control rats (Figures 3A and E, respectively). The administration of LPS was followed by a significant increase in iNOS immunopositivity (Figures 3B and F). The administration of cerebrolysin resulted in a dose-dependent decrease in iNOS expression in neurons of cortex (Figures 3C and D) and striatum (Figures 3G and H).

3.3.3. *Cleaved caspase-3 immunoreactivity*

No caspase-3 immunoreactivity was observed in the cytoplasm of neurons in in cortex and striatum of control rats (Figures 4A and E). Caspase-3 immunostaining was observed in neurons distributed around the damage area and the number of immunopositive neurons increased after treatment with LPS (Figures 4B and F). On the other hand, caspase-3 immunostaining gradually decreased under treatment with cerebrolysin in a dose-dependent manner (Figures 4C, D, G, and H).

3.4. *Liver histopathology*

Figure 5A shows the normal hepatic architecture. In the liver sections from rats given only LPS injection,

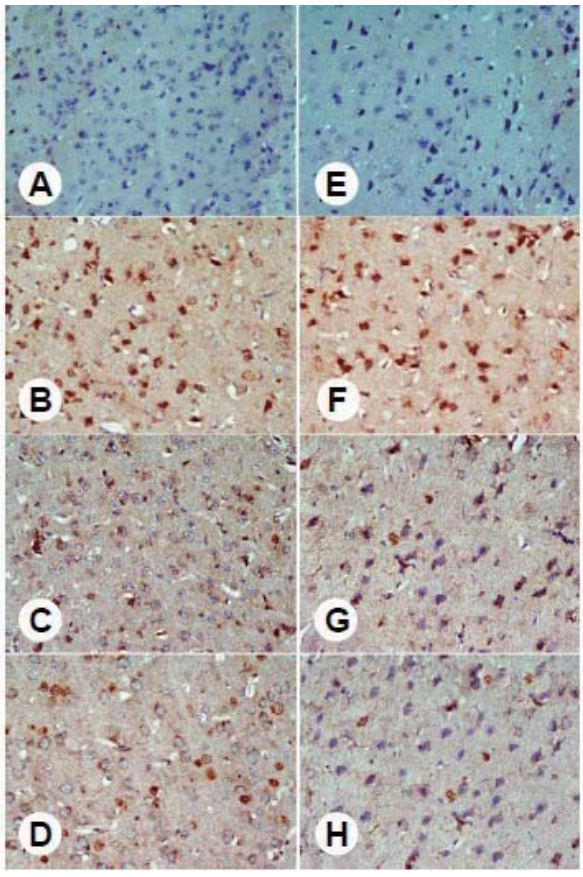

Figure 3. iNOS immunohistochemistry of rat cortex and striatum. (**A**) cortex of control rat: iNOS-immunopositive neurons; (**B**) significant increase in iNOS immunopositivity in cortical neurons after LPS injection; (**C**) cortex after injection of LPS and cerebrolysin at 43 mg/kg: markedly decreased iNOS expression compared to LPS control; (**D**) cortex after injection of LPS and cerebrolysin at 86 mg/kg: minimal iNOS expression. (**E**) striatum of control rat: no positive immunostaining; (**F**) striatum after LPS injection: significant increase in iNOS immunopositivity; (**G**) striatum after injection of LPS and cerebrolysin at 43 mg/kg: markedly decreased iNOS expression compared to LPS control; (**H**) striatum after injection of LPS and cerebrolysin at 86 mg/kg: minimal iNOS expression (iNOS immunohistochemistry, haematoxylin counterstain, ×400). Brown color indicates positive.

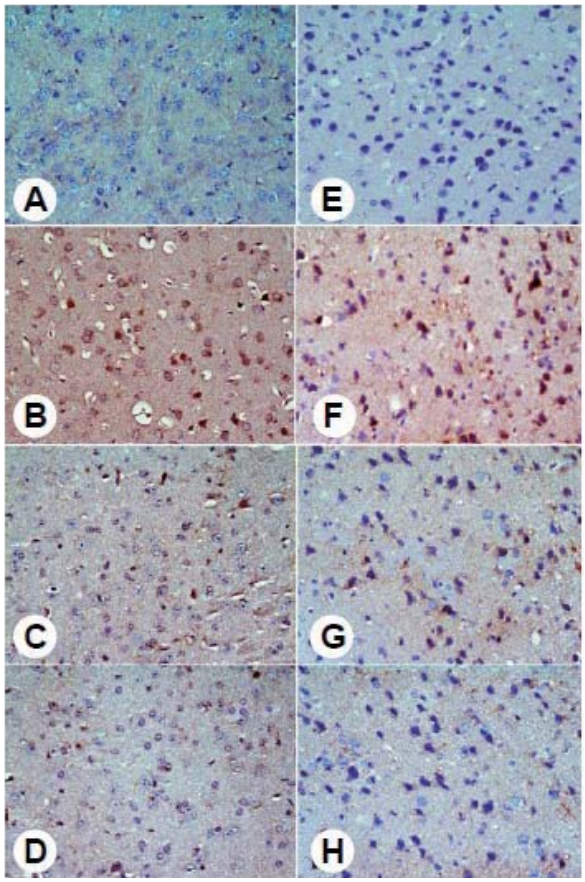

Figure 4. Expression of caspase-3 in cortical and striatal neurons. (**A**) normal rat cortex: caspase-3 immunohistochemistry not present; (**B**) cortex of LPS-treated rat: there is increased caspase-3 expression; (**C**) cortex after injection of LPS and cerebrolysin at 43 mg/kg; markedly decreased caspase-3 expression; (**D**) cortex after injection of LPS and cerebrolysin at 86 mg/kg: markedly decreased caspase-3 expression. (**E**) striatum of control rat: caspase-3 immunohistochemistry not present; (**F**) striatum of LPS-treated rat: there is increased caspase-3 expression; (**G**) striatum after injection of LPS and cerebrolysin at 43 mg/kg; markedly reduced caspase-3 expression to near normal; (**H**) striatum after injection of LPS and cerebrolysin at 86 mg/kg: caspase-3 expression nearly normal (Caspase-3 immunohistochemistry, haematoxylin counterstain, ×400). Brown color indicates positive.

large areas of pericentral necrosis with loss of hepatic architecture, vacuolar fatty change and inflammatory cell infiltration comprised predominantly of mononuclear cells and macrophages, have been found (Figures 5B and C). Treatment with cerebrolysin was associated with a dose-dependent improvement in the liver morphology (Figures 5D-F). When given at 43 mg/kg, the drug resulted in amelioration of liver damage with few necrotic areas being present (Figure 5E). The higher dose of 86 mg/kg almost completely prevented liver necrosis, showing minimal hepatic damage (Figure 5F).

3.5. *Liver immunohistochemistry*

3.5.1. *COX-2 expression*

In saline control group, negligible COX-2-immunopositive cells were seen in liver tissue (Figure 6A). However, after LPS injection increased expression of COX-2 immunopositivity was detected in the cytoplasm (Figure 6B). This was attenuated by cerebrolysin in a dose-dependent manner (Figures 6C and D).

3.5.2. *iNOS expression*

Negligible iNOS immunopositivity in the livers of control rats was noticed (Figure 7A). LPS intoxication increased iNOS immunoreactivity in necrotic areas (Figure 7B) which was slightly ameliorated by cerebrolysin at the dose of 21.5 mg/kg. Cerebrolysin given at 43 mg/kg markedly reduced cytoplasmic iNOS immunoreactivity as compared to the lower dose (Figure 7C), whereas in those treated with cerebrolysin at 86 mg/kg, iNOS expression was similar to controls (Figure 7D).

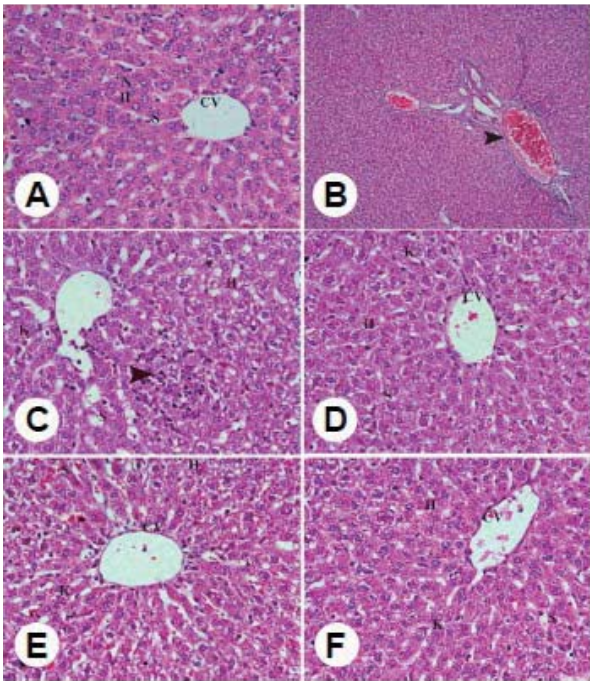

Figure 5. H & E stained sections from the rat liver. (**A**) normal liver with central vein (CV) and surrounding hepatocytes (H), sinusoids (S) and nucleus (N); (**B**) after LPS injection showing dilatation and congestion of portal tract with inflammatory cell infiltration around portal tract (arrow head); (**C**) after LPS injection showing pericentral necrosis with inflammatory cell infiltration (arrow head), degeneration of hepatocytes (H), dilatation and congestion of hepatic sinusoids (S) and activated Kupffer cells (K); (**D**) after injection of LPS and cerebrolysin at 21.5 mg/kg showing damage of hepatic cells with degeneration of some hepatocytes (H), dilatation of hepatic sinusoids (S) and activated Kupffer cells (K); (**E**) after injection of LPS and cerebrolysin at 43 mg/kg showing normal hepatic cells with less degeneration of some hepatocytes (H), dilatation of hepatic sinusoids (S) and activated Kupffer cells (K); (**F**) after injection of LPS and cerebrolysin at 86 mg/kg showing markedly reduced number of hepatocytes with normal hepatic cells (H), few dilatation of hepatic sinusoids (S) and activated Kupffer cells (K) (H & E, ×400).

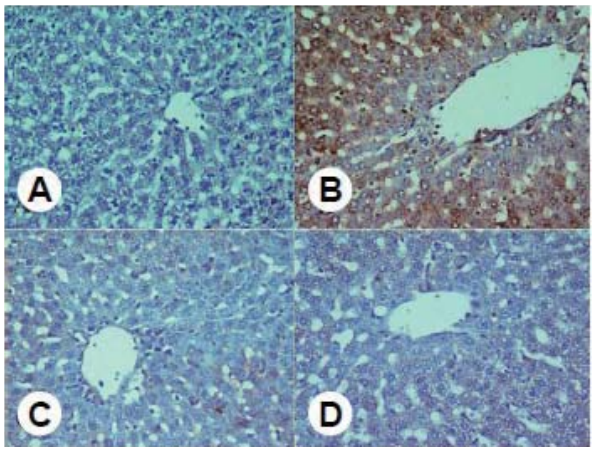

Figure 6. COX-2 immunohistochemistry of rat liver. (**A**) negligible positive immunostaining in normal rat; (**B**) strong COX-2 expression after LPS injection; (**C**) LPS and cerebrolysin at 43 mg/kg: nearly normal COX-2 expression; (**D**) LPS and cerebrolysin at 86 mg/kg: nearly normal COX-2 expression (COX-2 immunohistochemistry, haematoxylin counterstain, ×400). Brown color indicates positive.

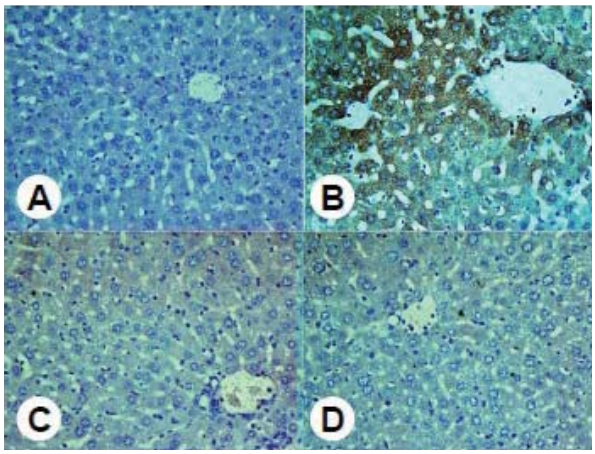

Figure 7. iNOS immunohistochemistry of liver. (**A**) control rat: negligible iNOS immunopositivity; (**B**) after LPS injection: markedly increased iNOS immunoreactivity in necrotic areas; (**C**) LPS and cerebrolysin at 43 mg/kg: more decrease in cytoplasmic iNOS immunoreactivity compared with the previous section; (**D**) LPS and cerebrolysin at 86 mg/kg: iNOS expression nearly normal (iNOS immunohistochemistry, haematoxylin counterstain, ×400). Brown color indicates positive.

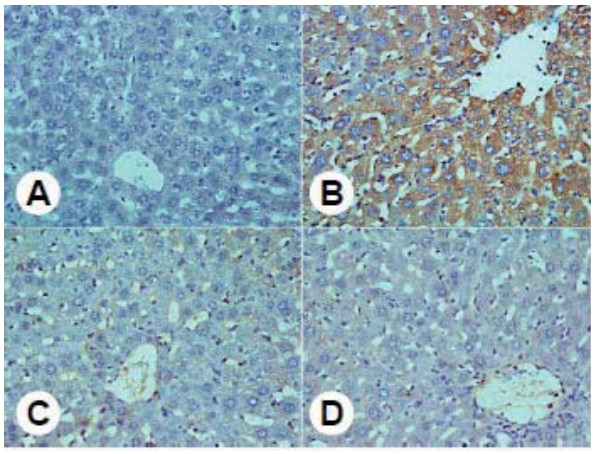

Figure 8. Caspase-3 immunohistochemistry in liver. (**A**) control rat: negligible caspase-3 immunopositivity; (**B**) LPS-treated rat: increased caspase-3 expression; (**C**) LPS and cerebrolysin at 43 mg/kg: markedly reduced caspase-3 expression; (**D**) LPS and cerebrolysin at 86 mg/kg: caspase-3 immunopositivity nearly normal (Caspase-3 immunohistochemistry, haematoxylin counterstain, ×400). Brown color indicates positive.

3.5.3.*Caspase-3 immunoreactivity*

Negligible caspase-3 immunopositivity was observed in the livers of control rats (Figure 8A). However, after LPS treatment a significant increase in caspase-3 immunoreactivity in the cytoplasm of hepatocytes was found (Figure 8B). This was subsequently reduced under treatment with different doses of cerebrolysin (Figures 8C and D).

4. Conclusion

This study examined the effect of cerebrolysin, a mixture of neurotrophic factors, on the development of oxidative stress and brain injury induced in rats by LPS endotoxin. The study demonstrates for the first time that cerebrolysin decreased the oxidative stress and the neuroinflammatory response and neuronal damage induced by peripherally injected LPS. The transcription factor NFκB, a central mediator of the immune response, which is critical for inducible expression of multiple genes involved in inflammatory responses is also reduced by the drug. These data suggest the usefulness of cerebrolysin in systemic inflammatory conditions involving the brain. We also showed that treatment with cerebrolysin decreased the LPS-induced liver injury.

The administration of LPS was associated with an increase in lipid peroxidation (measured as increased malondialdehyde) and a drop in GSH level, which indicates the development of oxidative stress and consumption of GSH by the increased generation of free radicals. Other researchers have reported decreased brain GSH and glutathione reductase activity in rats after the administration of LPS (1 mg/kg, *i.p.*) (*12*). Similarly, a single intraperitoneal dose of LPS (250 µg/mouse) was associated with GSH depletion, and lipid peroxidation and impairment in mitochondrial redox activity (*11*). Cerebrolysin at the highest dose examined caused a mild yet a significant decrease in brain MDA which was associated with an increase in GSH. Glutathione, a tripeptide of glycine, glutamic acid, and cysteine, is the most abundant nonprotein thiol in almost all aerobic species and which participates non-enzymatically and enzymatically in supporting cellular redox balance and in protecting against oxidative damage by reactive oxygen species (*26*). Studies have shown decreased glutathione content in brain of patients suffering from a number of neurological diseases (*27*), thereby implicating GSH consumption by free radicals in the pathogenesis of these disorders.

NF-κB is a ubiquitously expressed transcription factor that activates transcription of various inflammatory cytokines, adhesion molecules, and chemokines involved in the generation of acute inflammation (*18*). NF-κB is thus a critical intracellular mediator of the inflammatory cascade. Stimulation of cells by bacterial endotoxin or cytokines *e.g.*, TNF-α, and IL-1β leads to a dissociation of NF-κB from its inhibitory subunit IκBα and a rapid translocation of free NF-κB to the nucleus (*18*). NF-κB can also be activated by reactive oxygen species (*28*). In the present experiments, cerebrolysin decreased NF-κB levels in the brain after LPS challenge in a dose-dependent manner. This ability of cerebrolysin to decrease the induction of NF-κB activity might be involved in its neuroprotective effects by decreasing brain inflammation under pathological circumstances.

Reduced PON1 activity has been observed in the serum from patients with neurodegenerative diseases *e.g.*, Alzheimer disease and mixed dementia (*29*). This enzyme which possesses an organophosphatase, arylesterase, and lactonase activity and hydrolyzes many different substrates (*30*) is largely though to protect cellular membranes against oxidative stress (*31*). In the present study, markedly decreased PON1 activity was observed in the brain and liver after endotoxin challenge. Cerebrolysin was able to reverse the decline in PON1 activity after LPS injection, suggesting a stimulatory effect for cerebrolysin on the enzyme or reduction of oxidative stress by cerebrolysin with consequent sparing of PON1.

Cerebrolysin demonstrated a strong inhibitory effect on nitric oxide levels in brain after LPS challenge. The drug also attenuated the increased expression of iNOS in brain tissue. Increased generation of nitric oxide occurs during inflammatory conditions due to the action of the inducible form of nitric oxide synthase (iNOS). Glial cells (astrocytes and microglia) synthesize nitric oxide after the transcriptional expression of a Ca^{2+}-independent iNOS (*32*). Overproduction of reactive nitrogen species or nitrosative stress results in nitrosylation reactions that can alter the structure

of proteins and so inhibit their normal function (*33*). Synthesis of nitric oxide by both the inducible and constitutive NOS isoforms also contribute to the activation of apoptotic pathways in the brain during systemic inflammation induced by LPS (*34*). Moreover, LPS-activated microglia has been shown to mediate oligodendrocyte progenitor cell death involving nitric oxide-dependent oxidative pathway (*35*). In this way systemic inflammatory responses can affect neurogenesis, a process by which new neurons are added in the adult mammalian brain with the consequently the repair/replacement of the lost neuronal systems (*36*). Cerebrolysin thus by decreasing brain inflammation is likely to protect neurogenesis from oxidative and nitrosative mediated cell damage. In this context, there are data to suggest a beneficial effect for cerebrolysin on the process of neurogenesis. Thus in APP tg mice cerebrolysin might rescue the alterations in neurogenesis in APP tg mice by protecting neural precursor cells and decreasing the rate of apoptosis (*5*). Moreover, cerebrolysin treatment initiated 24 and 48 h after experimental stroke enhanced neurogenesis in the ischemic brain and improved functional outcome (*6*).

The inducible form of the enzyme cyclooxygenase, the rate limiting step in prostaglandin synthesis (COX-2) is undetectable in most tissues, but its expression can be induced by a variety of stimuli including LPS related to inflammatory response. Peripherally administered LPS results in increased expression of COX-2 in brain (*14*) and prostaglandin E2 (PGE2) generated in brain *via* COX-2 have been implicated in endotoxin-induced fever. LPS-induced COX-2 expression and PGE2 production appear to be mediated through NF-κB *via* activation of TLR4 (*37*). COX-2 has also been implicated in age-related neurodegenerative diseases *e.g.*, Parkinson's disease (*38*). The present study shows the presence of COX-2-immunopositive neurons in the cortex and striatum after LPS injection; this COX-2 expression being markedly reduced by cerebrolysin.

The activation of caspase proteases, especially caspase-3 is crucial for the execution of programmed cell death (apoptosis) (*39*). Caspase activation is an integral process of programmed cell death during various brain injuries (*40*). This study which measured caspase-3 expression by immunohistochemistry indicated significant increase of caspase-3 positive cells in cortex and striatum after LPS challenge. Cerebrolysin was found to inhibit the appearance of cells positive for caspase-3, suggesting that the drug protect cortical and striatal neurons at least partly by interfering with the activation of capsase-3.

Two different types of cholinesterases hydrolyze the neurotransmitter acetylcholine. AChE (EC 3.1.1.7) terminates the action of acetylcholine at the post-synaptic membrane in the neuromuscular junction. The other enzyme is BChE (EC 3.1.1.8) which hydrolyses acetylcholine as well as many other esters (*41*). The role of AChE in cholinergic neurotransmission is well established and the use of AChE inhibitors has been associated with improved cognition, behaviour, activities of daily living, and global functioning in mild-to-moderate Alzheimer's disease (*42*). The physiological functions of BChE are however, still unresolved. Severely demented Alzheimer's disease patients had significantly lower AChE and BChE activities in CSF than the controls had (*43*). In the present study, systemic endotoxin injection was associated with a decreased activity of both cholinesterases within the brain, suggesting a deleterious effect for systemic inflammation on brain function. This decline in the activity of both AChE and BChE was reversed by cerebrolysin, thereby, suggesting a neuroprotective effect for the drug. Markedly raised BChE activity above normal values after cerebrolysin treatment was however observed. The distribution of BChE in brain suggested that this enzyme may play a unique role in neuronal function (*44*). Studies also suggest a key role of BChE during neurogenesis (*45*). This might provide a possible explanation for the rise in BChE by cerebrolysin observed in the present study since the drug has been shown to promote neuronal growth (*3*) and enhances neurogenesis (*6*).

Although cerebrolysin is essentially a neuroprotective agent used in various cerebral pathologies, the present study also investigated its effects on the liver tissue integrity during endotoxaemia. It has been shown that in liver, TLR4 is expressed by all parenchymal and non-parenchymal cell types, and contributes to tissue damage due to different etiologies (*46*). Interestingly, lipid peroxidation induced by LPS in liver was markedly decreased by the drug despite no effect on GSH level. LPS causes iNOS expression in Kupffer cells and hepatocytes of the liver and consequent increased generation of nitric oxide (*47*) which can result in oxidant stress in the liver and consequent cell injury. In this respect, cerebrolysin, displayed marked inhibitory effect on nitric oxide level and on iNOS expression in hepatic tissue. The drug also reversed the LPS-induced depression of PON1 activity in the liver. Serum levels of PON1 decreases in chronic hepatitis and liver cirrhosis (*48*) and might be a potential test for the evaluation of liver function (*49*). Moreover, caspase-3 activation and COX-2 expression were inhibited by the agent in a dose-dependent manner. Histologically, cerebrolysin dose-dependently attenuated liver necrosis, inflammatory cell infiltration and the loss of hepatic architecture induced by LPS. These observations suggest a potential utility for this peptide mixture in reducing liver injury during endotoxaemia.

In summary, the present study showed that cerebrolysin significantly attenuated oxidative stress and nitric oxide levels in brain and liver after LPS challenge in rats. The drug also reduced the activation

of NF-κB, increased PON1, AChE, and BChE activities in brain. Moreover, cerebrolysin decreased caspase-3 activity, COX-2 and iNOS expression in cortex, striatum and liver and attenuated the brain and liver damage induced by LPS endotoxin, thus suggesting a neuroprotective and a hepatoprotective effect of the drug in endotoxaemia.

References

1. Panisset M, Gauthier S, Moessler H, Windisch M, The Cerebrolysin Study Group. Cerebrolysin in Alzheimer's disease: a randomized, double-blind, placebo-controlled trial with a neurotrophic agent. J Neural Transm. 2002; 109:1089-1104.
2. Wong GKC, Zhu XL, Poon WS. Beneficial effect of cerebrolysin on moderate and severe head injury patients: result of a cohort study. Acta Neurochir. 2005; 95 (Suppl): 59-60.
3. Hartbauer M, Hutter-Paier B, Skofitsch G, Windisch M. Antiapoptotic effects of the peptidergic drug cerebrolysin on primary cultures of embryonic chick cortical neurons. J Neural Transm. 2001; 108:459-473.
4. Onishchenko LS, Gaikova ON, Yanishevskii SN. Changes at the focus of experimental ischemic stroke treated with neuroprotective agents. Neurosci Behav Physiol. 2008; 38:49-54.
5. Rockenstein E, Mante M, Adame A, Crews L, Moessler H, Masliah E. Effects of Cerebrolysin™ on neurogenesis in an APP transgenic model of Alzheimer's disease. Acta Neuropathol. 2007; 113:265-275.
6. Zhang C, Chopp M, Cui Y, Wang L, Zhang R, Zhang L, Lu M, Szalad A, Doppler E, Hitzl M, Zhang ZG. Cerebrolysin enhances neurogenesis in the ischemic brain and improves functional outcome after stroke. J Neurosci Res. 2010; 88:3275-3281.
7. Allegri RF, Guekht A. Cerebrolysin improves symptoms and delays progression in patients with Alzheimer's disease and vascular dementia. Drugs Today (Barc). 2012; 48 (Suppl A):25-41.
8. Warner DS, Sheng H, Batinic-Haberle I. Oxidants, antioxidants and the ischemic brain. J Exp Biol. 2004; 207:3221-3231.
9. Perry VH, Cunningham C, Holmes C. Systemic infections and inflammation affect chronic neurodegeneration. Nat Rev Immunol. 2007; 7:161-167.
10. Halliwell B. Reactive oxygen species and the central nervous system. J Neurochem. 1992; 59:1609-1623.
11. Noble F, Rubira E, Boulanouar M, Palmier B, Plotkine M, Warnet JM, Marchand-Leroux C, Massicot F. Acute systemic inflammation induces central mitochondrial damage and amnesic deficit in adult Swiss mice. Neurosci Lett. 2007; 424:106-110.
12. Jacewicz M, Czapski GA, Katkowska I, Strosznajder RP. Systemic administration of lipopolysaccharide impairs glutathione redox state and object recognition in male mice. The effect of PARP-1 inhibitor. Folia Neuropathol. 2009; 47:321-328.
13. Wang X, Quinn PJ. Endotoxins: lipopolysaccharides of gram-negative bacteria. Subcell Biochem. 2010; 53:3-25.
14. Quan N, Whiteside M, Herkenham M. Cyclooxygenase 2 mRNA expression in rat brain after peripheral injection of lipopolysaccharide. Brain Res. 1998; 802:189-197.
15. Turrin NP, Gayle D, Ilyin SE, Flynn MC, Langhans W, Schwartz GJ, Plata-Salamán CR. Pro-inflammatory and anti-inflammatory cytokine mRNA induction in the periphery and brain following intraperitoneal administration of bacterial lipopolysaccharide. Brain Res Bull. 2001; 54:443-453.
16. Qin L, Wu X, Block ML, Liu Y, Breese GR, Hong JS, Knapp DJ, Crews FT. Systemic LPS causes chronic neuroinflammation and progressive neurodegeneration. Glia. 2007; 55:453-462.
17. Spencer SJ, Mouihate A, Pittman QJ. Peripheral inflammation exacerbates damage after global ischemia independently of temperature and acute brain inflammation. Stroke. 2007; 38:1570-1577.
18. Baeuerle PA. The inducible transcription activator NF-κB: Regulation by distinct protein subunits. Biochim Biophys Acta. 1991; 1072:63-80.
19. Paget GE, Barnes JM. Toxicity testing. In: Evaluation of Drug Activities Pharmacometics (Laurence DR, Bacharach AL, eds.). Academic Press, London, UK, 1964; pp. 1-135.
20. Beurel E, Jope RS. Lipopolysaccharide-induced interleukin-6 production is controlled by glycogen synthase kinase-3 and STAT3 in the brain. J Neuroinflammation. 2009; 6:9.
21. Ruiz-Larrea MB, Leal AM, Liza M, Lacort M, de Groot H. Antioxidant effects of estradiol and 2-hydroxyestradiol on iron-induced lipid peroxidation of rat liver microsomes. Steroids. 1994; 59:383-388.
22. Ellman GL. Tissue sulfhydryl groups. Arch Biochem. 1959; 82:70-77.
23. Moshage H, Kok B, Huizenga JR. Nitrite and nitrate determination in plasma: A critical evaluation. Clin Chem. 1995; 41:892-896.
24. Higashino K, Takahashi Y, Yamamura Y. Release of phenyl acetate esterase from liver microsomes by carbon tetrachloride. Clin Chim Acta. 1972; 41:313-320.
25. Gorun V, Proinov I, Baltescu V, Balaban G, Barzu O. Modified Ellman procedure for assay of cholinesterases in crude enzymatic preparation. Anal Biochem. 1978; 86:324-326.
26. Wang W, Ballatori N. Endogenous glutathione conjugates: Occurrence and biological functions. Pharmacol Rev. 1998; 50:335-356.
27. Schulz JB, Lindenau J, Seyfried J, Dichgans J. Glutathione, oxidative stress and neurodegeneration. Eur J Biochem. 2000; 267:4904-1143.
28. Schmidt KN, Amstad P, Cerutti P, Baeuerle PA. The roles of hydrogen peroxide and superoxide as messengers in the activation of transcription factor NF-κB. Chem Biol. 1995; 2:13-22.
29. Wehr H, Bednarska-Makaruk M, Graban A, Lipczyńska-Łojkowska W, Rodo M, Bochyńska A, Ryglewicz D. Paraoxonase activity and dementia. J Neurol Sci. 2009; 283:107-108.
30. La Du BN. Human serum paraoxonase: arylesterase. In: Pharmacogenetics of Drug Metabolism (Kalow W, ed.). Pergamon Press, New York, USA, 1992; pp. 51-91.
31. Rodrigo L, Hernández AF, López-Caballero JJ, Gil F, Pla A. Immunohistochemical evidence for the expression and induction of paraoxonase in rat liver, kidney, lung and brain tissue. Implications for its physiological role. Chem Biol Interact. 2001; 137:123-137.
32. Moncada S, Bolanos JP. Nitric oxide, cell bioenergetics and neurodegeneration. J Neurochem. 2006; 97:1676-1689.

33. Valko M, Leibfritz D, Moncol J,. Cronin MTD, Mazur M, Telser J. Free radicals and antioxidants in normal physiological functions and human disease. Int J Biochem Cell Biol. 2007; 39:44-84.
34. Czapski GA, Cakala M, Chalimoniuk M, Gajkowska B, Strosznajder JB. Role of nitric oxide in the brain during lipopolysaccharide-evoked systemic inflammation. J Neurosci Res. 2007; 85:1694-1703.
35. Pang Y, Campbell L, Zheng B, Fan L, Cai Z, Rhodes P. Lipopolysaccharide-activated microglia induce death of oligodendrocyte progenitor cells and impede their development. Neuroscience. 2010; 166:464-475.
36. Bithell A, Williams BP. Neural stem cells and cell replacement therapy: Making the right cells. Clin Sci (Lond). 2005; 108:13-22.
37. Shih RH, Yang CM. Induction of heme oxygenase-1 attenuates lipopolysaccharide-induced cyclooxygenase-2 expression in mouse brain endothelial cells. J Neuroinflammation. 2010; 7:86.
38. Bartels AL, Leenders KL.Cyclooxygenase and neuroinflammation in Parkinson's disease neurodegeneration. Curr Neuropharmacol. 2010; 8: 62-68.
39. Porter AG, Jänicke RU. Emerging roles of caspase-3 in apoptosis. Cell Death Differ. 1999; 6:99-104.
40. Yakovlev AG, Faden AI. Caspase-dependent apoptotic pathways in CNS injury. Mol Neurobiol. 2001; 24:131-144.
41. Chatonnet A, Lockridget O. Comparison of butyrylcholinesterase and acetylcholinesterase. Biochem J. 1989; 260: 625-634.
42. Thompson S, Lanctôt KL, Herrmann N. The benefits and risks associated with cholinesterase inhibitor therapy in Alzheimer's disease. Expert Opin Drug Saf. 2004; 3:425-440.
43. Sirviö J, Kutvonen R, Soininen H, Hartikainen P, Riekkinen PJ. Cholinesterases in the cerebrospinal fluid, plasma, and erythrocytes of patients with Alzheimer's disease. J Neural Transm. 1989; 75:119-127.
44. Tago H, Maeda T, McGeer PL, Kimura H. Butyrylcholinesterase-rich neurons in rat brain demonstrated by a sensitive histochemical method. J Comp Neurol. 1992; 325:301-312.
45. Mack A, Robitzki A. The key role of butyrylcholinesterase during neurogenesis and neural disorders: An antisense-5'butyrylcholinesterase-DNA study. Prog Neurobiol. 2000; 60:607-628.
46. Guo J, Friedman SL. Toll-like receptor 4 signaling in liver injury and hepatic fibrogenesis. Fibrogenesis Tissue Repair. 2010; 3:21.
47. Duval DL, Miller DR, Collier J, Billings RE. Characterization of hepatic nitric oxide synthase: Identification as the cytokine-inducible form primarily regulated by oxidants. Mol Pharmacol. 1996; 50:277-284.
48. Ferre N, Camps J, Prats E, Vilella E, Paul A, Figuera L, Joven J. Serum paraoxonase activity: A new additional test for the improved evaluation of chronic liver damage. Clin Chem. 2002; 48:261-268.
49. Camps J, Marsillach J, Joven J. Measurement of serum paraoxonase-1 activity in the evaluation of liver function. World J Gastroenterol. 2009; 15:1929-1933.

(*Received March 18, 2013; Revised March 28, 2013; Re-revised December 9, 2013; Accepted December 10, 2013****)***

Author Index (2013)

Subject Index (2013)

Policy Forum

Reviews

Brief Reports

Original Articles

Case Report

Commentary

DD&T
Drug Discoveries & Therapeutics

Guide for Authors

1. Scope of Articles

Drug Discoveries & Therapeutics welcomes contributions in all fields of pharmaceutical and therapeutic research such as medicinal chemistry, pharmacology, pharmaceutical analysis, pharmaceutics, pharmaceutical administration, and experimental and clinical studies of effects, mechanisms, or uses of various treatments. Studies in drug-related fields such as biology, biochemistry, physiology, microbiology, and immunology are also within the scope of this journal.

2. Submission Types

Original Articles should be well-documented, novel, and significant to the field as a whole. An Original Article should be arranged into the following sections: Title page, Abstract, Introduction, Materials and Methods, Results, Discussion, Acknowledgments, and References. Original articles should not exceed 5,000 words in length (excluding references) and should be limited to a maximum of 50 references. Articles may contain a maximum of 10 figures and/or tables.

Brief Reports definitively documenting either experimental results or informative clinical observations will be considered for publication in this category. Brief Reports are not intended for publication of incomplete or preliminary findings. Brief Reports should not exceed 3,000 words in length (excluding references) and should be limited to a maximum of 4 figures and/or tables and 30 references. A Brief Report contains the same sections as an Original Article, but the Results and Discussion sections should be combined.

Reviews should present a full and up-to-date account of recent developments within an area of research. Normally, reviews should not exceed 8,000 words in length (excluding references) and should be limited to a maximum of 100 references. Mini reviews are also accepted.

Policy Forum articles discuss research and policy issues in areas related to life science such as public health, the medical care system, and social science and may address governmental issues at district, national, and international levels of discourse. Policy Forum articles should not exceed 2,000 words in length (excluding references).

Case Reports should be detailed reports of the symptoms, signs, diagnosis, treatment, and follow-up of an individual patient. Case reports may contain a demographic profile of the patient but usually describe an unusual or novel occurrence. Unreported or unusual side effects or adverse interactions involving medications will also be considered. Case Reports should not exceed 3,000 words in length (excluding references).

News articles should report the latest events in health sciences and medical research from around the world. News should not exceed 500 words in length.

Letters should present considered opinions in response to articles published in Drug Discoveries & Therapeutics in the last 6 months or issues of general interest. Letters should not exceed 800 words in length and may contain a maximum of 10 references.

3. Editorial Policies

Ethics: Drug Discoveries & Therapeutics requires that authors of reports of investigations in humans or animals indicate that those studies were formally approved by a relevant ethics committee or review board.

Conflict of Interest: All authors are required to disclose any actual or potential conflict of interest including financial interests or relationships with other people or organizations that might raise questions of bias in the work reported. If no conflict of interest exists for each author, please state "There is no conflict of interest to disclose".

Submission Declaration: When a manuscript is considered for submission to Drug Discoveries & Therapeutics, the authors should confirm that 1) no part of this manuscript is currently under consideration for publication elsewhere; 2) this manuscript does not contain the same information in whole or in part as manuscripts that have been published, accepted, or are under review elsewhere, except in the form of an abstract, a letter to the editor, or part of a published lecture or academic thesis; 3) authorization for publication has been obtained from the authors' employer or institution; and 4) all contributing authors have agreed to submit this manuscript.

Cover Letter: The manuscript must be accompanied by a cover letter signed by the corresponding author on behalf of all authors. The letter should indicate the basic findings of the work and their significance. The letter should also include a statement affirming that all authors concur with the submission and that the material submitted for publication has not been published previously or is not under consideration for publication elsewhere. The cover letter should be submitted in PDF format. For example of Cover Letter, please visit http://www.ddtjournal.com/downcentre.php (Download Centre).

Copyright: A signed JOURNAL PUBLISHING AGREEMENT (JPA) must be provided by post, fax, or as a scanned file before acceptance of the article. Only forms with a hand-written signature are accepted. This copyright will ensure the widest possible dissemination of information. A form facilitating transfer of copyright can be downloaded by clicking the appropriate link and can be returned to the e-mail address or fax number noted on the form (Please visit Download Centre). Please note that your manuscript will not proceed to the next step in publication until the JPA form is received. In addition, if excerpts from other copyrighted works are included, the author(s) must obtain written permission from the copyright owners and credit the source(s) in the article.

Suggested Reviewers: A list of up to 3 reviewers who are qualified to assess the scientific merit of the study is welcomed. Reviewer information including names, affiliations, addresses, and e-mail should be provided at the same time the manuscript is submitted online. Please do not suggest reviewers with known conflicts of interest, including participants or anyone with a stake in the proposed research; anyone from the same institution; former students, advisors, or research collaborators (within the last three years); or close personal contacts. Please note that the Editor-in-Chief may accept one or more of the proposed reviewers or may request a review by other qualified persons.

Language Editing: Manuscripts prepared by authors whose native language is not English should have their work proofread by a native English speaker before submission. If not, this might delay the publication of your manuscript in Drug Discoveries & Therapeutics.

The Editing Support Organization can provide English proofreading, Japanese-English translation, and Chinese-English translation services to authors who want to publish in Drug Discoveries & Therapeutics and need assistance before submitting a manuscript. Authors can visit this organization directly at http://www.iacmhr.com/iac-eso/support.php?lang=en. IAC-ESO was established to facilitate manuscript preparation by researchers whose native language is not English and to help edit works intended for international academic journals.

4. Manuscript Preparation

Manuscripts should be written in clear, grammatically correct English and submitted as a Microsoft Word file in a single-column format. Manuscripts must be paginated and typed in 12-point Times New Roman font with 24-point line spacing. Please do not embed figures in the text. Abbreviations should be used as little as possible and should be explained at first mention unless the term is a well-known abbreviation (*e.g.* DNA). Single words should not be abbreviated.

Title page: The title page must include 1) the title of the paper (Please note the title should be short, informative, and contain the major key words); 2) full name(s) and affiliation(s) of the author(s), 3) abbreviated names of the author(s), 4) full name, mailing address, telephone/fax numbers, and e-mail address of the corresponding author; and 5) conflicts of interest (if you have an actual or potential conflict of interest to disclose, it must be included as a footnote on the title page of the manuscript; if no conflict of interest exists for each author, please state "There is no conflict of interest to disclose"). Please visit Download Centre and refer to the title page of the manuscript sample.

Abstract: The abstract should briefly state the purpose of the study, methods, main findings, and conclusions. For article types including Original Article, Brief Report, Review, Policy Forum, and Case Report, a one-paragraph abstract consisting of no more than 250 words must be included in the manuscript. For News and Letters, a brief summary of main content in 150 words or fewer should be included in the manuscript. Abbreviations must be kept to a minimum and non-standard abbreviations explained in brackets at first mention. References should be avoided in the abstract. Key words or phrases that do not occur in the title should be included in the Abstract page.

Introduction: The introduction should be a concise statement of the basis for the study and its scientific context.

Materials and Methods: The description should be brief but with sufficient detail to enable others to reproduce the experiments. Procedures that have been published previously should not be described in detail but appropriate references should simply be cited. Only new and significant modifications of previously published procedures require complete description. Names of products and manufacturers with their locations (city and state/country) should be given and sources of animals and cell lines should always be indicated. All clinical investigations must have been conducted in accordance with Declaration of Helsinki principles. All human and animal studies must have been approved by the appropriate institutional review board(s) and a specific declaration of approval must be made within this section.

Results: The description of the experimental results should be succinct but in sufficient detail to allow the experiments to be analyzed and interpreted by an independent reader. If necessary, subheadings may be used for an orderly presentation. All figures and tables must be referred to in the text.

Discussion: The data should be interpreted concisely without repeating material already presented in the Results section. Speculation is permissible, but it must be well-founded, and discussion of the wider implications of the findings is encouraged. Conclusions derived from the study should be included in this section.

Acknowledgments: All funding sources should be credited in the Acknowledgments section. In addition, people who contributed to the work but who do not meet the criteria for authors should be listed along with their contributions.

References: References should be numbered in the order in which they appear in the text. Citing of unpublished results, personal communications, conference abstracts, and theses in the reference list is not recommended but these sources may be mentioned in the text. In the reference list, cite the names of all authors when there are fifteen or fewer authors; if there are sixteen or more authors, list the first three followed by *et al*. Names of journals should be abbreviated in the style used in PubMed. Authors are responsible for the accuracy of the references. Examples are given below:

Example 1 (Sample journal reference):
Nakata M, Tang W. Japan-China Joint Medical Workshop on Drug Discoveries and Therapeutics 2008: The need of Asian pharmaceutical researchers' cooperation. Drug Discov Ther. 2008; 2:262-263.

Example 2 (Sample journal reference with more than 15 authors):
Darby S, Hill D, Auvinen A, *et al*. Radon in homes and risk of lung cancer: Collaborative analysis of individual data from 13 European case-control studies. BMJ. 2005; 330:223.

Example 3 (Sample book reference):
Shalev AY. Post-traumatic stress disorder: Diagnosis, history and life course. In: Post-traumatic Stress Disorder, Diagnosis, Management and Treatment (Nutt DJ, Davidson JR, Zohar J, eds.). Martin Dunitz, London, UK, 2000; pp. 1-15.

Example 4 (Sample web page reference):
World Health Organization. The World Health Report 2008 – primary health care: Now more than ever. *http://www.who.int/whr/2008/whr08_en.pdf* (accessed September 23, 2010).

Tables: All tables should be prepared in Microsoft Word or Excel and should be arranged at the end of the manuscript after the References section. Please note that tables should not in image format. All tables should have a concise title and should be numbered consecutively with Arabic numerals. If necessary, additional information should be given below the table.

Figure Legend: The figure legend should be typed on a separate page of the main manuscript and should include a short title and explanation. The legend should be concise but comprehensive and should be understood without referring to the text. Symbols used in figures must be explained.

Figure Preparation: All figures should be clear and cited in numerical order in the text. Figures must fit a one- or two-column format on the journal page: 8.3 cm (3.3 in.) wide for a single column, 17.3 cm (6.8 in.) wide for a double column; maximum height: 24.0 cm (9.5 in.). Please make sure that artwork files are in an acceptable format (TIFF or JPEG) at minimum resolution (600 dpi for illustrations, graphs, and annotated artwork, and 300 dpi for micrographs and photographs). Please provide all figures as separate files. Please note that low-resolution images are one of the leading causes of article resubmission and schedule delays. All color figures will be reproduced in full color in the online edition of the journal at no cost to authors.

Units and Symbols: Units and symbols conforming to the International System of Units (SI) should be used for physicochemical quantities. Solidus notation (*e.g.* mg/kg, mg/mL, mol/mm^2/min) should be used. Please refer to the SI Guide www.bipm.org/en/si/ for standard units.

Supplemental data: Supplemental data might be useful for supporting and enhancing your scientific research and Drug Discoveries & Therapeutics accepts the submission of these materials which will be only published online alongside the electronic version of your article. Supplemental files (figures, tables, and other text materials) should be prepared according to the above guidelines, numbered in Arabic numerals (*e.g.*, Figure S1, Figure S2, and Table S1, Table S2) and referred to in the text. All figures and tables should have titles and legends. All figure legends, tables and supplemental text materials should be placed at the end of the paper. Please note all of these supplemental data should be provided at the time of initial submission and note that the editors reserve the right to limit the size and length of Supplemental Data.

5. Submission Checklist

The Submission Checklist will be useful during the final checking of a manuscript prior to sending it to Drug Discoveries & Therapeutics for review. Please visit Download Centre and download the Submission Checklist file.

6. Online submission

Manuscripts should be submitted to Drug Discoveries & Therapeutics online at http://www.ddtjournal.com. The manuscript file should be smaller than 5 MB in size. If for any reason you are unable to submit a file online, please contact the Editorial Office by e-mail at office@ddtjournal.com

7. Accepted manuscripts

Proofs: Galley proofs in PDF format will be sent to the corresponding author *via* e-mail. Corrections must be returned to the editor (proof-editing@ddtjournal.com) within 3 working days.

Offprints: Authors will be provided with electronic offprints of their article. Paper offprints can be ordered at prices quoted on the order form that accompanies the proofs.

Page Charge: A page charge of $140 will be assessed for each printed page of an accepted manuscript. The charge for printing color figures is $340 for each page. Under exceptional circumstances, the author(s) may apply to the editorial office for a waiver of the publication charges at the time of submission.

(Revised February 2013)

Editorial and Head Office:

Pearl City Koishikawa 603
2-4-5 Kasuga, Bunkyo-ku
Tokyo 112-0003
Japan
Tel: +81-3-5840-9697
Fax: +81-3-5840-9698
E-mail: office@ddtjournal.com

DD&T
Drug Discoveries & Therapeutics

JOURNAL PUBLISHING AGREEMENT (JPA)

Manuscript No.:

Title:

Corresponding author:

The International Advancement Center for Medicine & Health Research Co., Ltd. (IACMHR Co., Ltd.) is pleased to accept the above article for publication in Drug Discoveries & Therapeutics. The International Research and Cooperation Association for Bio & Socio-Sciences Advancement (IRCA-BSSA) reserves all rights to the published article. Your written acceptance of this JOURNAL PUBLISHING AGREEMENT is required before the article can be published. Please read this form carefully and sign it if you agree to its terms. The signed JOURNAL PUBLISHING AGREEMENT should be sent to the Drug Discoveries & Therapeutics office (Pearl City Koishikawa 603, 2-4-5 Kasuga, Bunkyo-ku, Tokyo 112-0003, Japan; E-mail: office@ddtjournal.com; Tel: +81-3-5840-9697; Fax: +81-3-5840-9698).

1. Authorship Criteria

As the corresponding author, I certify on behalf of all of the authors that:

1) The article is an original work and does not involve fraud, fabrication, or plagiarism.
2) The article has not been published previously and is not currently under consideration for publication elsewhere. If accepted by Drug Discoveries & Therapeutics, the article will not be submitted for publication to any other journal.
3) The article contains no libelous or other unlawful statements and does not contain any materials that infringes upon individual privacy or proprietary rights or any statutory copyright.
4) I have obtained written permission from copyright owners for any excerpts from copyrighted works that are included and have credited the sources in my article.
5) All authors have made significant contributions to the study including the conception and design of this work, the analysis of the data, and the writing of the manuscript.
6) All authors have reviewed this manuscript and take responsibility for its content and approve its publication.
7) I have informed all of the authors of the terms of this publishing agreement and I am signing on their behalf as their agent.

2. Copyright Transfer Agreement

I hereby assign and transfer to IACMHR Co., Ltd. all exclusive rights of copyright ownership to the above work in the journal Drug Discoveries & Therapeutics, including but not limited to the right 1) to publish, republish, derivate, distribute, transmit, sell, and otherwise use the work and other related material worldwide, in whole or in part, in all languages, in electronic, printed, or any other forms of media now known or hereafter developed and the right 2) to authorize or license third parties to do any of the above.

I understand that these exclusive rights will become the property of IACMHR Co., Ltd., from the date the article is accepted for publication in the journal Drug Discoveries & Therapeutics. I also understand that IACMHR Co., Ltd. as a copyright owner has sole authority to license and permit reproductions of the article.

I understand that except for copyright, other proprietary rights related to the Work (*e.g.* patent or other rights to any process or procedure) shall be retained by the authors. To reproduce any text, figures, tables, or illustrations from this Work in future works of their own, the authors must obtain written permission from IACMHR Co., Ltd.; such permission cannot be unreasonably withheld by IACMHR Co., Ltd.

3. Conflict of Interest Disclosure

I confirm that all funding sources supporting the work and all institutions or people who contributed to the work but who do not meet the criteria for authors are acknowledged. I also confirm that all commercial affiliations, stock ownership, equity interests, or patent-licensing arrangements that could be considered to pose a financial conflict of interest in connection with the article have been disclosed.

Corresponding Author's Name (Signature):

Date: